MULTI-MODAL SMART SENSING NETWORK FOR MARINE ENVIRONMENTAL MONITORING

by

Dian Zhang, B.Eng.

Submitted in partial fulfilment of the requirements

for the Degree of Doctor of Philosophy

Dublin City University

School of Electronic Engineering

Supervisor: Prof. Noel E. O'Connor, Prof. Fiona Regan

June, 2015

Declaration

I hereby certify that this material, which I now submit for assessment on the programme of study leading to the award of Doctor of Philosophy is entirely my own work, that I have exercised reasonable care to ensure that the work is original, and does not to the best of my knowledge breach any law of copyright, and has not been taken from the work of others save and to the extent that such work has been cited and acknowledged within the text of my work.

Signed: _____
Dian Zhang (Candidate)

ID: _____

Date: _____

ACKNOWLEDGEMENTS

Firstly, I wish to express my deepest thanks to my supervisors Prof. Noel E. O'Connor and Prof. Fiona Regan for giving me the opportunity to pursue this interesting and challenging project and for invaluable guidance and support that I have received. The constant encouragement and inspiration that they provided especially during the bemused periods for which I will always be grateful. In DCU, I have been very lucky to work with experts from a variety of research centres. From marine scientists to microtronic system engineers, from chemists to computer scientists who have provided me with valuable domain knowledge. I have been also very lucky to work within Insight and MESTECH, where I have had the opportunity to work with many excellent researchers. Dr. Edel O'Connor who kept dragging me back on the right path of my research. Dr. Kevin McGuinness, the founder of McGuinness Consultant, who gave the solutions to all the problems that I have encountered during my PhD and saved mine and many other PhD students' life. I would also like to greatly thank Dr. Timothy Sullivan, who I worked a lot with over the years and provided a breadth of knowledge such as bio-fouling, nanocomposites and polydimethylsiloxane, which upto now I still have no clue about. Dr. Jogile Kuklyte, for sharing her feelings as the previous free range student. My colleagues from MESTECH, Ciprian Briciu-Burghina and Brendan Heery, who made my experience over the last few years very enjoyable.

A special thanks to Dr. Kevin Fraser, Dr. Timothy Sullivan, Ruth Blayney and Niall Durham, who translated this thesis from Chinglish to English. If you are still confused about any part of the writing please contact them respectively.

On a personal note, I want to thank my wife Xiaodong Liu, my parents Xun Zhang and Zhongru Zhang and all the other members of my family for their constant support. I want to also thank the people from the Full Shilling, where I have been working in the past thirteen years, for their continuous support since I came to Ireland.

Finally, thanks to QUESTOR centre and Beaufort Marine Research Awards, which funded this research.

TABLE OF CONTENTS

LIST OF PEER-REVIEWED PUBLICATIONS

Journal

- Murphy, Kevin, Brendan Heery, Timothy Sullivan, Dian Zhang, Lizandra Paludetti, King Tong Lau, Dermot Diamond, Ernane Costa, Noel E. O'Connor and Fiona Regan. "A low-cost autonomous optical sensor for water quality monitoring." Talanta 132 (2015): 520-527.

- Zhang, Dian, Timothy Sullivan, Ciprian Briciu-Burghina, Kevin Murphy, Kevin McGuinness, Noel E. O'Connor, Alan F. Smeaton, and Fiona Regan. "Detection and classification of anomalous events in water quality datasets within a smart city-smart bay project." International Journal on Advances in Intelligent Systems 7, no. 1&2 (2014): 167-178.

Conference

- Zhang, Dian, Timothy Sullivan, Noel E. O'Connor, Randy Gillespie, and Fiona Regan. "Coastal Fog Detection Using Visual Sensing." In Ocean 15, Genova, Italy, 18-21 May 2015.

- Zhang, Dian, Edel O'Connor, Timothy Sullivan, Kevin McGuinness, Fiona Regan,

and Noel E. O'Connor. "Smart multi-modal marine monitoring via visual analysis and data fusion." In Proceedings of the 2nd ACM international workshop on Multimedia analysis for ecological data, pp. 29-34. ACM, 2013.

- Sullivan, Tim and Zhang, Dian and O'Connor, Edel and Briciu Burghina, Ciprian Constantin and Heery, B. and Gualano, Leonardo and Smeaton, Alan F. and O'Connor, Noel E. and Regan, Fiona (2013) "Improving data driven decision making through integration of environmental sensing technologies." In Ocean 13, Bergen, Norway, 10-13 June 2013.

- Regan, Fiona, Dian Zhang, Timothy Sullivan, Ciprian Briciu, Helen Cooney, Kevin Murphy, Edel O'Connor, Noel O'Connor, and Alan Smeaton. "A smart city-smart bay project-establishing an integrated water monitoring system for decision support in Dublin Bay." In SENSORCOMM 2013, The Seventh International Conference on Sensor Technologies and Applications, pp. 75-82. 2013.

- Zhang, Dian, Edel O'Connor, Kevin McGuinness, Noel E. O'Connor, Fiona Regan, and Alan Smeaton. "A visual sensing platform for creating a smarter multi-modal marine monitoring network." In Proceedings of the 1st ACM international workshop on Multimedia analysis for ecological data, pp. 53-56. ACM, 2012.

- O'Connor, Edel, Dian Zhang, Alan F. Smeaton, Noel E. O'Connor, and Fiona Regan. "Multi-modal sensor networks for more effective sensing in Irish coastal and freshwater environments." In Ocean 12, pp. 1-9. IEEE, 2012.

Oral Presentation

- Zhang, Dian, Noel E. O'Connor, and Fiona Regan. "Intelligence in Multi-Modal Wireless Sensor Network for Marine Environment Monitoring." In Environ 2015: 25th Irish Environmental Researchers' Colloquium, 8th - 10th April 2015, Sligo, Ireland

- Zhang, Dian, Timothy Sullivan, Noel E. O'Connor, and Fiona Regan. "Smart Sensing for Marine Monitoring and Decision Making ." In Environ 2014: 24th Irish Environmental Researchers' Colloquium, 26th - 28th February 2014, Dublin, Ireland

- O'Connor, Edel, Dian Zhang, Alan F. Smeaton, Noel E. O'Connor, and Fiona Regan. "Smarter sensing through the integration of diverse sensing modalities into environmental monitoring networks." In SESEH 2012: Sino-European Symposium on Environment and Health, 20th - 25th August, 2012, Galway, Ireland.

LIST OF FIGURES

LIST OF TABLES

ABSTRACT

MULTI-MODAL SMART SENSING NETWORK FOR

MARINE ENVIRONMENTAL MONITORING

Dian Zhang

There is an imperative need for long-term, large-scale marine monitoring systems that will allow decisions to be made based on the analysis of collected data to avoid or limit negative impacts on the ecosystem. Modern marine environmental sensing technologies, such as autonomous wireless sensor networks (WSNs), provide the capability to meet the challenges of high spatial and temporal scales. However, the significant amount of data generated from WSNs is a significant challenge for manual analysis. These multitudinous data need to be automatically processed, indexed and catalogued in a smarter way that can be more easily understood, accessed and managed by operators, scientists and policy makers. Moreover, current research works show that WSNs have their own limitations, for example, reliability issues and the fact that they are passive systems and provide context-less data. Thus, it is becoming increasingly clear that in order to adequately monitor marine environments, they need to be characterised from multiple perspectives. Combining multiple technologies and sensing modalities in environmental monitoring programmes can provide not only advantages of reliability and robustness for sensing systems, but also enhanced understanding of environmental processes. In addition, considerable advances can be made if robust sensing technology can be combined with sophisticated methods of data analysis, classification and cataloguing. The aim of this work is to bridge the gap between current aquatic monitoring systems and futuristic ideal large scale multi-modality smart sensing networks for marine environmental monitoring. To illustrate this, a smart sensing system is proposed and two case studies are used to show data processing from *in-situ* measurements and from camera based visual sensing data automatically using machine learning techniques. Abnormal events detection results from an *in-situ* sensor and shipping traffic detection results from visual sensor are combined to illustrate the benefit of coupling multiple sensing modalities.

CHAPTER 1

INTRODUCTION

1.1 Overview

With an estimated coastline length of $3,171$ km and Exclusive Economic Zone (EEZ) covering an estimated 89 million hectares, the Irish marine resource provides vital and increasing exploitation opportunities. According to the Integrated Marine Plan for Ireland 2012 [1], the Irish ocean economy will generate €6.4 billion a year in turnover by 2020, contribute 2.4 % of GDP (direct and indirect Gross Value Added) by 2030, and support approximately 1 % of the total workforce. In Ireland, 99.5 % of foreign trade is facilitated through seaports, of which 42 % of the gross domestic product (GDP) is exported through Dublin Port [2]. From the global economic perspective, marine related activities are estimated to contribute 2 % of the world's GDP and approximately 4 % of Europe's GDP (in 2007). Approximately 80 % of all international trade is carried by sea [3]. These increasingly exploited resources must be monitored, managed and protected efficiently and effectively.

Water quality is also a key factor to human and halobios health. 3.4 million people die each year from water related diseases [4]. Contaminated water can transmit diseases such as diarrhoea, cholera, dysentery, typhoid and polio. According to the U.S. National

Library of Medicine [5], contaminated water is estimated to cause more than $500,000$ diarrhoeal deaths each year. Generally, sea water does not have significant influence on human health because water cannot stagnate and its saltiness stems bacteria proliferation. However, open water in estuaries can easily become contaminated due to sewage, surface runoff or infections spread by wildlife. Bacteria, such as *Escherichia coli* (E. coli) and *faecal coliform*, get into the human body by direct contact or though the food chain and can cause illness, such as acute enterocolitis and bloody diarrhea.

Fish kills, which are often the first visible signs of environmental stress, may be caused by a variety of reasons. Dumping of sewage, which has nutrients, such as phosphate, stimulates aquatic plants that use up oxygen as they decompose (known as eutrophication). The rapid growth of marine flora blocks light to deeper water, further reducing oxygen levels due to the decrease in the photosynthesis process. Fish and other living vertebrate die as a result of suffocation. The Irish Central Fisheries Board annual report stated that 53 fish kills were recorded nationally during 2013. Among those, 12 kills were caused by agricultural practice, 7 by industrial operations and 5 by municipal works. However, the cause of 28 kills (53 %) are unknown. According to some sources[1], over 600 mass death events were reported in 76 countries in 2014. Approximately 470 out of all those events are related to the aquatic environment and the causes of the majority of these kills are undiscovered. Thus, from both economic and ecosystem well-being perspectives, there is an imperative need for long-term, large-scale marine monitoring systems.

Modern marine environmental sensing technologies, such as autonomous wireless sensor networks (WSN), provide the capability to meet challenges of high spatial and temporal scales [6, 7]. In recent years, the development of sensing technology is reaching a maturational stage in terms of cost and accuracy, which presents the opportunity to monitor large geographical areas with high temporal frequency. However, there are substantial challenges to widespread deployment of devices to collect data on large spatial scales, and such goals are not yet achievable in a cost-effective manner, particularly in aquatic monitoring programmes. High installation and operating costs of deployment infrastruc-

[1] http://www.end-times-prophecy.org/mass-animal-deaths-2014.html accessed: Nov 2014

ture coupled with sensor unreliability stemming from factors such as sensor drift and biofouling result in inadequate spatial coverage of most aquatic zones [8, 9]. In addition, the significant amount of data generated from *in-situ* sensor networks cannot be handled based on manual analysis. These multitudinous data need to be automatically processed, indexed and catalogued in a smarter way that can be easier understood, accessed and managed by operators, scientists and policy makers. Moreover, current research works show that WSNs have their own limitations, for example, reliability issues, the use of passive systems and context-less data. Aquatic environments, especially marine environments, are very aggressive and sensors are subject to noise, failure or damage. Probes, optical based sensors in particular, can be blocked by particles which results in noisy readings that may not reflect the true property of a water body. Malfunctioning sensors may produce unreliable information or gaps in coverage.

In [10], the author defined *in-situ* sensing as a technology used to acquire information about an object when the distance between the object and the sensor is comparable to or smaller than any linear dimension of the sensor. In contrast, the distance between the object and the sensor is much greater than any linear dimension of the sensor in remote sensing.

Current *in-situ* sensors are passive systems (all the settings are pre-configured and do not vary during the period of deployment), which are easy to develop, configure and deploy. However, pre-configured sensors do not adapt based on the occurrences at the scene. In contrast, active systems adapt based on the dynamics on site, which can provide richer details of environmental phenomena by increasing sampling rate when it is occurring and expand life time, especially for reagent based analysers a that contains limited amount of reagent or battery powered systems, by reducing sampling rate when no events arise. Also, single modality *in-situ* sensors result in a lack of surrounding information that could assist environmental scientists to better understand the causes and the effects of abnormal events.

Thus, it is becoming increasingly clear that in order to adequately monitor marine environments, they need to be characterised from multiple perspectives. Combining multiple

technologies and sensing modalities in environmental monitoring programmes can potentially provide not only advantages of reliability and robustness for sensing systems, but also enhanced understanding of environmental processes. In addition, considerable advances can be made if robust sensing technology can be combined with sophisticated methods of data analysis, classification and cataloguing.

Automated collection and storage of datasets related to environmental water quality is now becoming commonplace, however, challenges remain in automated detection of important events within these datasets and thus determination of the value and ecological significance of the collected data. This challenge can only increase as the vision of futuristic multimodality smart sensing system containing integrated sensing networks becomes a reality.

Decision-making is the process of reaching a decision based on adequate judgement, including identification of the problem, recognition of the solution and ability to evaluate all options, ultimately reaching the best decision after evaluation of the available data. High quality, high frequency environmental datasets are required to facilitate this process and ideally, environmental data would be measured once and utilised in multiple applications for different purposes.

The aim of this work is to bridge the gap between current aquatic monitoring systems and the futuristic ideal of large scale multimodality smart sensing networks for marine environmental monitoring. To illustrate this, we propose our vision of a smart sensing system, showing two case studies of automated data processing from *in-situ* measurements and from camera based visual sensing data. Ultimately, we combine unusual event detection results from *in-situ* sensors and shipping traffic detection from a visual sensor to illustrate the benefit of coupling multiple sensing modalities. Both case studies demonstrate how state-of-the-art computer science technologies can be applied to the marine environment monitoring domain to provide next generation information that supports marine scientists and policy makers in better understanding marine ecosystems and to allow well informed decision making.

1.2 Motivation

Historically, investment in the monitoring of both European and global water bodies has been low, partly owing to the high costs associated with sample collection and subsequent analyses in the laboratory. However, monitoring of water, globally and within Europe, will increase over the coming years to comply with legislative requirements such as the EU Water Framework Directive [11] and the Water Floods Directive [12], and in response to the pressures of climate change, which will lead to resource scarcity and water quality changes. The traditional "spot and grab" sampling approach using conventional sampling and laboratory based techniques can introduce a significant financial burden, and is unlikely to provide a reasonable estimate of the true maximum and/or mean concentration for a particular physico-chemical variable in a water body with marked temporal variability. The use of relatively inexpensive *in-situ* sensors offers the potential to reduce costs considerably, making it possible to monitor an increasingly wider set of parameters in the field, as well as providing more useful, continuous monitoring capabilities to give an accurate idea of changing environmental and water quality. *In-situ* in the context of environmental sensing means sensors in direct contact with the medium of interest, as opposed to methods such as remote sensing where no contact is made between the sensor and the analyte. The accurate measurement and detection of environmental pollutants is feasible under laboratory-controlled conditions but doing so with continuous *in-situ* monitors remains the most challenging aspect of environmental sensing. One of the advantages of wireless sensor networks, *in-situ* sensor or sensors with wireless communication functionality, is that they enable remote continuous monitoring of the environment. Data from monitoring systems can now be used for a variety of applications in addition to protection of the environment [13, 14, 15].

Although it is evident that some elements of the ideal monitoring system are in place, ongoing research and development is required in several areas related to both sensor technology and field-testing. The ideal monitoring system of the near future might consist of a network of sensors, deployed at key locations, capable of autonomous operation in

the field, for long periods (annual to decade time scales). Currently, the building blocks necessary to achieve the ideal scenario of the measurement, of multiple water quality parameters, simultaneously and in real-time are available [16]. However, as a scientific community, we need to improve the quality of some of the more sophisticated sensors for nutrients, while using the simpler devices in cleverer ways in embedded networks to make this idea truly achievable. Another consideration is that a common platform for data validation and sensor verification has yet to be universally implemented to improve data quality. Data transmission in wireless networked sensors has become one of the most dynamic and important areas of multi-disciplinary research [17, 18]. Data from monitoring stations can be analysed and communicated by wireless technology to the laboratory, for statistical processing and interpretation by expert systems. Alerts can be issued to relevant personnel - through an alarm sent to their mobile devices, such as smart phones, tablets or laptops - when worrying trends for any constituent of interest or breaches of Environmental Quality Standards (EQS) are detected through the evaluation of water quality parameters measured numerous times per day. These personnel can then intercept serious pollution incidents or lead the response deemed to be appropriate.

Existing works in both academia and industry have already showed the power of such smart systems in terms of better environmental understanding, cost reduction, nature resource saving and improved city management. The city of Dubuque, Iowa, U.S., has used computer science technology to analysis the data collected from $22,000$ smart water meters. Based on the feedback provided by the system, users changed their behaviours, which resulted in water consumption decreasing by 6.6 % [19]. In addition, using the information provided by the Electric Consumption Feedback System, which analyses the data captured from 765 smart electric meters in Dubuque, householders reduced their electricity use by 3.7 % [20]. Such reductions lead to less CO_2 emissions and ecosystem damage, which have significant positive environmental impacts.

In Ireland, Dublin City Council (DCC) is already working with IBM on a smart city project analysing the use of transport within the city, which the council claims has already led to improved services for users. Insight, a research center at Dublin City University,

launched a smart gas project that monitored gas emissions at landfill sites using smart gas sensor [21]. The research findings showed that a smart sensor enabled monitoring system presents an effective tool that assists people in better understanding their domiciliary environments and as a result taking further actions or even changing hardware infrastructure to reduce their resource usage. In this work, we take the concept underpinning these works and adapt it to marine water quality monitoring domain.

1.3 Objectives and Research Hypotheses

The objective of this research is to design and investigate novel solutions to address the gap between current existing single modality *in-situ* water quality sensors and the future ideal of multi modality smart sensing networks for marine environmental monitoring. We aim to explore how state-of-the-art machine learning techniques can be used to automate the processing of raw sensing data from different modalities thus providing comprehensive information that is more suitable for management. Such information can potentially provide an improved operator view of the functioning of environments and hence improve decision making capability. As a result, the system can support scientists in better understanding and modelling the marine ecosystem and decision makers in constructing new policies to better protect environmental and coastal resources.

1.3.1 Hypotheses

In this research the following hypotheses are investigated:

- *Machine learning techniques can convert measuring devices to smart sensors that provide enhanced intelligence to improve marine water quality monitoring operation and support decision making.*
- *The use of camera enabled multimodality sensor networks can enhance the use of a single modality in-situ sensor to provide context information to assist scientists in*

better understanding the ecosystem.

1.3.2 Research Questions

In order to explore the above hypotheses, the following research questions need to be addressed:

1. *Can machine learning methods be used to automate the detection of abnormal events in the marine environment from in-situ sensing modalities?*

2. *Can machine learning techniques further group automatically detected abnormal events into catalogues based on their similarities to assist marine scientists in finding their causes?*

3. *What information can be extracted from a visual sensor to enhance the deployed wireless sensor network? Can this information be used to classify the abnormal events detected by in-situ sensors to assist the marine scientists in better understanding and modelling the ecosystem?*

4. *Can a multi-modal smart sensor framework combine various data sources to provide a broader picture of monitoring sites and to assist the operators in monitoring large scale marine environments more efficiently and effectively?*

1.4 Contribution

Inspired by the current smart sensing technologies in various domains, we adopt and adapt the concept of smart sensing to marine water quality monitoring applications. In this work, a multi-modal smart sensing framework, corresponding to visual support for *in-situ* sensors, for marine environmental monitoring is designed. State-of-the-art computer science technologies are investigated to automate the processing of data generated by both sensing modalities to provide novel information. This work provides a complete framework for unusual event detection and categorisation in a marine environment,

which can potentially assist marine scientists to better understand, manage and protect the ecosystem. The investigation results are promising and provide a number of avenues for further research.

1.5 Thesis Outline

Chapter 1: In this chapter, the need for high spatial and temporal monitoring of a marine environment is identified from both economical and ecosystem well being perspectives. Current smart sensing technologies applied in various domains have been discussed, which provides the inspiration for this research. The objectives, hypotheses and research questions are introduced in this section.

Chapter 2: This chapter provides an overview of the key concepts from the literature in relation to marine environmental monitoring. Existing marine environmental monitoring applications are reviewed and the key features of these systems are discussed. This chapter also provides a general introduction to data processing and machine learning techniques applicable to the targeted application domain.

Chapter 3: In order to address the proposed hypotheses, a multi-modal smart sensing framework is designed. The framework provides a high level infrastructure for a cloud based, large scale marine sensing system regardless of the number of sensors or sensing modalities deployed or the number of observing sites. New sensor(s) or site(s) can be seamlessly plugged into this framework to create a truly dynamic modular system.

Chapter 4: The test site, Dublin Bay, and the technologies deployed along with the issues are described in this chapter.

Chapter 5: This chapter shows a case study of the *in-situ* data processing. Anomalies are first isolated from *in-situ* sensor measurements then grouped into events. Abnormal events are further catalogued into sub-classes based on their similarities. The experiments carried out in this section address the first two research questions, which validates hypothesis 1.

Chapter 6: A second case study is carried out to illustrate the benefits of visual data

processing. The first part of this chapter investigates the development and evaluation of a shipping traffic model. The outcome can subsequently be used to evaluate some of the abnormal events detected from the *in-situ* data processing stream, which demonstrates the benefit of coupling multiple sensing modalities. This chapter relates to research questions 3 and 4 and validates hypothesis 2.

Chapter 7 The outcomes of this research are summarised in this chapter along with the overall conclusions in relation to the research hypotheses. Possible future research directions are also suggested.

CHAPTER 2

LITERATURE REVIEW

2.1 Introduction

In this chapter, an overview of some key concepts from the literature in relation to environmental monitoring is provided. It starts with an introduction of the concept of autonomous wireless sensor networks (WSNs), which provide the fundamental physical infrastructure for environmental monitoring systems. WSN is a key factor to long-duration and large-scale environmental monitoring and is the essential component of smart monitoring systems. The design, such as choosing the network topology and data communication method, is the first important step of establishing a marine environmental monitoring system. Progress of WSNs is highlighted along with the challenges still to be addressed. Visual sensing as an alternative sensing modality for marine environmental monitoring is also introduced. Data processing techniques, such as anomaly detection and unusual event detection, are discussed, which introduces intelligence to WSN systems. To conclude, an overview of current existing marine monitoring systems is provided in this chapter.

2.2 Wireless Sensor Networks

Wireless Sensor Networks (WSNs) have gained significant attention in recent years, particularly with the concept of the Internet of Things (IoT) [22, 23] and Smart Planet [24, 25]. A WSN typically consists of a number of sensor nodes (a few to thousands) working together to monitor a region to obtain data about the environment [26]. These sensor nodes are often small and inexpensive compared to traditional sensors but with limited processing resources. In the context of this thesis, a sensor node resident in a WSN means a device that measures one or multiple physical conditions, for example turbidity, salinity and temperature levels. A sensor node may also contain a power unit, a control unit, on board storage and a data transmission component. The power unit provides the energy source and the control unit controls the processes of data collection and transmission. The data transmission unit is used to synchronize the signals between a node to other nodes or a so-called sink node[1]. It allows the exchange of data remotely without the need to travel to the observation site, which is useful when the sensor unit is deployed at a restricted area or a location that is not easily accessed, such as deep underwater. Wireless Sensor Networks provide the fundamental components of a new generation of developments that involve observation, understanding and controlling of the physical world.

The advancements in WSNs have resulted in the development of low-cost, low-power, diminutive and multifunctional devices that consist of sensing, data processing and transmitting components [26]. These low-cost smart units have been successfully employed in many exciting application domains, such as surveillance, environment, sports, health, automobile industry etc., and are key components in applications, such as smart bay, smart home, smart transport, smart product etc. Sensor networks essentially provide a gateway through which the digital world can sense and respond to changes in the real world [27]. Both Cisco and Ericsson, the world leading communication technology providers, predict that 50 billion "things" will be connected to the Internet by the year 2020, all sensing, controlling or providing information about the physical world. WSNs also offer new so-

[1] In WSNs, a sink node is the unit that establishes and maintains a communication channel between a WSN deployed at the site and a base station for data exchange.

lutions for monitoring marine ecosystems in real time. Figure 2.1 (Source: [17], Sensor, Volume 10, Issue 7, page 6952, with modification) shows a general structure of a WSN for oceanographic monitoring. Two network topologies, star (point to point) and mesh (multi-hop), are illustrated.

Generally, devices in a WSN are catalogued in three types, corresponding to sensor node (treetop), router node (branch) and sink node (trunk). A sensor node may consist of sensing probes that measure the physical parameters of a body of water; an analogue to digital converter that digitalizes readings; a wireless transceiver module that sends or receives data; a power supply module and a micro-controller that controls the whole process. A router node connects to multiple sensor nodes and other router nodes or sink nodes depending on the topology applied. The role of router node is to establish and maintain a data communication channel between sensor node and sink node. The role of a sink node is to communicate with the base station through various data communication approaches.

Generally, when developing and deploying a WSN, two aspects need to be emphasised: the topology of the network and the data transmission method.

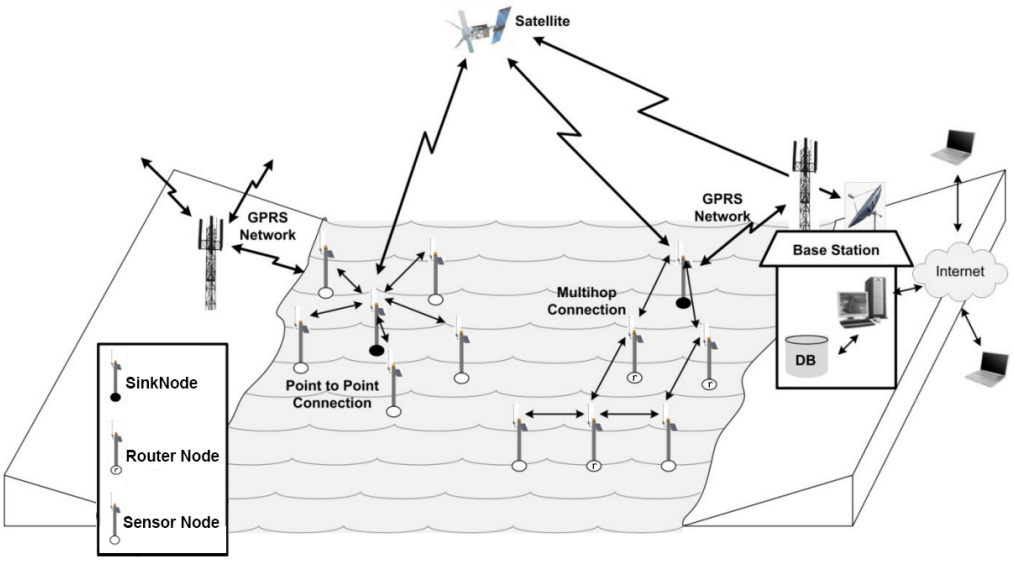

Figure 2.1: General structure of a WSN for oceanographic monitoring.
Source: Sensor, Volume 10, Issue 7, page 6952 (with modification)

2.2.1 Topologies

Many network topologies exist in WSNs. The choice of network architecture for a WSN is entirely dependent on the application [28]. It depends on the amount and frequency of data that needs to be transmitted, energy usage, data transmission distance, mobility of the sensor node, etc [29]. However, the most commonly used topologies in marine environmental monitoring systems are star, tree and mesh (shown in Figure 2.2, Source: [30], Sensor, Volume 14, Issue 9, page 16938).

In star topology, all sensor nodes in the network are connected to the sink node directly. All data passes through the sink node before reaching the base station. The advantages of star topology are easy configuration, low power consumption and network latency. Sensor node(s) can be easily connected or removed without disrupting the network. Fault detection is also much simpler in a star topology. Since the sensor node communicates with the sink node directly, the network latency is smaller. The disadvantage of this topology is that there is only one communication channel between sensor node and sink node. If this channel fails, the sensor node is disabled in the network. In addition, there is too much dependency on the sink node, if it fails the entire WSN goes down. Also, the maximum number of nodes in the network depends on the capacity of the sink node.

In a mesh topology, sensor nodes communicate with router nodes, which connect to other router nodes and finally the sink node, instead of communicating with the sink node directly. The benefit of mesh topology is it can cover a longer range and provides a fault tolerance to increase network reliability and the size of the sensor network can be easily scaled. However, the power consumption is much higher compared with star architecture and network traffic latency exists. It is also more complicated to maintain a mesh network and sophisticated routing protocols are required to avoid network traffic collision.

The tree (sometimes referred to as cluster) topology is a hybrid star-mesh architecture, which takes the advantage of low energy usage from star architecture as well as the extended range and fault tolerance of mesh topology [30].

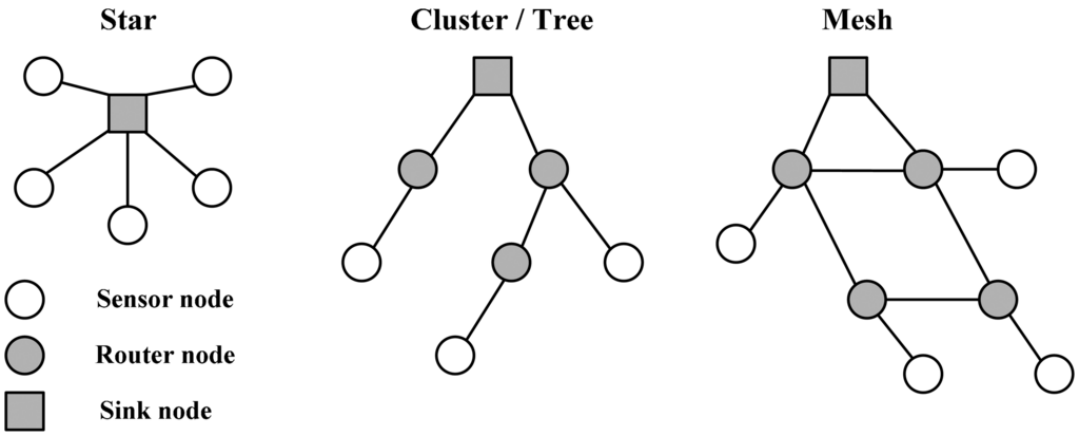

Figure 2.2: General WSN topologies in marine environmental monitoring systems. Source: Sensor, Volume 14, Issue 9, page 16938

2.2.2 Data Communication

In order to communicate to the base station, sensor nodes in a WSN incorporate a radio module. Various data transmission technologies exist. The optimal data transmission method for a WSN is task dependent, normally based on three main factors: bandwidth, distance and power consumption. However, the underlying protocols, such as Hypertext Transfer Protocol (HTTP) or Transmission Control Protocol and the Internet Protocol (TCP/IP), are typically not considered by operators when deploying WSNs. Some commonly used wireless data transfer technologies are listed below and discussed in terms of these factors.

- *WiMax*: Worldwide Interoperability for Microwave Access is a wide range wireless communications standard [31] designed to provide high speed connection over long distance. It can reach 10 Mbps at 10 km with line-of-site (optical visibility). However, it is a power intensive technology and requires significant electrical support. In addition, the installation and operational costs are very high. Weather conditions, such as rain, could also affect the signal.

- *Wi-Fi*: It is defined as any Wireless Local Area Network (WLAN) that is based on *IEEE 802.11* standards [32]. *Wi-Fi* is an ad-hoc network, where devices equipped with a wireless network interface controller connect to a hotspot and the data is transferred to the Internet or other devices on the local network. *Wi-Fi* is cheap to

deploy and maintain. There is no mobile carrier cost if there is a Wi-Fi or Ethernet connection available on site. Depending on the standards that the devices support, the data communication speed can reach 300 Mpbs up to 100 meters. The disadvantage of a *Wi-Fi* enabled sensor is that it consumes relatively high power compared to other technologies, such as Bluetooth and NFC.

- *Mobile Network*: In the past decade, mobile network operators have started providing fast mobile broadband connection services, over 3G and 4G technologies, along with existing voice and text services based on GSM (Global System for Mobile Communications) and GPRS (General Packet Radio Service) technologies. The main advantages of mobile broadband are speed, coverage and cost. The throughput of mobile broadband connection is between a few hundred kilobits and tens of megabits per second. According to the Ericsson Mobility Report 2012 [33], more than 85 % of the world's population is expected to have 3G coverage by 2017. In Ireland, almost all areas in the country are covered by cellular carriers and broadband contracts are as cheap as €10 per month. However, mobile broadband has a few limitations. The power requirement is high. A USB 3G dongle may consume a few watts when transmitting data. Also, the connection is less reliable compared to others. Mobile network technology is also commonly used in WSNs for data transmission. Many sensors have a GSM module and can send data to another GSM enabled device or an on-line data portal for further processing. GSM has great coverage throughout the world and the cost of purchase, deployment, maintenance and operation is low. The greatest disadvantage of GSM is the bandwidth. It is not suitable for large amounts of data such as image data. Also, if a WSN contains hundreds of nodes, the cost of sending sensor readings is considerable.

- *Bluetooth*: It is designed for exchanging data over short distances for fixed and mobile devices. The new Bluetooth 4.0 includes Classic Bluetooth, Bluetooth high speed and Bluetooth Low Energy (Bluetooth LE, BLE, marketed as Bluetooth Smart). Bluetooth Low Energy [34], the key new feature, is aimed at very low power applications running off small cell batteries while still providing long range

and high speed functionality. The power consumption is between 0.01 to 0.5 Watt depending on use case and it allows 0.27 Mbps throughput and can cover up to 100 meters. Bluetooth is commonly used for inner WSNs communication, where one sensor node exchanges data with another or other nodes.

- *ZigBee*: Similar to Bluetooth, it is designed for low power communication over short distances. ZigBee is typically used in low data rate applications that require long battery life. Data rates vary from 20 kbit/s to 250 kbit/s and the range is between 10 to 100 meters. The high power version can reach up to 1500 meters however, the power consumption is 60 times (60 mW) higher than the standard version (1 mW). The cost of deploying and maintaining a ZigBee network is relatively low. However, like Bluetooth, Zigbee is commonly used for inner node data transmission. Data communication between site and base stations may still require other types of technologies.

- *NFC*: Near Field Communication (ISO/IEC 14443 and ISO/IEC 18000-3), is a form of contactless communication between devices. There are three modes in NFC: NFC target (acting like a credential), NFC initiator (as a reader) and NFC peer-to-peer. The main advantages of NFC are it consumes very little power and does not need to pair like Bluetooth, which allows connection to be quickly established (less than 1 second). NFC is a relatively new technology and has not been tested in a marine monitoring system. It may be very useful for on-site data collection, where a handheld device (reader) can download data from sensor nodes (credentials) within a close range. Since the NFC target consumes very little power, it can significantly improve sensor lifetime. However, due to its low power, the transmission distance is limited (approx. 10 cm).

2.2.3 Issues with WSNs

Sensor networks represent a significant improvement when compared to traditional sensors. However, this brings new challenges. Deployment of a large scale sensor network in

an environment is generally limited in numbers due to issues related to cost, power, maintenance and data transmission capabilities, especially in an aquatic environment [35]. Current deployments of these devices are still relatively small.

Sensing devices are also prone to data faults and node failure. Xu et al. [36] listed factors that may lead to the failure of WSN, such as hardware or software malfunction, radio interference, battery depletion or malicious damage. In addition to this, "data fault" is another recessive failure [37]. Although the sensor is "functioning", it provides inaccurate information that can lead to incorrect conclusions at the application layer. Previous research has shown this to be a major issue that still requires further analysis [37].

In addition, sensor networks in marine environments pose unique challenges. Devices, especially sensing probes, are subject to harsh conditions, which in turn requires greater levels of protection [27]. Energy consumption is generally much higher in marine environments since WSNs often need to cover large distances and require attenuated data transmission channels. Mains power sources may not be available for offshore nodes, hence energy needs to be harvested on site. Movements of water surface, such as waves, can cause damage due to friction, such as cable or chain cut. Allowance must be made for movement of sensor nodes. The cost of installation and maintenance of sensors in marine environments is much higher than a land-based system [17]. Bio-fouling, the growth of nuisance or unwanted biofilms on the surface of probes, is one of the major issues in aquatic monitoring, limiting sensor deployment periods. Developing anti-fouling materials for sensors in coastal or inland aquatic environments is still an active field of research [9]. Although the cost of sensing instruments are dropping [35], deploying and maintaining such sensing systems are still at a high cost. Chemo-Bio based sensors can only store a limited amount of reagent and generally consume much more power [35]. Thus, only a fixed amount of sampling can be performed before maintenance is required.

At application level, raw sensor data generally provides a lack of high level information that can be easily understood and managed. Hence, techniques for increasing efficiency and effectiveness of deployed instruments and the adoption of alternative sensing modalities such as visual sensors, as investigated in this thesis, are worth exploring.

2.2.4 The Future of WSNs

Current research works in WSNs are not limited to a single domain. The development of new and reliable physical/chemical sensors, new anti-fouling solutions is still ongoing. However, in recent years it has been realised that existing WSNs can be significantly enhanced by introducing alternative sensing modalities [27].

Visual sensing, sensing from camera or satellite-based imaging instruments, has been proposed as an alternative sensing modality in a variety of contexts in the literature. A number of initiative research projects [38, 39, 40] have illustrated that visual sensing represents a very valuable sensing modality for complementing the use of *in-situ* sensor networks. It provides visual evidence that can be used to validate *in-situ* measurements or context information that can be used to control WSNs. For example, operators can query image data during the period of an event, which is detected by an *in-situ* sensor and examine whether the event is caused by local activities. In addition, activities detected by visual sensors can be used to trigger *in-situ* sensor measuring or increase their sampling rate (adaptive sampling) to increase *in-situ* sensor efficiency.

The rapid growth of social media, such as Facebook[2], Twitter[3], Flickr[4], Google+[5], Tumblr[6] etc., with billions of registered users, million of images and zillions of messages shared daily, establishes a new form of WSNs. In contrast to traditional WSNs, the social media constructs a "virtual wireless sensor network". Users on social media act as "sensor nodes" and the images and messages that they share are "sensor measurements". However, unlike traditional WSNs, these sensor measurements are highly heterogeneous and very unreliable. Many projects have already started to investigate how social media data can be used for some types of monitoring [41, 42]. Moreover, social media has played a great part in response to environment significance. During the earthquake in Haiti, social media users were used as a base for volunteers by Ushahidi, a piece of soft-

[2]https://www.facebook.com
[3]https://twitter.com/
[4]https://flickr.com
[5]http://plus.google.com
[6]http://www.tumblr.com

ware that allows digital volunteers to create maps for first responders in a disaster zone [43]. In [44], Starbird et al. analysed the use of Twitter, an on-line social media service that allows users to send and read short messages called "tweets", during the Red River Valley flooding event in America and Canada in March and April 2009. They concluded that social media activities can be connected to environmental threats.

It has also been realized that the introduction of intelligence into the sensor networks by adopting state-of-the-art computer science technologies, particularly from the machine learning domain, can significantly enhance existing WSNs. In [27], O'Connor applied a trust and reputation system to WSNs. The system identifies unreliable sensor nodes and removes them from the network to maintain the overall system reliability. Diamond et al. [35] notes that less reliable but more abundantly low cost sensors can be used as indicators to modify the operating characteristics of more sophisticated nodes. Information retrieved from relatively dumb sensors can be used to trigger the delicate nodes. These sophisticated sensors can subsequently confirm or dispute the information coming from the less reliable sensors. This can shorten the duty cycle of the more delicate sensors, which reduces the energy required and their overall efficiency and increases their lifetime in the field, while maintaining high resolution sensing. Intelligence on chip can also reduce communication costs. Data pre-processing, such as anomaly detection, can be performed locally and only unusual measurements are sent back to the operation centre. This can significantly reduce the energy consumption since data transmission, especially over long distance, consumes the majority of energy in WSNs [45].

Information integration is not a new topic and has existed in many forms in various research areas [46, 47, 48]. Information integration, in the context of environmental monitoring, involves combining data from sensors, either heterogeneous or homogeneous, in order to provide a more complete, a more accurate overall picture of the underlying ecology which is being sensed [49]. Research works in [49, 50, 51] demonstrated the potential usefulness of such an integration system. In this thesis, the focus is to investigate what is possible with a single such multi-modal system in the context of long term marine environmental monitoring. Due to the high cost and the limitation of the test sites currently

available, multiple deployments of many such systems into a WSN is the subject of future work.

2.3 Marine Water Quality Monitoring Systems

During the past decade, many marine environment monitoring systems have been developed and deployed. In this section, a comprehensive review of related projects, systems and techniques in the literature on marine environment monitoring based on wireless sensor networks is presented.

O'Connor et al. [52] proposed a multi-modal event monitoring system based on WSNs and visual images for event detection at rivers and estuaries. They investigated the use of a multi-modal sensor network where visual sensors, such as cameras, along with context information can be used to complement and enhance the usefulness of a traditional *in-situ* sensor network in measuring and tracking some features of a river or coastal location. A study has also been conducted in [52] to illustrate how context information can be extracted from images and further used to evaluate *in-situ* sensor measurements.

Khan et al. [53] proposed a decentralized ad-hoc wireless sensor network for ocean pollution detection. To extend the network deployment duration and to improve its quality of service, they focused on the deployment of sensors, protocol stacks, synchronization and routing algorithms.

In [54], Perez et al. presented a small scale WSN based monitoring system for a coastal shallow water body. The system was tested in a real environment in the Mar Menor coastal lagoon, situated in the South-East of Spain. Two solar panels were equipped for energy harvesting on site. A data portal was developed using LabVIEW (Laboratory Virtual Instrumentation Engineering Workbench) prototype software package. Inner network communication (between nodes) was implemented using ZigBee, and GPRS was used for communicating with a base station. The project focused on the design and testing of the hardware infrastructure for general oceanographic observation purposes, where

no sophisticated data processing was presented.

Alkandari et al. [55] showed a case study of monitoring water characteristics, such as temperature, pH, dissolved oxygen, etc., at sea surface. An architecture of a WSN along with a data acquisition, transmission and visualization platform was introduced. A web portal, which allows operators to access sensor readings via Internet was also provided. SquidBee (Adruino and XBee based open hardware device) was used as the sensing nodes and ZigBee data transfer protocol was applied for data communication between sensing nodes and cluster head node (sink node). The cluster head node has Wi-Fi capability, which sends data to a server. The system was tested in the laboratory and planned to be deployed at Kuwait Gulf. High level data processing was not presented in this work.

Regan et al. [56] described the development and testing of a multi-sensor heterogenous real-time water monitoring system that measured water quality parameters, such as pH, temperature, conductivity, turbidity and dissolved oxygen. The features that are required for such monitoring systems were introduced. The challenges of design, development, maintaining water quality monitoring systems in real word environment were listed and the possible solutions were discussed in this work. The system was deployed at five sites on the River Lee, Ireland. A ZigBee data transmission system was developed to enable data acquisition and dissemination at the site. Trend analysis was carried out in this work.

In [57], Cesare et al. designed and deployed a WSN-based seawater luminosity, temperature and moisture monitoring system. It has been deployed with success at Moreton Bay, Brisbane, Australia, to monitor the water conditions of a segment of the Australian Coral Reef. Data transmission followed the ZigBee protocol. ZigBee standard was used for data communication between node and gateway and ZigBee high power was used for information exchange between gateway and base station. A graphical user interface was developed for data browsing.

In addition to the research works discussed above there are many other WSNs based marine monitoring systems outlined in the literature [58, 59, 60, 61]. However, the majority of these research works focus on the design and the development of hardware infrastruc-

ture and data communication protocols, which demonstrate the lack of data processing at a higher level. Very little work has been done to bring intelligence into WSNs and to automate data processing to convert raw data into information that is easier to interpret and understand. WSN developers are usually not, or not completely aware, of the potential that computer science technologies can offer. On the other hand, computer science researchers are not familiar with all the real problems and subtle requirements of WSN systems [62]. For this reason, in this research, the focus is to bring these two fields together. Specifically, applying the state-of-the-art machine learning and image processing techniques to automate the processes of raw sensor data from multiple sensing modalities to create a rich content based information repository that is more suitable for management.

2.4 Anomaly Detection

In order to detect and catalogue events in aquatic environments, anomalous sensor measurements need to be isolated from the input data stream. To achieve this, an anomaly detection technique is generally applied. *Anomaly detection* refers to the problem of finding values in sensor readings that do not conform to expected behaviour. These non-conforming values are often referred to as anomalies, outliers, discordant observations, or exceptions depending upon the application domain [63]. Anomaly detection is an important problem that has been studied within diverse research areas and application domains [64, 65]. Many anomaly detection techniques have been developed over time. In [63], Chandola et al. listed a number of challenges to be faced when developing an anomaly detection method:

- Defining a normal region that encompasses every possible normal behaviour is very difficult.
- Normal behaviour keeps evolving and a current notion of normal might not be sufficiently representative in the future.
- The exact notion of anomaly is different for different application domains.

- Availability of labelled data for training/validation of models used by anomaly detection techniques is usually a major issue.

Due to these facts, most of the existing anomaly detection techniques solve a specific formulation of the problem. Some of the popular techniques are density based [66, 67, 68], machine learning and data mining based [69, 70, 71, 72, 73, 74].

Anomalies can be classified as point anomalies, where an individual data instance is significant from the rest of the data; contextual anomalies, where a data instance is anomalous in a specific context, but not otherwise; collective anomalies, where individual instance is normal but a collection of related data instances is anomalous with respect to the entire dataset [75]. All the above types of anomalies exist in marine monitoring systems. For example, an excessive turbidity measurement may be caused by blockage of the sensor probe, a high temperature reading is normal in summer time but is abnormal during the winter period and tide levels may not follow the sine wave pattern as expected.

To develop an anomaly detection algorithm and the subsequent evaluation protocol, a set of labelled (sometimes referred to as annotated or ground truth dataset) data is generally required. In other research domains, such as image processing, many organizations provide public annotated datasets that can be used to develop, evaluate and compare different methods proposed by researchers. However, obtaining such a dataset that is accurate as well as representative of all types of behaviours is often difficult and expensive, and not yet available in marine environmental monitoring research domains.

Machine learning and data mining based anomaly detection methods can be categorised into three modes: supervised, semi-supervised and unsupervised. Supervised detection methods require labelled training data to build a model, and then can be used to classify a new given instance. However, these methods are not commonly used due to a number of issues. Firstly, the number of anomalous instances are far less than normal instances, which will introduce an imbalanced class distribution. This issue has been addressed in the data mining and machine learning literature [76, 77]. New methods are still being developed to solve this issue [78, 79, 80]. Secondly, supervised learning methods tend to

work well on the data that have been seen but may perform poorly on unobserved data as supervised learning requires more accurate and representative training data that ideally describes all scenarios. However, in real marine environments, gathering such a training dataset is prohibitive. For example, a natural disaster event may only happen once over many years. In addition, building a model requires a set of training data, which means it cannot perform the detection task until the training phase is completed. Semi-supervised detection is a situation in which the training data of some of the samples are labelled. Semi-supervised methods are able to make use of unlabelled data to better capture the nature of the underlying data distribution and generalize better to new instances. This method also operates when only normal data is available, which can be used to build a normal model. A limited set of anomaly detection techniques exists that assume only anomaly samples are available for training [81, 82, 83]. These methods are not commonly used as it is difficult to obtain a training data set that covers all possible anomalous scenarios. Unsupervised anomaly detection techniques detect anomalies in an unlabelled test data set under the assumption that the majority of the instances in the data set are normal and proceed by looking for instances that seem to fit least to the remainder of the data set. Such techniques typically suffer from high false alarm rate [84]. Anomaly detection is the first step of the detection of unusual events, which consist of a single or a collection of anomalies.

2.5 Unusual Event Detection and Clustering in WSNs

Unusual event detection is a key component for many WSN applications [85, 86]. An unusual event can be defined as a collection of a single or multiple consecutive anomalies in the environmental parameters. It is one of the most important tasks in WSN applications because it is an efficient way for mining meaningful information out of huge volumes of sensor data [86].

The prevailing approach is to use a single or combined multi-threshold primitives also known as SQL-like semantics [85, 87, 88, 89]. For example, select all anomalous events

with temperature value greater than 30 °C and/or salinity level lower than 20 NTU. However, this simple threshold solution may not be always suitable especially in a dynamic environment, where the ambient conditions are constantly changing. Defining and maintaining suitable thresholds in a dynamic environment is very difficult. Complex events with spatio-temporal variety in the environment can typically not be captured by a simple cut-off method [90]. There is also no clear border between normal and unusual data instances. In some applications, unusual event patterns are predefined by field experts, who have made thorough analyses of historical data in an off-line fashion. This manual process is labour intensive and in many areas such domain knowledge is limited [86]. Furthermore, unusual events may be of different varieties. For example, a wind storm is an abnormal event in the context of marine environment while a heavy rainfall is also an unusual event but these two events have very different characteristics. A solution to these issues is to learn these event patterns through a training process, known as machine learning. In 1959, Arthur Samuel defined machine learning as a "Field of study that gives computers the ability to learn without being explicitly programmed" [91]. Tom M. Mitchell provided a widely quoted, more formal definition: "A computer program is said to learn from experience *E* with respect to some class of tasks *T* and performance measure *P*, if its performance at tasks in *T*, as measured by *P*, improves with experience *E*" [92]. Machine learning, a sub-field of artificial intelligence (AI), is the design and development of algorithms that take in empirical data, such as sensor readings, and make informed decisions. Algorithms can take the advantage of examples (training data) and capture patterns of interests and predict properties of unknown data. Machine learning has been widely used in the fields of natural language processing, computer vision, information retrieval, object recognition, pattern recognition etc. Machine learning algorithms can be organized into the following categories: supervised learning, unsupervised learning and reinforcement learning.

- Supervised learning is the machine learning task, which creates a function from a training data set with ground truth. Each data entry in the data set is a pair consisting of a set of values (called feature vector) that represent some object and a

desired output value. In some cases, more than one features are extracted from an object and they are grouped together to represent the object. For convenience, these features are called low level features and the grouped feature set is refereed as descriptor. A supervised learning algorithm analyses this data set and produces an inferred function, which is called a classifier, to be able to predict the correct output label for new valid instances that may not yet have been seen. Supervised learning is often referred as concept learning in human and animal psychology research domains. Classification, an instance of supervised learning, is to solve the problem of identifying the sub-class to which a new instance belongs. An example of a classification problem would be the vehicle classification, in which the aim is to assign each input vector (e.g. size, weight) to one of the finite number of discrete categories (e.g. car, van, bus or truck). Regression analysis, another instance of supervised learning, is to estimate the relationship between a dependent variable and one or more independent variables. An example of a regression problem would be the prediction of water level as a function of visual features such as the appearance of a rock or the position of a floating dock within an image.

- In unsupervised learning, the training data consists of a set of raw input vectors without any corresponding target values. The system tries to learn the hidden structure within the data set. The goal of unsupervised learning may be to discover groups of similar examples within the data, known as clustering, or to determine the distribution of data within the input space, called density estimation, or to project the data from a high-dimensional space down to low-dimensions for the purpose of data visualization or reducing the amount of data to be further processed. Since the examples given to the learner are unlabelled, there is no error or reward signal to evaluate a potential solution.

- In reinforcement learning, an algorithm is responsible for making decisions, and it periodically receives some sort of award or utility for its actions. Reinforcement learning is learning by interacting with an environment [93]. It is defined not by characterizing learning methods, but by characterizing a learning problem. A good

example of reinforcement learning is a robot navigation system. A negative penalty will be given if its collision sensor detects that the robot has hit an object. Eventually the robot will correlate the range finder sensor data with the collision sensor data and the directions that it sends to the wheels. This will finally make the navigation decisions that result in the robot not bumping into barriers.

2.6 Evaluating Classification Results

There are many approaches that can be used to measure performance of a classifier, from more generally used Precision and Recall, to more considered metrics that suit certain experimental use cases [94, 95, 96]. When evaluating the performance of a classifier, there are four basic outputs: true positives (TP), true negatives (TN), false positives (FP), and false negatives (FN). These outputs are normally arranged into 2 x 2 contingency table, referred as a confusion matrix, with columns corresponding to actual value and rows corresponding to classification value as shown in Table 2.1.

	classification value	
actual value	TP	FN
	FP	TN

Table 2.1: Confusion matrix table.

Precision is the fraction of retrieved instances that are relevant, while *recall* is the fraction of relevant instances that are retrieved. Both precision and recall are based on an understanding and measure of relevance. The precision and recall values can be calculated as follows:

$$precision = \frac{TP}{TP + FP} \tag{2.1}$$

$$recall = \frac{TP}{TP + FN} \tag{2.2}$$

The *F-score* is a measure of a test's accuracy, which considers both precision and recall

of the test to compute a single accuracy measure [97]. *F-score* can be interpreted as a weighted average of precision and recall. The most commonly used F-score is the balanced F-score referred as *F1-score*, which is the harmonic mean of precision and recall. The *F1-score* reaches its best value at 1 and worst score at 0:

$$F_1 = 2 \cdot \frac{\text{precision} \cdot \text{recall}}{\text{precision} + \text{recall}}. \tag{2.3}$$

Another commonly used performance metric for classification algorithms is the Receiver Operating Characteristic (ROC), where the true positive rate is plotted against the false positive rate at varied classification threshold settings. This performance metric has been widely used in anomaly detection and abnormal event detection applications [98, 99, 100]. In ROC space, the lower left point represents the strategy of never alarming, the upper right point represents the strategy of always alarming, the upper left point represents perfect classification, and the diagonal line (bottom left to upper right) represents the strategy of randomly guessing the class. Informally, one point in ROC space is better than another if it is to the upper left (TP is higher, FP is lower, or both). ROC analysis provides tools to illustrate the behaviour of a classifier without regard to class distribution or error cost, and so decouples classification performance from these factors [101]. It is also common to calculate the area under the ROC curve (AUC), which is the line that connects the set of points of the corresponding classifier in ROC space, for model comparison. The larger area the curve covers indicates a better classification performance.

2.7 Summary

In this chapter, an overview of the key concepts from the literature in relation to marine environmental monitoring is provided. The current and future progress of sensor networks are discussed. As outlined in [16], the basic hardware infrastructure is now in place for long term marine environment monitoring. Although there is ongoing research and development in the areas relating to both sensor and wireless data transmission technolo-

gies, there is a clear need to investigate innovative methods to manage these monitoring systems effectively and efficiently. Anomaly detection, the first element of introducing intelligence to WSNs is highlighted in this chapter followed by the discussion of unusual event detection and clustering in WSNs. Standard classification performance evaluation methods, which are used to evaluate the experimental result in this thesis, are also introduced.

CHAPTER 3

A FRAMEWORK FOR A MULTI-MODAL SMART SENSING SYSTEM

3.1 Introduction

In order to investigate the proposed hypotheses in Section 1.3.1, a multi-modal smart sensor network framework must be designed. Figure 3.1 illustrates the proposed structure of the system. This framework is architected in a flexible manner that can be deployed in a computing cloud. A computing cloud is a model for enabling ubiquitous, convenient, on-demand network access to a shared pool of configurable computing resources (e.g. networks, servers, storage, applications, and services) that can be rapidly provisioned and released with minimal management effort or service provider interaction [102]. Deploying the designed multi-modal smart sensing system in a cloud has a number of benefits. In a real deployment, the amount of information available will grow quickly over time. As the volume of the data grows, the computational and storing resources that are required to process and store this data increases. Cloud computing offers an attractive solution that such resources can be located on-demand with minimal modification and costs. Whilst the cloud-based repository presents an attractive proposition from a storage perspective, this information is only useful if it can be easily accessed after the fact.

The framework consists of three layers corresponding to data collection, data processing and information layers. The data collection layer takes input from multiple resources at various observation sites and provides formulated data segments to the data processing layer. The data processing layer acquires these formulated data segments from the data repository (resident in the data collection layer), detects and catalogues real world events, which may be interesting depending on user requirements. The information layer provides an interactive graphical user interface (GUI) that allows end user queries in the sensor network, via the cloud, to support a rich set of queries. High level content-based knowledge is provided at this layer, which can be easily understood and accessed by the end user.

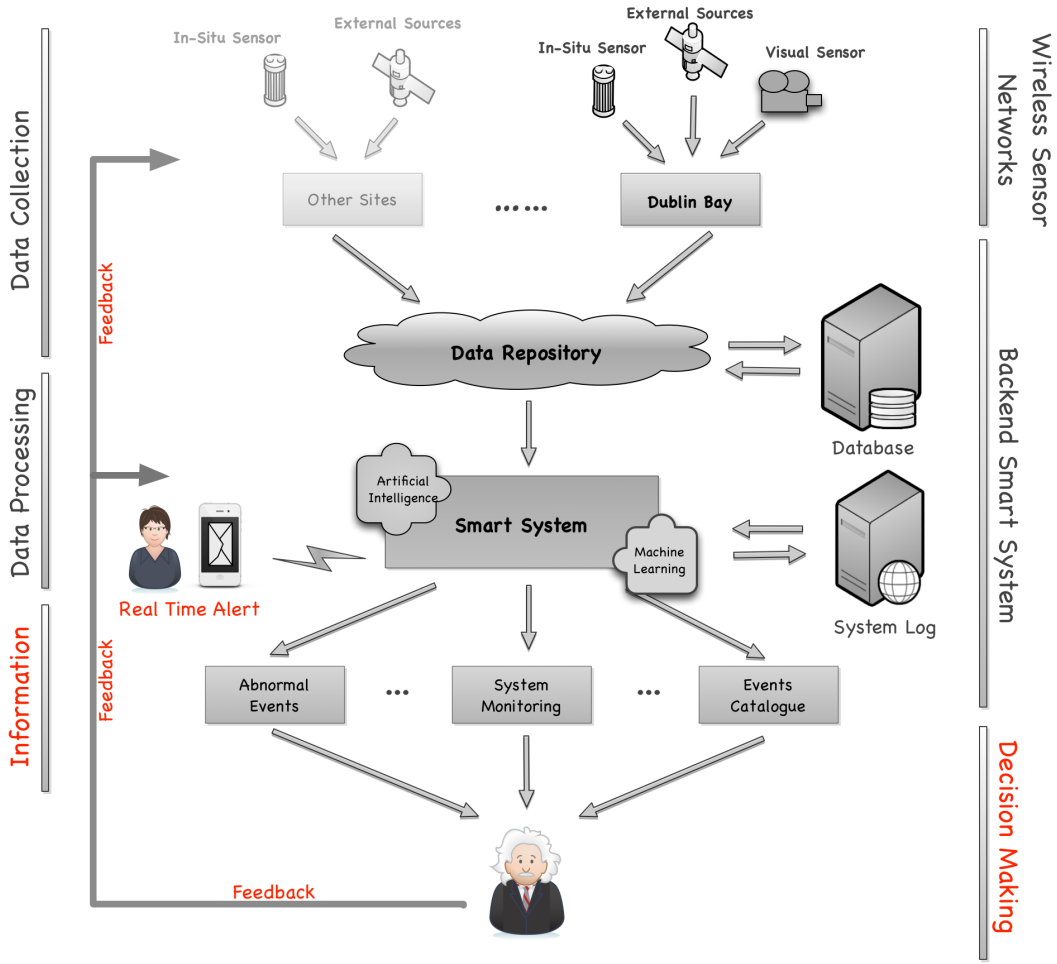

Figure 3.1: A schematic outlining the architecture of the proposed multi-modal smart monitoring system, including treatment of the data and the feedback mechanisms for decision-making.

3.2 Data Collection Layer

The data collection layer is the middle tier that sits between deployment sites and back-end system, rendering the sites and various sensing modalities transparent to the data process. This virtual data aggregation system, as shown in Figure 3.2, allows the number of observing sites and the number of sensors equipped at each site to expand dynamically. The designed architecture of the data collection layer is flexible and extendible allowing other sites and data sources to be added without overly increasing complexity.

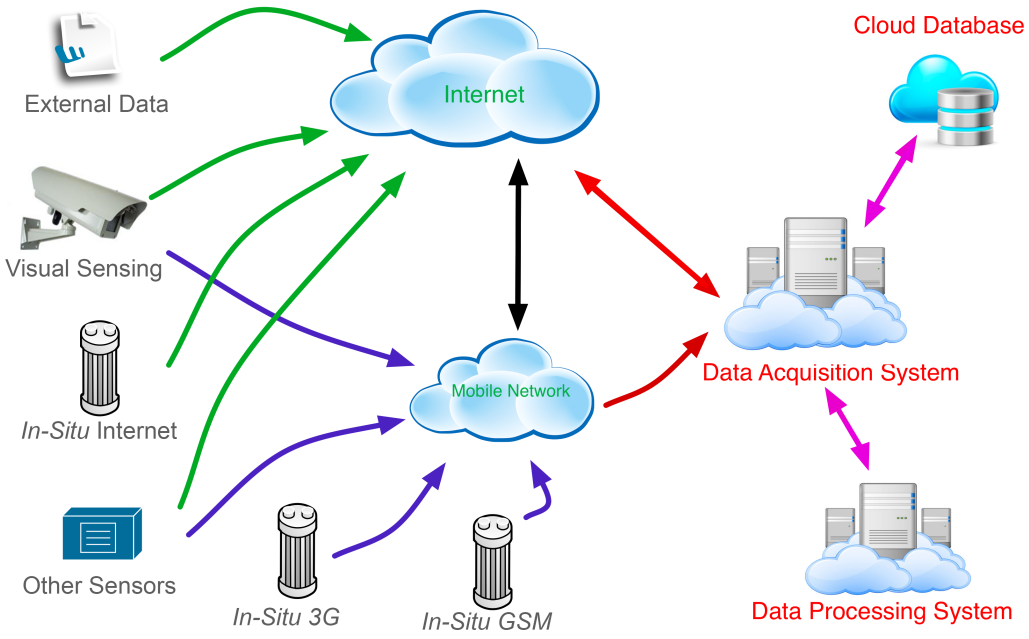

Figure 3.2: Block diagram of the data collection system. Data acquisition system extracts data from various sensors through different communication methods and stores data to a centralized repository. The system also provides formatted data segments to the back-end data processing system. All the data acquisition, storage and processing systems can be deployed on a computing cloud, which can be expanded on-demand.

The data collection layer takes inputs from multiple resources at various observation sites, e.g. multi-parameter *in-situ* sensors (*in-situ* Internet, *in-situ* 3G, *in-situ* GSM), visual sensors, external data sources (meteorological data for instance) and save them to a centralized data repository (e.g. a cloud data centre). Each sensor modality may have its own data and communication format. For instance, an *in-situ* sensor sends plain text measurements to the server via GSM network. In contrast, an image sensor sends a sequence of images to a data centre through the 3G mobile internet connection. Furthermore, exter-

nal resources, such as rain gauge data and tidal information, which are relevant to water quality parameters may all have different data formats. The data collection layer provides a Universal Serial Bus (USB) like interface. Once the data format and the data communication method of a sensor modality are defined, it can simply be plugged into the data aggregation system. Ideally, the multi-modal sensing system would integrate as many sensing modalities as possible and fuse all data into a centralised location to be processed. Access to such data sources can potentially provide much greater understanding of environment than any one modality along [51, 52].

3.3 Data Processing Layer

The smart system, resident in the data processing layer, pulls a set of formulated data segments from the data repository and then processes it using the state-of-the-art machine learning techniques to convert raw sensor measurements into organized knowledge that can be easily understood and accessed by end users. Various machine learning techniques can be applied to process data gathered from all sensor modalities and generate multiple outputs according to a user's interests. The system can also send real time alerts, via text message or e-mail, to operators if an abnormal event is being detected, so that they can react quickly to avoid or limit negative impacts. In this work, a sensor communication malfunction alerting system is developed using Nexmo. The alerting system tracks the inputs from all sensors and if any sensor is off-line longer than a pre-defined period, a text message will be sent to system operators. Nexmo[1] is a cloud-based Short Message Service (SMS) and Voice API (application program interface) that provides the service of sending and receiving high volume of messages at wholesale rates.

[1] https://www.nexmo.com/

3.4 Information Layer

The information layer provides a graphic user interface (GUI) for end users to interact with. For example, show all the events detected by a visual sensor along with *in-situ* sensor readings during these periods. Also, the end user could query all turbidity abnormal events in the last N months and browse the image data associated with these events. Within this list of abnormal events, find events that are similar in terms of sensor measurement patterns from the previous year. Based on the information provided, operators can send feedback to the deployed system, for instance to reduce the redundancy in the sensor network or increasing/decreasing the sampling rate. New policies can be specified based on the analysis of the information provided by the system. For example, re-scheduling the discharging of waste water to make less impacts to the aquatic environments.

3.5 Summary

In this chapter, a multi-modal smart sensing system framework has been designed and the structure of the system discussed. The framework is architected in a flexible manner that can be deployed on a computing cloud. The system is designed to meet the requirement of future large scale multi-modality sensor networks, whereby sites and sensors can be dynamically added or removed. The system also provides a user interface that allows a rich set of queries from end users. In the next chapter it is explained how this system was deployed at a specific test site. In Chapter 5 and 6, two case studies have been carried out to illustrate how the designed system could perform in practice. The first case study (Chapter 5) shows how raw *in-situ* water quality parameters can be converted into organized event based information and the second case study (Chapter 6) exhibits how the smart system can be used to detect events from a visual sensor. Subsequently, an example of how these multi-modality information can be combined at the information layer is presented. The two case studies show an implementation of the proposed multi-modal smart sensing system at one test site (Dublin Bay) from data collection layer to data

processing and information layers as illustrated in Figure 3.1. Future work shall involve the evaluation of the proposed methods used in the two case studies on multiple test sites once they become available, which completes the implementation of the overall proposed framework.

CHAPTER 4

TEST SITE AND SYSTEM DEPLOYMENT

4.1 Introduction

The following chapter describes Dublin Bay, Ireland, as a test site along with the equipment used for collection of continuous monitoring data. This corresponds to a practical implementation of the framework described in the previous chapter. Both the *in-situ* and visual sensing modalities deployed at the site, are described in detail in this chapter along with practical issues concerning deployment in a real environment.

4.2 Dublin Bay

Dublin Bay (latitude: 53°20'39", longitude: -6°12'59") is located on the lower Liffey Estuary in Dublin Ireland (Figure 4.1). The River Liffey, which flows through the centre of Dublin, plays an extremely important role in terms of water management in Dublin as around 60 % of its flow is abstracted for drinking water and to supply industry. Much of this makes its way back into the river after purification in waste water treatment plants (WWTP). The catchment area of the River Liffey is $1,256\ km^2$. The long term average flow rate of the River Liffey is 18.0 Cubic Metres per second (m^3/s) [103]. The ESB

Dublin Bay hydroelectric power plant, the Poolbeg generation station and the Celtic Anglian waste water treatment plant (as shown in Figure 4.1) are also located at the estuary, which all contribute to the local ecosystem.

The estuary hosts a diverse ecosystem including benthic communities, fish and shellfish, sea bird populations and marine mammals [104, 105]. The topography of the estuary has been greatly modified, and is constrained by walls along its whole length and is regularly dredged to remove accumulated sediments. The sediments in Dublin Bay at the lower limit of the estuary are predominantly sand. Muddy sediments are also presented starting from Dublin Bay to the upstream of the River Liffey [106].

Figure 4.1: Overview of the Dublin Bay area, indicating the location of the deployed pilot system , which provided the datasets used in this research. The ESB Dublin Bay hydroelectric power plant, the Poolbeg generation station and the Celtic Anglian waste water treatment plant are also located at the estuary, which all contribute to the local ecosystem Dublin Bay background image source: Google Maps. Retrieved: 2014-04-11

The research site is located in the upper part of the estuary, where the ship traffic is less intensive. Average water depth in the area is approximately 8 m and the width of the channel is approximately 260 m. It is a very complex site in terms of marine environmental monitoring, as the estuary is macrotidal (the tidal range is in excess of 4 m) with strong salinity gradients and seawater flushes into and out of the port, which causes water column stratification. In [106], Briciu-Burghina et al. built vertical profiles of the water column for salinity, temperature, DO and pH. It was shown that the column stratification occurs at depths between 1 and 2 meters at the estuary.

Anthropogenic disturbances include input of pollutants (runoff, storm drains, discharges from sewage treatment plant, industrial discharges, port activity and recreational boating) and the modification of flow (upstream dam releases). All these episodic changes dictate the chemical, physical and biological parameters at the site and thus increase its complexity [106]. In addition, Dublin Bay is a busy port environment with a diverse ecosystem. The area is subject to a large amount of recreational and commercial activity and the port is heavily used with a high amount of shipping traffic.

Figure 4.2: A YSI 6600EDS V2-2 multi-parameter water quality sonde with simultaneous measurement of turbidity, dissolved oxygen, temperature, salinity, and depth. Source: https://www.ysi.com/6600-V2-4

Given the large amount of activity at the site and its importance from an environmental

and ecological perspective, the site was equipped with a multi-parameter *in-situ* sonde (YSI 6600EDS V2-2 as shown in Figure 4.2). The sonde unit contains individual sensors for turbidity, dissolved oxygen, temperature, conductivity and depth, and was deployed along with a visual sensing system. From the data processing perspective, more data may contribute additional information to the machine learning method, thus produce a more accurate model. If it does not provide useful inputs to the model, it can be removed at processing stage. Moreover, water quality sensors are point sensors, a single sensor may not reflect the true property of a large water body. However, due to the high cost and the requirement of labour intensive maintenance work as well as the hosting agreement issue, only one multi-parameter sonde is deployed at the site.

4.3 Deployed System

The system deployed at Dublin Bay consists of two parts - the *in-situ* sensor and the visual sensor. Each sensing modality has its own communication methods capable of transmitting data to a server. The *in-situ* sensor node measures physical parameters in the water body, whereas the visual sensor captures the surroundings above the water surface. Figure 4.3 shows the relative position of the sonde and the camera deployed at the marina.

4.3.1 In-Situ Sensor

A multi-parameter sonde (YSI 6600EDS V2-2), equipped to measure turbidity (Nephelometric Turbidity Units (NTU)), optical dissolved oxygen ($mgL^{-1}/\%$ saturation), temperature ($^{\circ}\mathrm{C}$), salinity (ppt), depth (m) and telemetry system (EcoNet) were purchased from YSI Hydrodata UK [1].

The unit was powered with a 12 V external battery and data recorded onto an internal logger, before sending to a cloud data server via GSM. The sonde was deployed at a depth of 2.5 m from the water surface, and data was collected from 1st of Oct 2010 with

[1] http://www.ysi.com/index.php

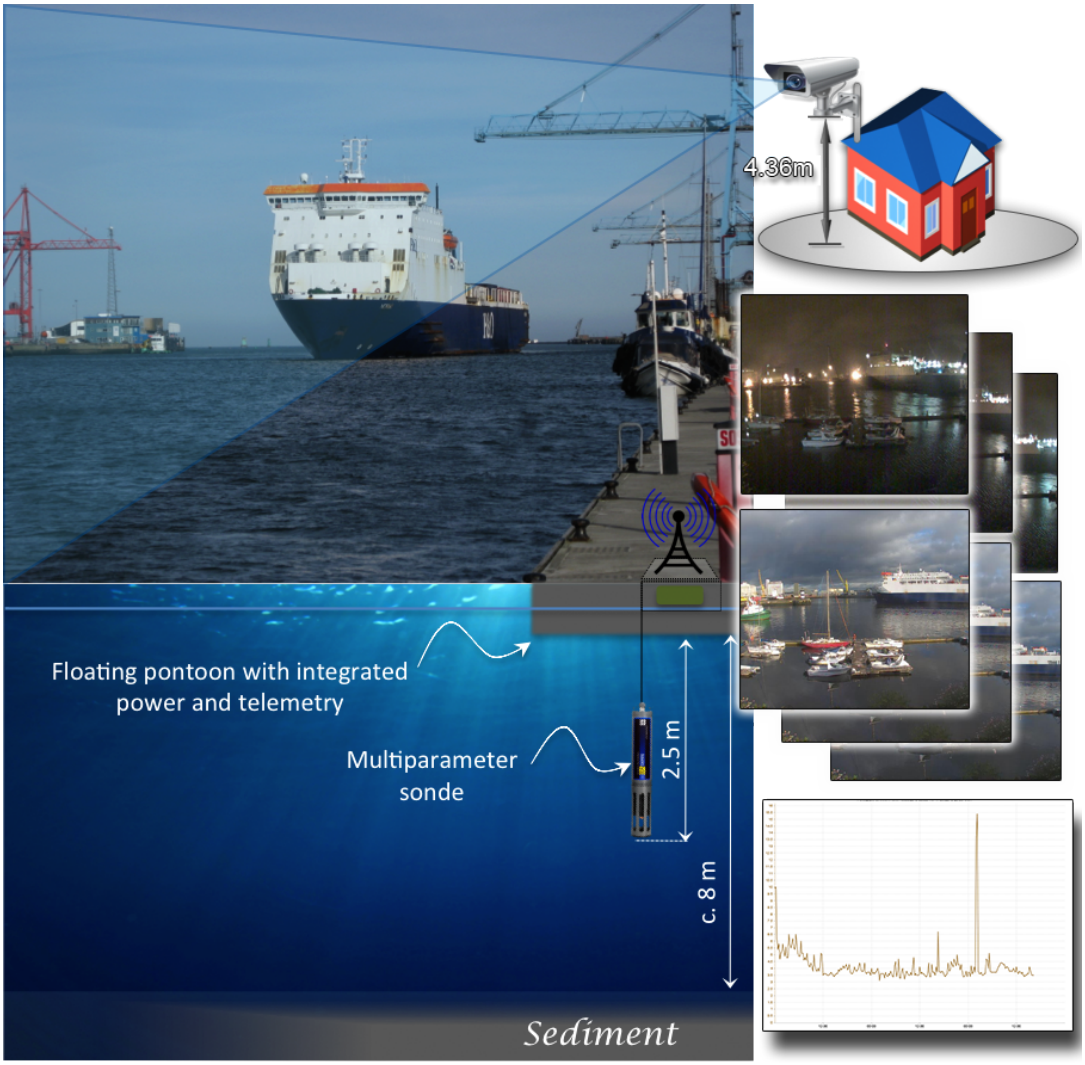

Figure 4.3: The relative positions of the in-situ and visual sensor deployed at Dublin Bay.

a sampling interval of 15 mins.

Temperature, dissolved oxygen and salinity were checked using a ProPlus handheld multi-parameter instrument (YSI Hydrodata UK) and turbidity was validated using a portable turbidity meter Turb® 430 IR (VWR Ireland [2]). Both hand held instruments were calibrated in the laboratory prior to deployment as per manufacturer's protocols. Site visits were undertaken fortnightly in winter and weekly in spring for cleaning, calibration and validation. A protocol for the operation and maintenance of a continuous water quality monitor at sites with rapidly changing conditions was adapted from [107]. The following maintenance procedures were performed every time on arrival at the scene:

[2]https://ie.vwr.com/

1. Readings and time are recorded from both the lab calibrated meters and the sonde. The clock drift, due to the precision of the onboard real-time clock, of the sonde is logged. If the drift is significant, over 5 mins, the on-board clock is reset.

2. To compare the measurements between the *in-situ* sensor and the calibrated device, an ambient water sample was taken in an insulated bucket. Both of the instruments were placed inside this sample, and both systems allowed to run in parallel. The disparity between the two instruments was recoded.

3. The sonde is cleaned and step 2 is repeated multiple times to ensure readings are accurate.

4. The sonde is rinsed thoroughly and the sensors calibration is finally checked following the calibration criterion.

5. If the calibration criterion is breached, the sonde is recalibrated.

Calibration criterion: Temperature $\pm 0.2\ ^{\circ}\mathrm{C}$, DO $\pm 0.3\ mg/l$, Specific Conductance $\pm 3\ \%$ of the measured value and Turbidity $\pm 5\ \%$ of measured value. Copper tape and mechanical wipers (for the optical oxygen and turbidity sensors) were used to control biofouling of sensor systems. However, it can only suppress the growth of microorganisms. Figure 4.4 shows an example of biofouling (6 weeks after deployed) on the deployed sensor at the test site.

4.3.2 Visual Sensor

The components of the visual sensing unit are shown in Figure 4.5. The camera installed at the test site is an *Axis P1344-E* IP camera, which is an IP66-rated camera that has protection against dust, rain, snow and sunlight, and can operate in temperature as low as $-40\ ^{\circ}\mathrm{C}$. It also provides 1 Mega Pixel HDTV $720p$ resolution, day and night image and/or video streams. Another advantage of this camera is that it can be either powered by an $8 - 20$ V external power source or powered over Ethernet (POE). It also consumes

Figure 4.4: An example of biofouling (6 weeks after deployed) on the deployed sensor at Dublin Port during May-June 2013.

relatively low power (max. 6.4 W) compared to other commonly used IP cameras (e.g. Vivoteck IP8352 IP camera consumes max. 10 W). The camera was mounted on a pole at a height of 4.36 m above the ground and approximately 20 m from the river bank wall. This position is suitable for monitoring the shipping traffic while also being close to the location of the sonde. The camera is connected to a *Fit-PC2i* control board through Ethernet cable. For this pilot system, the visual sensor is connected to the mains electricity.

Figure 4.5: The visual sensor unit, which consists of an IP66-rated Axis P1344-E IP camera for image capturing, a Huawei E353 3G modem for image data transmission and a Fit-PC2i nettop for controlling.

The Fit-PC is a tiny, light, fan-less, inexpensive nettop computer. It supports the main operating systems such as Window and Linux. It consumes relatively low power, 6 W at low load and 8 W at full load. It supports a Wi-Fi connection by using a Wi-Fi network

card and a 3G mobile network by using a mobile broadband modem, WiMAX network connection by using a WiMax dongle or RJ45 wired Internet connection. It also provides standard USB and HDMI ports, which are convenient for on-site diagnostics. In this initial system, Fit-PC is chosen due to its convenience for development and on-site diagnostics. For a future release version of visual sensing system, a much more cost effective embedded board, such as Raspberry Pi (10 % of the cost and 30 % of the power consumption compare to Fit-PC), could be investigated. The control board connects to the IP camera through RJ45 connection and retrieves image data from it via HTTP protocol. Image data are then sent back to a cloud server through a 3G mobile network. At our test site, the frame rate of the camera is set to 1 frame every 10 seconds. This is due to two main reasons: the network speed at the location and the duration of the target events. From human inspection, we found that the fastest object moving on the water surface is speeding boats. The configured frame rate will capture at least one image of such an event. In some cases, there may also a upper limit of the amount of data that can be transmitted, e.g. the monthly data allowance of some mobile broadband package allows 10 Gigabytes data per month. Mobile broadband is one of the wireless internet connection mechanisms that is based on third generation wireless broadband technologies (3G). A mobile broadband service can be used anywhere within a coverage area. It provides high speed upload internet access. Current HSDPA (one of the 3G standards) deployments support down-link speeds of up to 42 Mbps and up-link speeds of up to 5.76 Mbps. In this work, a *HuaWei E353* 3G modem with Meteor mobile carrier is used. Figure 4.6 shows the results of Meteor 3G mobile broadband upload and download speed tests at various locations in Dublin. From the graph, it can be seen that the minimum upload speed is 0.75 Mbps. At the test site (Dublin Bay), the upload speed is 2.7 Mbps. The upload speed that the system requires is 0.31 Mbps when uploading image data at 1 frame per second. Thus, 3G mobile broadband provides sufficient bandwidth for the visual sensor.

The main technical issue of the visual sensing system is the unreliable 3G connection. The control board has to restart itself to establish a new connection, which can result in a small disruption to the image data stream (2 minutes data lost).

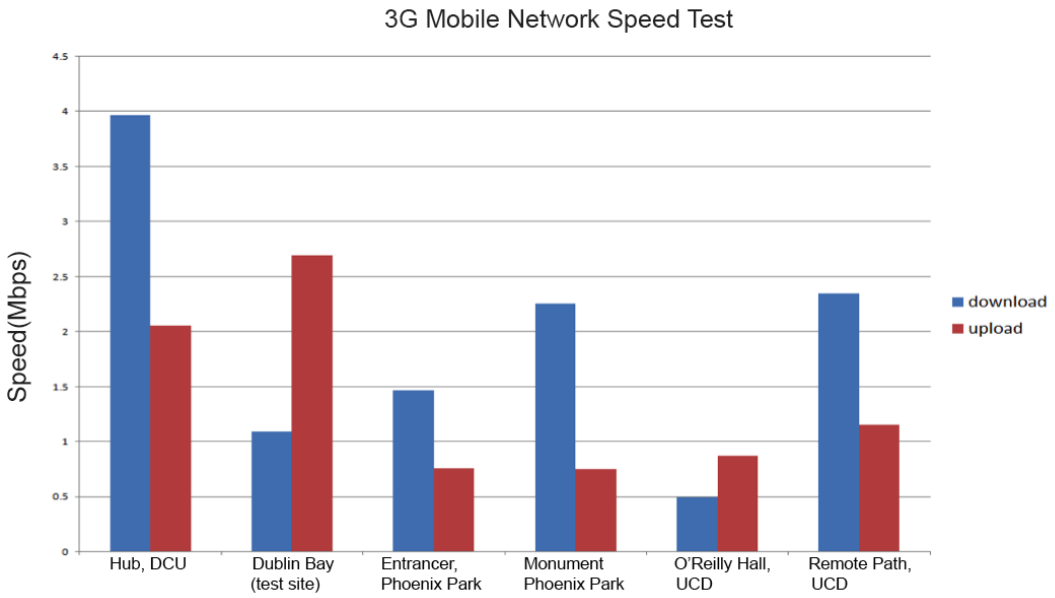

Figure 4.6: Meteor 3G mobile broadband upload and download speed test. Dublin Bay data is obtained from the test site.

4.4 Summary

This chapter provides an overview of the test location used for a practical deployment of the system introduced in the previous chapter and the complexity of the site is discussed. This test site presents a real challenge in environmental monitoring because of the complex interactions of parameters such as tide, stratification and human activities. The technologies deployed at the site are also discussed in this chapter along with their maintenance procedure. It should be noted that both of the sensors suffer real world issues such as biofouling and data communication issues.

CHAPTER 5

IN-SITU DATA PROCESSING

5.1 Introduction

In this chapter, a case study of abnormal event detection and clustering from *in-situ* sensor data is carried out. The case study illustrates how state-of-the-art computer science techniques can be used to automate the processing of raw sensing data measured from aquatic sensing instruments to provide comprehensive information, which is more suitable for management especially at a much larger scale. Anomaly sensor readings are first isolated from the input data stream and further grouped into events based on their temporal information. These abnormal events are then catalogued into clusters based on their similarities. This chapter is organized as follows. Section 5.2 introduces the importance of salinity and turbidity at estuaries. An abnormal event detection and clustering system framework is proposed in Section 5.3. The testing data, which is used for evaluating the proposed methods is described in Section 5.4 and statistical analysis of this testing dataset is carried out in Section 5.5. Section 5.6 shows how the parameters of the detection and clustering system are selected. The experimental results are described in Section 5.7 and 5.8 followed by a discussion in Section 5.9. The analysis carried out in this chapter relates to research question 1 and 2 in Chapter 1.

5.2 Importance of Salinity and Turbidity at Estuaries

There are numerous water quality parameters that can reflect overall water quality of estuaries, however, current state-of-the-art sensor technology may not capture them all. Developing reliable *in-situ* or portable sensors for marine or estuarine water quality parameters, such as *Escherichia coli* (*E. coli*), enterococci, phosphate and nitrate among others is still an active research domain. As previously described, a YSI V-6600 multi-parameter sonde was deployed at the pilot site to measure salinity (ppt), turbidity (NTU), temperature (°C), dissolved oxygen (mg/L and % saturation) and depth (m). In this work, the focus on salinity and turbidity measurements are investigated due to their high variance and complexity when compared with others, such as temperature and dissolved oxygen. The importance of salinity and turbidity in estuarine zones is discussed in detail in the sections 5.2.1 and 5.2.2 respectively.

5.2.1 Salinity

Salinity is the dissolved salt content contained in a body of water. Salinity is an important factor in determining many aspects of the chemistry of natural waters and of biological processes within it. It is a thermodynamic state variable that, along with temperature and pressure, governs physical characteristics like the density and heat capacity of the water. Intertidal environments in estuaries are critical exchange environments for both marine and freshwater systems. Salinity is the key tracer of freshwater input into coastal zones and directly contributes to seawater density and circulation patterns. However for environments like estuaries, where large salinity changes can occur on a daily and/or seasonal basis, prediction of levels is difficult. By their very nature, estuaries also exhibit considerable spatial and temporal heterogeneity in environmental parameters, which complicates study and understanding of transport processes. Characterisation of this heterogeneity through isolated point samples is commonly time-consuming, expensive and often unrepresentative. Additionally, estuarine environments are dynamic and complex systems where biotic and abiotic factors are often difficult to model and predict [108, 109]. Estu-

aries are therefore attractive locations for deployment of multi-modal sensing platforms [110]. Practical considerations such as ease of access to near-shore infrastructure, readily available power supplies and communications mean that such zones are generally convenient for testing and prototyping of novel systems.

An example requirement of estuarine and marine monitoring systems is the ability to predict water levels and changing freshwater inputs into any given system. Key goals include identifying relationships between catchment rainfall and runoff in an estuary, including the dominant forcing mechanisms affecting the transport of stormwater within the estuary, estimating volumes of storm water associated with high-precipitation events and predicting residence times of storm water within the system following monitored high-precipitation events. Understanding effects of flow rates and salinity gradients within estuarine systems are important when considering the effects of such forces on both natural and anthropogenic systems [111, 112]. For example, large variations in freshwater influx into a system can profoundly affect phytoplankton dynamics (believed to be related to nutrient transport or stratification-destratification events), or can significantly affect the probability of a flood event occurring. The ability to continuously monitor salinity and understanding of riverine discharge rates are thus crucial to many environmental phenomena occurring in otherwise complex estuarine systems. However, these goals cannot be achieved without isolating and cataloguing the significance from a long term salinity measurement stream. Salinity measurements from a YSI *In-Situ* sensor is determined automatically from the sonde conductivity and temperature readings according to algorithms found in standard methods for the examination of water and wastewater. The use of the practical salinity scale results in values that are unitless, since the measurements are carried out in reference to the conductivity of standard seawater at $15\ ^{\circ}\mathrm{C}$. However, the unitless salinity values are very close to those determined by the previously used method, where the mass of dissolved salts in a given mass of water (parts per thousand) was reported. Hence, the designation "parts per thousand (ppt)" is reported by the instrument to provide a more conventional output [113].

5.2.2 Turbidity

Turbidity is defined as the decrease in the transparency of a solution owing to the presence of suspended and some dissolved substances, which causes incident light to be scattered, reflected and attenuated rather than transmitted in straight lines [114]. Turbidity is now seen as a key water pollutant and is often used as a surrogate variable for suspended solids concentration [115, 116]. Turbidity levels are important drivers of population, community, and ecosystem level dynamics of phytoplankton and bacterioplankton in estuarine systems [117, 118]. Sustained and sporadic increases in turbidity levels are associated with fluctuations in microbial populations and concentration of re-suspended contaminants such as heavy metals or other pollutants [119, 120]. For a number of estuarine systems strong correlation has been found between suspended particle concentration and the number of attached bacteria, an important parameter in estimating microbial population of bacteria such as *Escherichia coli* and faecal coliforms [121]. Re-suspension of benthic sediment leading to higher turbidity levels, rather than runoff from surrounding lands, can create elevated *E. coli* concentrations in estuarine waters. Thus modelling of turbidity levels can enhance understanding of sediment effects on the fate and transport of *E. coli* in surface waters with subsequent implications for monitoring and management of microbiological water quality [121].

Turbidity levels can also influence photosynthetic activity and growth of phytoplankton cells by shortening the depth of the photic zone. For example, estuarine waters may often be rich in nutrients, but phytoplankton are unable to avail of these nutrients due to high turbidity resulting in high attenuation and light limitation of growth. Higher turbidity also increases water temperatures as suspended particles absorb more heat, thus altering the vertical stratification of heat in the water column. This, in turn, reduces the concentration of dissolved oxygen (DO) because warm water holds less DO than cold.

Many factors can contribute to changing turbidity levels within water bodies, especially in heavily industrialised urban river and estuarine waters where anthropogenic disturbance may influence natural systems [122]. In particular water movement from factors such as

rainfall, tide level, and shipping traffic can affect suspended sediment loads in complex ways. Rainfall levels directly contribute to run-off and discharge rates. Storm events and unusually high rainfall patterns are usually associated with increased turbidity generation, although propagation of storm-event turbidity pulses in urban river and estuarine systems are relatively poorly studied [122]. Together with rainfall levels, tidal dynamics are an important driver of turbidity levels within estuarine systems. The relationship between rainfall measurements and tide level are however often heavily estuary specific and are a function of local geology and localised features. Generally however, long, strongly tidal estuaries tend to have greater suspended particulate matter concentrations within their high-turbidity regions than shorter estuaries with comparable tidal ranges at their mouths, or weakly tidal estuaries [123]. In this study, the focus is on the integration of shipping traffic and turbidity significance. Future work would include the integration of other factors such as rainfall and tide levels into the smart system.

Shipping can regularly and profoundly affect turbidity levels through a number of mechanisms, including shore erosion from wakes, increased vertical mixing and stirring of the sediments, especially in the turning area outside harbours from large ships (150-200 m long) or indirectly through regular dredging [124]. Pressure changes, propeller suction, use of bow thrusters, drag and acceleration caused by shipping can result in visible water displacement, swell, pressure waves and turbulence. All of which results in periodic increases in mixing energy driving vertical mixing, artificial upwelling, temporary water currents and material transport [125]. Regular water column disturbance may result in partial or complete water column destratification and artificial upwelling. This in turn affects nutrient ava ilability [126], water temperature profiles [106] and dominant species in the locale [115]. Sediments that are frequently disturbed by re-suspension and subsequent deposition remain unconsolidated and relatively easy to erode. Such disturbance may either promote or interfere strongly with growth of planktonic and benthic organisms including cyanobacterial growth and bloom formation [117].

According to the YSI sonde operation manual [113], YSI measures turbidity with an optical sensor. Light from the emitter enters the sample and scatters off particles in the

water. The light, scattered at 90 degrees, enters a detector fibre and is measured by a photodiode. This follows the nephelometric technique of measurement, and values are expressed in nephelometric turbidity units (NTUs).

5.3 Abnormal Event Detection and Clustering from In-Situ Data

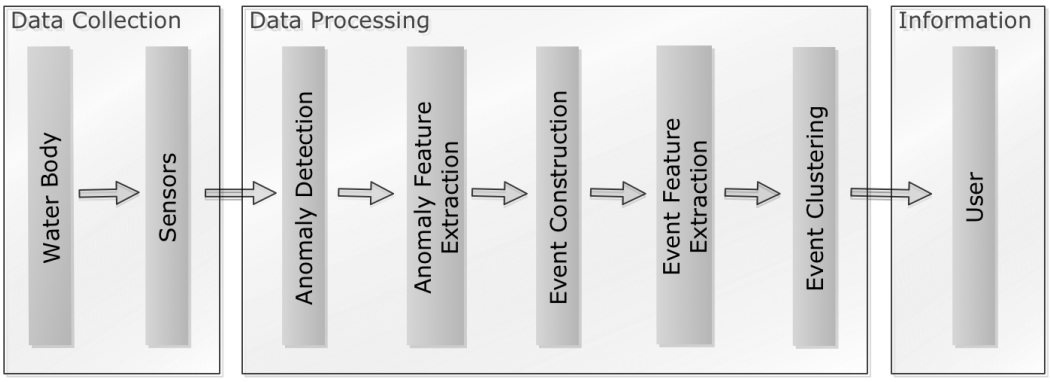

Figure 5.1: Flow diagram of the proposed system framework

To detect and cluster environmental events, anomalous sensor readings (also referred to as outliers) need to be extracted from a continuous data stream. These abnormal sensor measurements are then grouped into events based on proximity in time (temporal information). A set of features is extracted that is characteristic of different anomalies and is used to identify individual events. Each event might have different temporal characteristics; so to compare their similarities, a bag-of-words approach is adopted to encode these features as constant length descriptors. Bag-of-words is a nonlinear representation method that uses finite pre-trained ‘ words’ to represent inputs. Each feature set of the detected anomalies is matched against a pre-defined codebook (“a bag of words”) and the closest matching codeword is used to represent the feature. The event is then represented by the frequency of occurrence of each word. Once the feature vector of the event is constructed, a clustering method is applied to group these events into subclasses based on their similarities. Figure 5.1 shows the flow diagram of the proposed framework. Each step of the proposed framework is introduced in detail in the following sections.

5.3.1 Anomaly Detection

In order to detect abnormal events, unusual sensor measurements in the data stream need to be detected. An unusual or anomalous sensor measurement is defined as a sensor reading that differs considerably from recent observations. Thus, an anomaly can be detected by modelling previous sensor measurement trends. To achieve this, we have modified the pixel-based adaptive segmenter (MoPBAS) method originally proposed by Martin Hofmann et al. for image segmentation [127]. By examining the PBAS method, it is found that slightly modifying the original method, it meets the four challenges (See Section 2.4) of anomaly detection from *in-situ* sensor measurements in a marine environment. A non-parametric water quality background trend model is built based on a history of recently observed sensor readings, which defines a normal region (challenge 1). The model is updated over time according to the dynamics of the measurements. This ensures that the evolving normal behaviour is modelled accurately by the adaptive back ground trend model (challenge 2). The classification of an unusual reading depends on a decision threshold, which is constantly adapting based on the variations in the data stream. Thus, the definition of an anomaly varies based on how turbulent the water body is (challenge 3). When the water body has high variance, the increased threshold will decrease the sensitivity of the anomaly detection system, which will ignore relatively small changes. In contrast, the decreasing of the threshold will ensure that small variation will be detected during calm periods. The MoPBAS is an unsupervised learning method, no labelled data is required to train a trend model (challenge 4). Moreover, MoPBAS is computational inexpensive, which provides the opportunity of introducing intelligence on chip (implement anomaly detection algorithm on the sensor's control board). Above all, MoPBAS is a suitable method for anomaly detection in marine environments. Similar to any other machine learning method, MoPBAS has a number of tunable parameters, some are fixed values during the detection process and the others are constantly updating according to the variation of the inputs, which controls the sensitivity of the anomaly detection process. There are two ways to set the value of these parameters. They can be set by domain experts based on the analysis of how each parameter affects the MoPBAS model or using

parameter optimization algorithms. The advantage of the first method is it does not require a set of training data to obtain a set of optimized parameter value set. Initial values can be set based on the analysis of discrete samples that are collected from a site. Thus, the detection can be started as soon as an *in-situ* sensor is deployed. However, it may not achieve the best detection accuracy. In addition, it may require operators to evaluate the results at some point to confirm the initial values are appropriate. The main advantage of the second method is that the set of optimal values is obtained based on the data collected at the site, which produces a more accurate model. However, the main drawback of this method is that the detection may not be started until the training phase is over. How does each parameter affects the detection model and how to train a set of parameters using a parameter optimization algorithm are described in details in Section 5.6.

In the following, the process by which the MoPBAS method is used to detect abnormal sensor readings is described.

5.3.1.1 Background Trend Model and Anomaly Classification

To classify a new incoming value $I(t)$, a sensor reading trend model $B(t)$ is built. $B(t)$ is defined by an array of N recently observed values.

$$B(t) = \{B_1(t), ..., B_k(t), B_N(t)\} \tag{5.1}$$

As described by Hofmann et al. [127], incoming values are classified based on the total number of distances between input value $I(t)$ and all elements in $B(t)$ that are smaller than threshold $T(t)$. We found that comparing the minimum distance with the threshold is sufficient to differentiate the measurements.

$$I(t) = \begin{cases} 1, & \text{if min(dist}(I(t), B_k(t)) \text{)} > T(t) \\ 0, & \text{otherwise} \end{cases} \tag{5.2}$$

If the input value is classified as normal ($I(t) = 0$), it can be used for updating the background trend model. The update probability depends on the learning rate $L(t)$.

5.3.1.2 Update of the Decision Threshold

When monitoring water quality of estuarine waters, there can be periods of time where large variations occur in measured variables, such as after heavy rainfall, and time periods with little change or fluctuation. Ideally, for periods of high variability, the threshold $T(t)$ should be increased and for stable conditions, $T(t)$ should be decreased. To quantify this dynamic, the mean $\overline{d}_{min}(t)$ of the previous N minimum distances between input values and the trend model are calculated as the measure of the trend variations. For instance, assuming the water quality measurements remain constant, $\overline{d}_{min}(t)$ will be zero. In contrast, $\overline{d}_{min}(t)$ will be higher for more dynamic backgrounds. The decision threshold can then be adapted as follows:

$$T(t) = \begin{cases} T(t) \times (1 - T_{inc/dec}), & \text{if } T(t) > \overline{d}_{min}(t) \times T_{scale} \\ T(t) \times (1 + T_{inc/dec}), & \text{otherwise} \end{cases} \tag{5.3}$$

where $T_{inc/dec}$ is a static value that controls the threshold update rate and T_{scale} is also a fixed parameter, which stretches $\overline{d}_{min}(t)$ to the same range as $T(t)$. T_{lower} and T_{upper}, which are also fixed values, control the upper and lower bounds of the threshold, thus the threshold will not grow out of range.

5.3.1.3 Update of the Learning Rate

Another important parameter of MoPBAS is the trend model learning rate $L(t)$. Water quality measurements have characteristics that are significantly different from image segmentation data. Values measured by *in-situ* sensors are typically very noisy, have lower sampling rates (in terms of minutes compared to fraction of a second in the image processing domain) and vary from a baseline (they change gradually due to "global" effects, such as wind, tide etc.). Unlike background modelling in the image processing domain, in which foreground objects will be slowly merged into the background if it no longer

moves, water quality parameters will usually return to a baseline level after an event. Thus, we normalise ($R(t)/R_{upper}$) and invert the original learning rate ($R(t)$) proposed in the PBAS method. Here, the learning rate $L(t)$ is defined as follows:

$$R(t) = \begin{cases} R(t) + \frac{L_{inc}}{\overline{d}_{min}(t))}, & \text{if anomaly = true} \\ R(t) - \frac{L_{dec}}{\overline{d}_{min}(t))}, & \text{if anomaly = false} \end{cases} \tag{5.4}$$

$$L(t) = 1 - R(t)/R_{upper} \tag{5.5}$$

Where L_{inc} and L_{dec} are fixed values that control the increasing and decreasing intervals. The variation in $R(t)$ is limited by an upper and lower bound: $R_{lower} < R(t) < R_{upper}$. The learning rate also depends on the background dynamics ($\overline{d}_{min}(t)$). When an event occurs, measured values provided by the sensor will usually deviate greatly from the baseline level. Thus, the trend model should be updated slowly or not updated at all. In contrast, after an event occurs, sensor readings will usually stabilise or return to the baseline, and the trend model should be updated quickly. When an anomaly is first detected ($\overline{d}_{min}(t)$ is small), $R(t)$ increases rapidly, thus the learning rate $L(t)$ decreases sharply. However, $\overline{d}_{min}(t)$ will become large quickly when multiple anomalous readings are detected, which results in $R(t)$ and indeed $L(t)$ remaining constant or only changing slightly. When sensor readings stabilise or return to a normal range, $\overline{d}_{min}(t)$ becomes small and $L(t)$ will increase.

5.3.1.4 Update of the Trend Model

Updating the trend model, $B(t)$, is essential to capture global effects, such as tide or wind. The learning rate $L(t)$ is used as the update probability and an element in the trend model is randomly chosen and replaced by the incoming value. However, this process is only performed when no anomalous values are detected. This allows the incoming sensor measurement to be "learned" and incorporated into the trend model. In the original PBAS, a randomly chosen neighbouring pixel is also updated, however, as there is no "neighbour"

(image data is 2D as opposed to 1D water quality data) this step is not performed.

5.3.1.5 Distance Calculation

Rather than using common distance metrics, such as Euclidean distance, we use the root of the absolute square difference (RASD) to calculate the distance between incoming value and the ith element in the trend model.

$$D_i(t) = \sqrt{|I(t)^2 - B_i(t)^2|} \tag{5.6}$$

Figure 5.2 shows the ratio between our distance metric and the 1-D Euclidean distance (for illustration purposes, the input $I(t)$ range is set from 5 to 104 in steps of 1, background $B_i(t)$ is set to 5). It can be seen from Figure 5.2 that when the distance is large, the output is approximately equal to the 1-D Euclidean distance. However, the output is enhanced when the difference between $I(t)$ and $B_i(t)$ is small. This is a key factor when calculating the background dynamic $\overline{d}_{min}(t)$, as it smooths the effect of an event to $\overline{d}_{min}(t)$. Thus, the value of $\overline{d}_{min}(t)$ will not increase rapidly when an event occurs as shown.

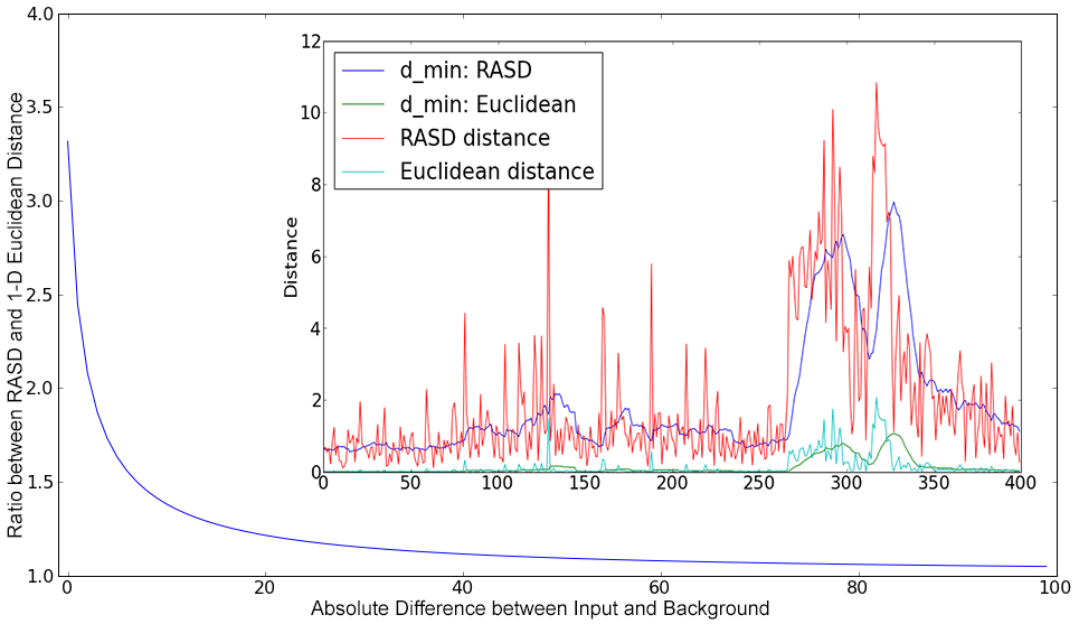

Figure 5.2: Demonstration of the ratio between RASD distance metrics and 1-D Euclidean distance, the inner graph shows RASD distance method, which enhances small distances, smoothing the variation of the background dynamics $\overline{d}_{min}(t)$.

5.3.2 Anomalous Feature Extraction

To capture the similarity in anomalies detected, and for further clustering of anomalous events, we need to extract a set of features that are sufficiently discriminative to allow us to classify unusual readings and subsequent events. As previously discussed, MoPBAS is a computational inexpensive technique, which can be potentially implemented on the *in-situ* sensor's control board. In addition, anomaly detection needs to be in real-time so that operators can be notified as soon as an irregular sensor measurement is being detected. Thus, a feature set is proposed using only the current sensor reading, the local variations between current sensor reading's contiguous measurements and the current values of two parameters from the MoPBAS trend model.

The feature set of an anomalous reading has the following components: the difference between the previous sensor measurement $I(t-1)$ and current sensor measurement $I(t)$, current sensor measurement $I(t)$, the difference between current sensor measurement $I(t)$ and the next sensor measurement $I(t+1)$, the minimum distance between sensor measurement and trend model d_{min}, and the distance between the minimum distance d_{min} and the threshold $T(t)$. The feature set $f(anomaly)$ can be represented as:

$$f = [I(t-1) - I(t), I(t), I(t) - I(t+1), d_{min}, d_{min} - T(t)] \tag{5.7}$$

5.3.3 Creating Event

Anomalies detected by the MoPBAS method are grouped into events according to their temporal information. To achieve this, agglomerative hierarchical clustering is applied. As shown in Figure 5.3, consecutive anomalies are combined together into a single event. In real environment, a sensor reading could be a noise (e.g. blockage of the sensor probe). A threshold T_{gap} is set to allow some tolerance to sensor readings. For example, if a sensor reading is classified as normal in a sequence of measurements, which all the rest values are classified as anomalies, then this "normal" reading is likely caused by noise, which will be ignored when creating an event. Thus, if the gap between a new anomaly

and previous outlier is smaller than a threshold, T_{gap}, the new anomalous value will be merged into the same event. In contrast, if this gap is greater than T_{gap}, a new event will be created.

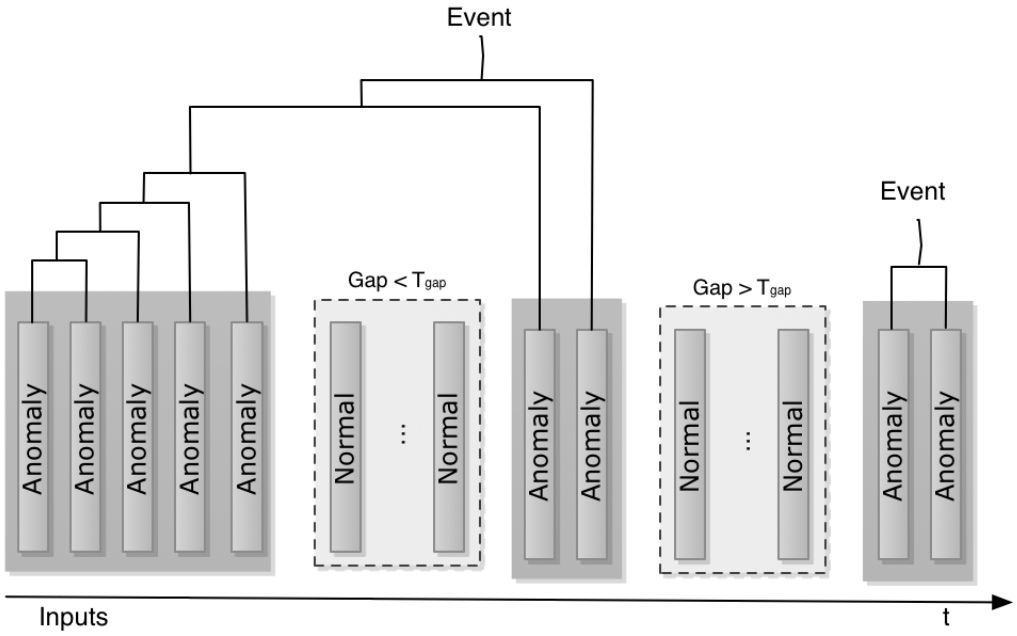

Figure 5.3: Anomalies are grouped into events using agglomerative hierarchical clustering based on their temporal information

5.3.4 Event Clustering

A Bag-of-Words approach is widely used in text document classification [128], content-based image retrieval [129] and image recognition tasks [130], where a document is represented as a bag of its "words" or a bag of small image patches (visual words) in the image processing domain. Most classification or clustering methods require a fixed number of feature dimensions. However, for many tasks, such as text document indexing, the number of features extracted from each file are generally different. The Bag-of-Words method represents these features by counting the frequency of occurrence of each "word" as the descriptor of the object. For text document processing, a "word" generally means an entry in a "codebook", which is the combination of a single word in a dictionary or a phrase. In the image processing domain, a word (some times referred as a "visual word") means a small image patch or fragment. As each environmental event may contain a different

number of anomalous values, each outlier feature set is represented by a "sensor word" in order to quantify the similarities between events, and the frequency of their occurrence is reconstructed as the descriptor of the event. To create a codebook, K-means clustering is performed over a set of training data. The centres of the learned clusters are then defined as codewords. Each anomaly feature set in an event is mapped to a certain codeword in the codebook and the event can be represented by the histogram of the occurrence of the codewords.

To divide events into groups, a clustering method known as robust on-line clustering [131] is used. Clustering is the process of dividing instances into groups in such a way that instances in the same group are more similar than elements in other groups. There are many common clustering methods that are widely used such as K-Means or Mean-shift. Current research indicates that there is no known single clustering method that categorically out performs all others in all tasks. The benefit of using robust on-line clustering in this context is that, unlike K-Mean or Mean-Shift, this method is not sensitive to "noisy" data. This is a key requirement for environmental monitoring tasks where highly variable data could indicate a significant event. Moreover, robust on-line clustering is an on-line method that can be used to process a continuous data stream provided by *in-situ* sensors.

5.4 In-Situ Test Data: Dublin Bay

The dataset that is used for evaluating the proposed abnormal event detection and clustering method was collected from deployed remote water quality monitoring systems in Dublin Bay between Oct 01 2010 and May 03 2011 (215 days) with a total number of $20,544$ measurements (at the sampling rate of 15 mins). Two water quality parameters, salinity and turbidity, are selected for evaluating the proposed system. One of the main reasons for choosing these two parameters is that they are much more complex compared to other water quality parameters, such as temperature or dissolved oxygen as previously discussed in Section 5.2. In addition, salinity and turbidity are not only affected by global

factors but local variations as well. The data exhibits a wide variety of environmental occurrences that include short-term events (such as human activities), mid-term natural phenomena (rainfall, tide for example), as well as long-term changes in measurements related to seasonal effects. To evaluate the results, both of the salinity and turbidity measurements are annotated manually. A total number of $2,416$ turbidity values and 753 salinity values are annotated as anomalous.

5.5 Statistical Analysis of In-Situ Data

The descriptive statistics of the *in-situ* sensor measurements are shown in Table 5.1.

Table 5.1: Descriptive statistics of in-situ measurements

Parameter(units)	No. of Samples	Range	Max	Min	Mean	Median
Turbidity (NTU)	20544	95	95.2	0.2	5.38	4.5
Salinity (ppt)	20544	14.05	31.00	16.95	30.35	30.5
	Std. Deviation	Variance				
Turbidity (NTU)	3.77	14.23				
Salinity (ppt)	0.706	0.499				

From the table, it can be seen that turbidity measurements have a very different distribution than salinity readings. Turbidity values have a much higher standard deviation and variance that indicates they are much noisier than salinity measurements. Figure 5.4 shows the scatter plot of turbidity readings vs. salinity values and their Spearman's correlation coefficient with the p-value. The Spearman's correlation is a non-parametric measure of the monotonicity of the relationship between two datasets. Unlike Pearson correlation, the Spearman's correlation does not assume that both datasets are normally distributed. Like other correlation coefficients, Spearman's correlation varies between -1 and $+1$ with 0 implying no correlation. Correlations of -1 or $+1$ imply an exact monotonic relationship. Positive correlations imply that as "x" increases, so does "y". Negative correlations imply that as "x" increases, "y" decreases. The p-value roughly indicates the probability of an uncorrelated system producing datasets that have a Spearman's correlation at least as extreme as the one computed from these datasets. The p-values are not

entirely reliable but are probably reasonable for datasets larger than 500 [132]. As can be seen from Figure 5.4, the correlation value between turbidity and salinity readings is very low, which indicates there is no strong monotonic relation between these two sensor parameters.

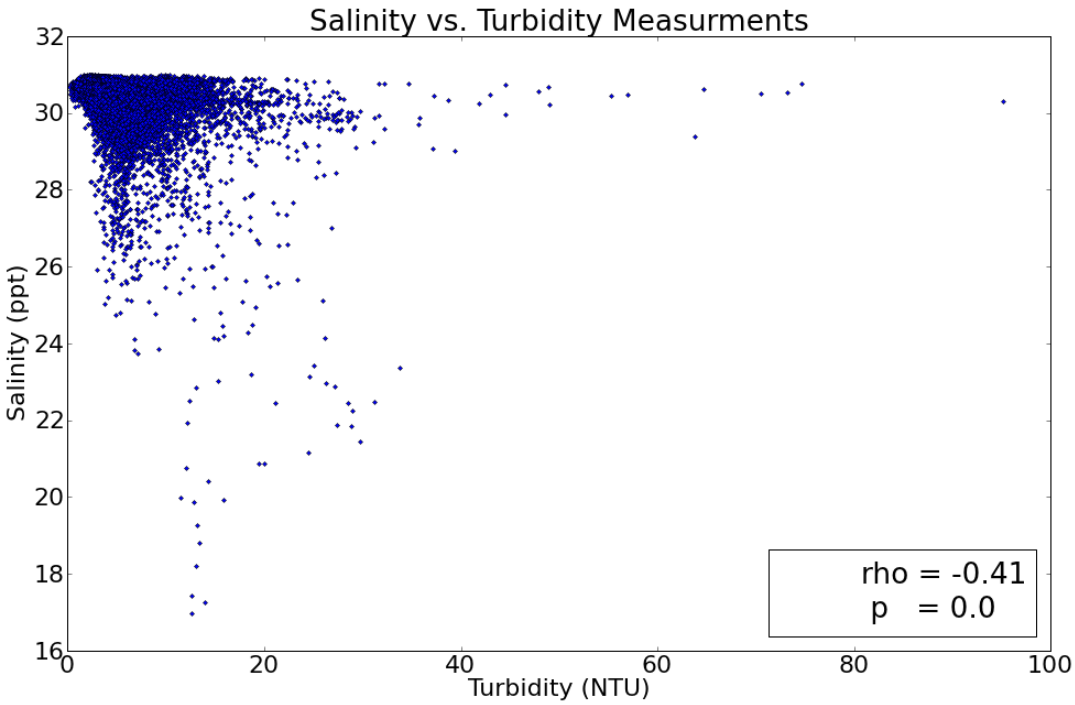

Figure 5.4: Scatter plot of Turbidity vs. Salinity and their Spearman's correlation coefficient(rho) and the p-value.

Figure 5.5 and 5.6 show the graphic representation of the distribution of salinity and turbidity with 50 bins. The inner graphs show the cumulative histogram of the salinity and turbidity measurements. As can be seen from the figures, a small number of bins have higher frequency than others. Due to the global effects such as seasonality, we cannot simply select a threshold to classify anomalies based on their occurrence frequency. Low turbidity measurements can be classified as normal values and high turbidity reading can be classified as abnormal values. However, the sensor readings in the middle range are more problematic as a value can be categorized as normal if previous inputs are lower and have low variation or as abnormal if the previous trend shows high variations. Thus, a simple threshold mechanism may not sufficient to separate anomalous sensor measurements. The same situation occurs in salinity sensor inputs as well, whereby middle range values are difficult to classify.

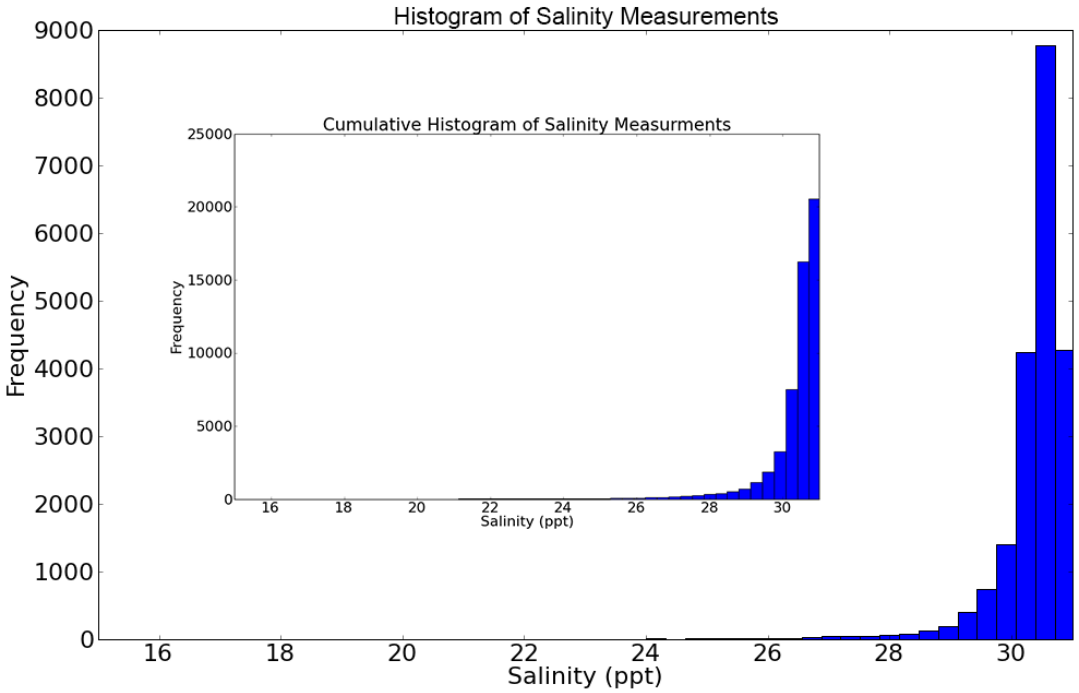

Figure 5.5: Salinity sensor measurements distribution.

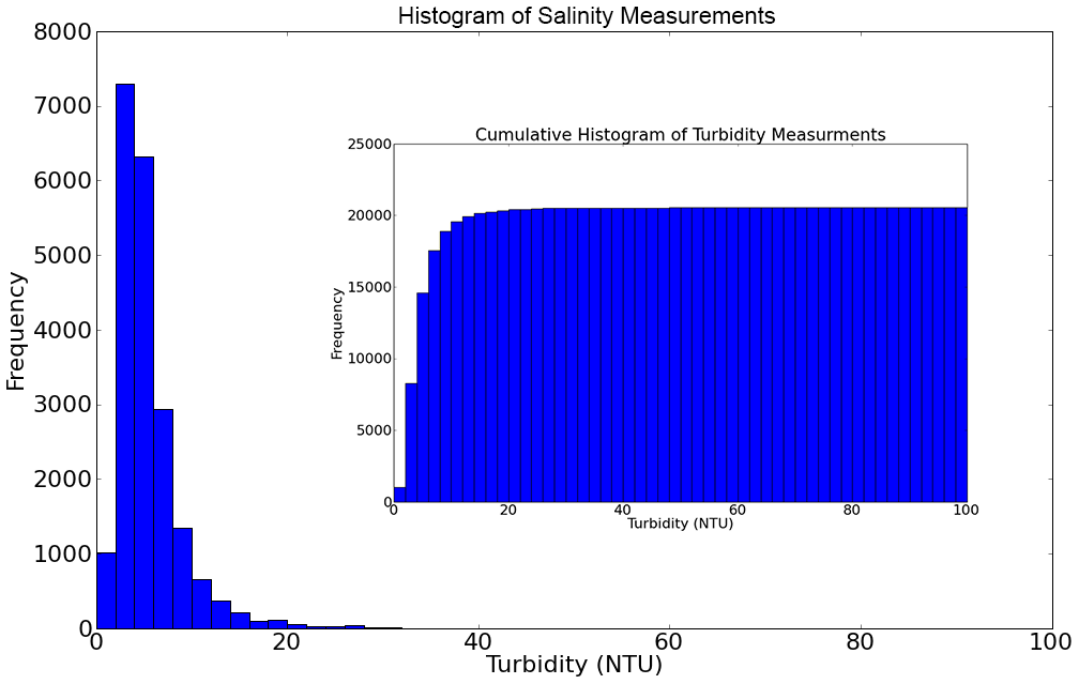

Figure 5.6: Turbidity sensor measurements distribution.

5.6 Parameter Settings

The MoPBAS method consists of a large number of tunable parameters, which can be used to control the sensitivity of the anomaly detection process. Some parameters, such

as the number of elements in the background trend model, upper and lower bonds of threshold, are fixed values during the whole process while others, model learning rate and decision threshold for instance, are updated automatically based on the variation of the input data. The optimal set of parameters, which gives the best performance is application dependent with the potential to be set by the user. Multiple states may be set where for instance one setting may capture all small changes, while another may only capture short-term rapid changes. As previously discussed, one way to obtain a set of values is to analyse the discrete water samples and the affects of each parameter to the model. The second way to obtain a set of parameters is to use a parameter optimizing algorithm. As turbidity readings have a different range and dynamics when compared to salinity measurements, it requires a different set of parameter values in order to detect turbidity anomalies. All the MoPBAS parameters are listed below and how they affect the model is discussed.

- N: is the number of elements of the trend model B. Increasing N will reduce the sensitivity of the system as there is high probability that there might be an element in the background model similar to the incoming sensor reading. However, only the normal values will be pushed into the trend model, thus further increases in N only duplicates existing elements (elements in the trend model are similar to each other) and results in an increase in memory and computational complexity.

- $T_{inc/dec}$: is the step by which the threshold T increases or decreases. Detection performance is not very sensitive to this value and this value is increased if the data exhibits a high degree of variability. This value depends on three main factors, the duration of an event, sampling rate and how fast sensor readings stabilise after an event. The number of $T_{inc/dec}$ should allow an increase of T from minimum to maximum longer than the duration of events and roughly the same length as the time required for stabilisation.

- T_{upper}: is the upper bound of the decision threshold. Increasing this value will reduce the sensitivity of anomaly detection i.e. only large variations will be classified

as anomalies (high precision). This value depends on the variation of sensor measurements at the site and how an outlier is defined. It is also related to the distance calculation method used.

- T_{lower}: is the lower bound of the decision threshold. Reducing this value will increase the sensitivity (high recall) of anomaly detection, smaller changes will be classified as an anomaly.

- T_{scale}: is the equilibrium factor, which stretches $\overline{d}_{min}(t)$ to the same range as the threshold. Lowering this value leads to low precision while a high value leads to low recall.

- L_{inc}: is the trend model learning rate control parameter R increasing interval.

- L_{dec}: is the trend model learning rate control parameter R decreasing interval. The value taken depends on the distribution of the background trend dynamic.

- R_{upper}: The upper bound of learning rate control parameter R. A lower value results a faster updated model. The value taken approximately equals the ratio between L_{inc} and the trend of $\overline{d}_{min}(t)$ values.

- R_{lower}: The lower bound of the learning rate control parameter R. This takes the form of a small positive number to avoid zero background model update probability. The ratio of R_{upper} and R_{lower} roughly defines how fast the learning rate increases.

Based on our understanding of the ecosystem at the site and the analysis of the discrete samples collected at the site, an initial range for each parameter is selected. The values are shown in Table 5.2. For anomaly detection at the test site, a set of parameter values can be chosen from this table.

Table 5.2: Initial Parameter Spaces Based on The Analysis of Discrete Water Samples

	N	T_{upper}	T_{lower}	$T_{inc/dec}$	T_{scale}
Turbidity	[10, 50]	[4.5, 5.5]	[0.5, 2.0]	[0.02, 0.10]	[2.0, 6.0]
Salinity	[10, 50]	[5.0, 13.0]	[2.0, 3.0]	[0.01, 0.10]	[0.5, 4.0]
	L_{inc}	L_{dec}	R_{upper}	R_{lower}	
Turbidity	[3.0, 6.0]	[0.05, 0.3]	[1.0, 5.0]	[0.05, 0.15]	
Salinity	[3.0, 8.0]	[0.05, 0.3]	[1.0, 5.0]	[0.05, 0.15]	

As previously discussed, to obtain one optimal set of parameters, which gives the best performance on the data set, Hyper-Parameter Optimization [133] was applied. Hyper-Parameter Optimization is the process of selecting a set of parameter values for a machine learning algorithm that obtain high performance with good generalization. Many widely-used machine learning algorithms take a significant amount of time to train from data. At the same time these same algorithms must be configured prior to training. These configuration variables are called *hyperparameters*. Hyperparameters generally have a significant effect on the success of machine learning algorithms, for instance, a poorly configured Support Vector Machine may perform no better than random selection. There are many Hyper-Parameter Optimization method in the literature, such as Sequential Model-based Global Optimization (SMBO) [134, 135], Gaussian Process Approach (GP) [136], Tree-Structure Parzen Estimator Approach (TPE) [133], Random Search for Hyper-Parameter Optimization [137]. HyperOpt [138] is a python library for optimizing the hyperparameters of machine learning algorithms which was developed by James Bergstra et al. HyperOpt provides algorithms and software infrastructure for carrying out hyperparameter optimization for machine learning algorithms. In this work, Random Search with HyperOpt implementation is selected due to its simplicity and availability. Moreover, in [138], the author reports that Random Search over the same domain is able to find models that are as good or better within a small fraction of the computation time. The loss function used to obtain the best set parameters for MoPBAS is the inverse of *F1* score $(1 - F1)$. The *F-Score* or *F-measure* is a measure of a statistic tests accuracy. It considers both precision p and recall r of the test to compute the score: p is the number of correct results divided by the number of all returned results and r is the number of correct results divided by the number of results that should have been returned. The *F1* score can be interpreted as a weighted average of the precision and recall, where an *F1* score reaches its best value at 1 and worst score at 0. To find an optimized set of parameters, we first set an initial range for each of the parameters based on the observation of the data and evaluate $1,000$ times on the training dataset to get an initial result. If the optimized parameter value returned is too close to the boundary of the initial range, the initial range of this parameter

is extended. Then we re-evaluate $50,000$ times with the adjusted initial range to obtain the best parameter set. The total number of evaluation loops is hardware dependent, on a standard desktop PC with Intel i7-2600 CPU, it requires approximately 45 hours to evaluate $50,000$ times on the training data. To avoid over fitting, we use the first $10,000$ continuous data points (approx. 50% of the whole dataset) to obtain the parameter values and use the rest data entries for testing. Because MoPBAS randomly selects and updates the element in the background trend model, we run the test 10 times and the averaged F1 score is reported. The initial parameter spaces for turbidity and salinity anomaly detection are shown in Table 5.2 and the results returned from HyperOpt are illustrated in Table 5.3. The results show that although the accuracy on the testing data is not as good as the result obtained from the training dataset, it still achieved comparative performance. This indicates that the parameter values returned from HyperOpt are good sets of parameters for the anomaly detection method and do not over-fit to the training dataset.

Table 5.3: Hyper-Parameter Optimizations Results

	N	T_{upper}	T_{lower}	$T_{inc/dec}$	T_{scale}	L_{inc}
Turbidity	20	5.00	1.73	0.055	4.42	3.60
Salinity	41	10.10	2.96	0.027	1.70	5.26
	L_{dec}	R_{upper}	R_{lower}	Best $F1_{train}$	Avg. $F1_{test}$	
Turbidity	0.20	2.77	0.07	0.86	0.844	
Salinity	0.187	1.85	0.09	0.895	0.841	

The histogram of the turbidity and salinity F1 scores, obtained from the parameter optimizing phase, are shown in Figure 5.7 and 5.8. Both of the figures show that within the initial parameters range, MoPBAS achieves relatively high accuracy. Majority random selected parameter set obtained over 0.8 F1 score. This indicates that MoPBAS anomaly detection is not very sensitive to the initial parameter values, the method can still return relativity high accurate results without tenuously tuned parameters. This also indicates that the initial range of the parameters, which are set based on the analysis of the discrete water sample and how each parameter affects the model are appropriate. A set of parameter values can be set manually. The main advantage of this is that when deploying an anomaly detection system at a new site, the operator can just give a loose set of pa-

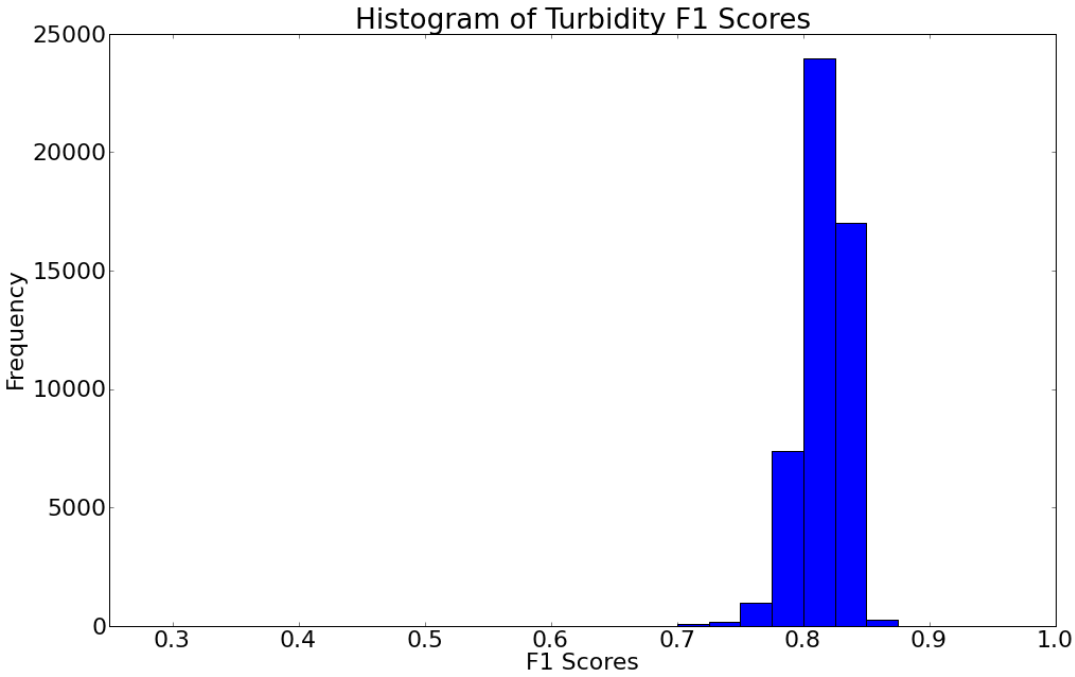

Figure 5.7: Histogram of turbidity MoPBAS HyperOpt training F1 scores (50,000 run)

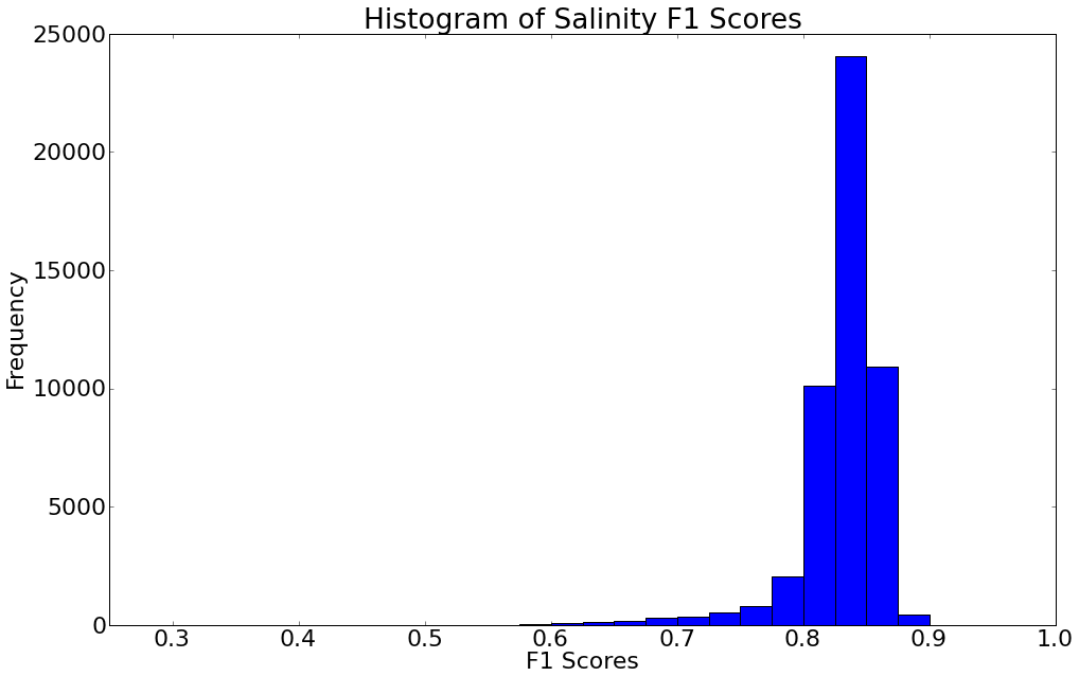

Figure 5.8: Histogram of salinity MoPBAS HyperOpt training F1 scores (50,000 run)

rameter values, which can be obtained from a site survey, to MoPBAS and it will return relatively accurate results. Anomaly detection can be started as soon as an *in-situ* sensor is deployed.

A major challenge of the bag-of-words approach is the estimation of the optimal size

of the codebook. If the codebook is too small, it may cause over-clustering with higher intra-class distortion. Therefore, it is common to choose an appropriately large value of codebook size, but that may cause a dispersive histogram and introduce more noise. One of the common methods to evaluate the codebook size is the Elbow method. The Elbow method is a widely used method for determining an optimal number of words for a codebook. The method starts with a small number of cluster centres K value and keeps increasing it. A plot of the average within cluster sum of squared error (ASSE) against a series of sequential cluster levels can provide a useful graphical way to choose an appropriate K. In general, as the number of clusters increases, ASSE should decrease because clusters are, by definition, smaller. An optimal K value can be defined as the solution at which the reduction in ASSE becomes steady (increasing K does not reduce ASSE dramatically). This produces an "elbow" in the plot of ASSE against number of clusters (words) K. The following measure represents the average within cluster sum of squared error between data points in a given cluster C_k and its cluster centre μ_k where x_i is the element in the cluster:

$$ASSE = \frac{1}{K}\sum_{k=1}^{K}\sum_{x_i \epsilon C_k} \|x_i - \mu_k\|^2 \tag{5.8}$$

The advantage of this method is its simplicity, the fact that it is computationally inexpensive and easy to interpret. However, in some cases, there will not be such an obvious break in the distribution of ASSE against number of words. To evaluate the codebook model, the range of K is set from 1 to 99 with step of 1. Due to the fact that the K-Means method randomly selects the initial cluster centres (some K-Means implementations choose these initial values in a smart way but may be still different), for each K value, we run the experiment 10 times and report the average ASSE and the standard deviation values. As the standard K-Means method uses Euclidean distance, features needs to be normalised. To normalise the features, feature scaling is applied.

$$x' = \frac{x - \min(x)}{\max(x) - \min(x)} \tag{5.9}$$

The first $10,000$ (approx. 50%) data entries are used to obtain the maximum and minimum value and these values are held constant for the rest of the experiments, which means the range of the normalised features are not limited to 0 and 1. There are a few reasons why normalisation is performed at this step rather than normalising the raw input sensor readings. Firstly, the MoPBAS anomaly detection method does not require normalised data. Although MoPBAS does need some prior knowledge about the range and the characteristics of the sensor readings in order to set the initial parameter values, these can be obtained from marine scientists or an initial site survey, which is generally carried out before deploying sensors. Secondly, MoPBAS only needs a few samples (N value) to start detecting anomalies, but the normalisation requires a much larger dataset to get an upper and lower bound. Moreover, any pre-processing will lead to the loss of information; thus, the normalisation should be only performed when necessary. In addition, if another method, feature set or distance measure, which does not require normalised inputs, is used for building a codebook, normalisation may not be required at all. All of the above suggest that normalisation is preferably performed at a later stage rather than on the raw data.

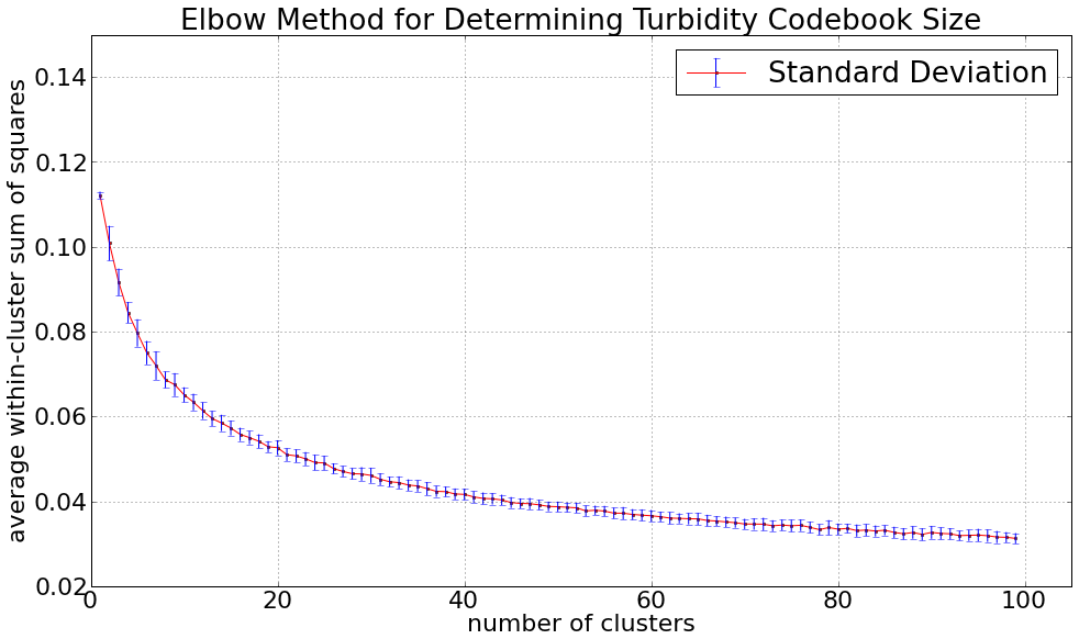

Figure 5.9: Determining the optimal size of turbidity codebook using the Elbow method

The average ASSE and the standard deviation values for each K are illustrated in Figure

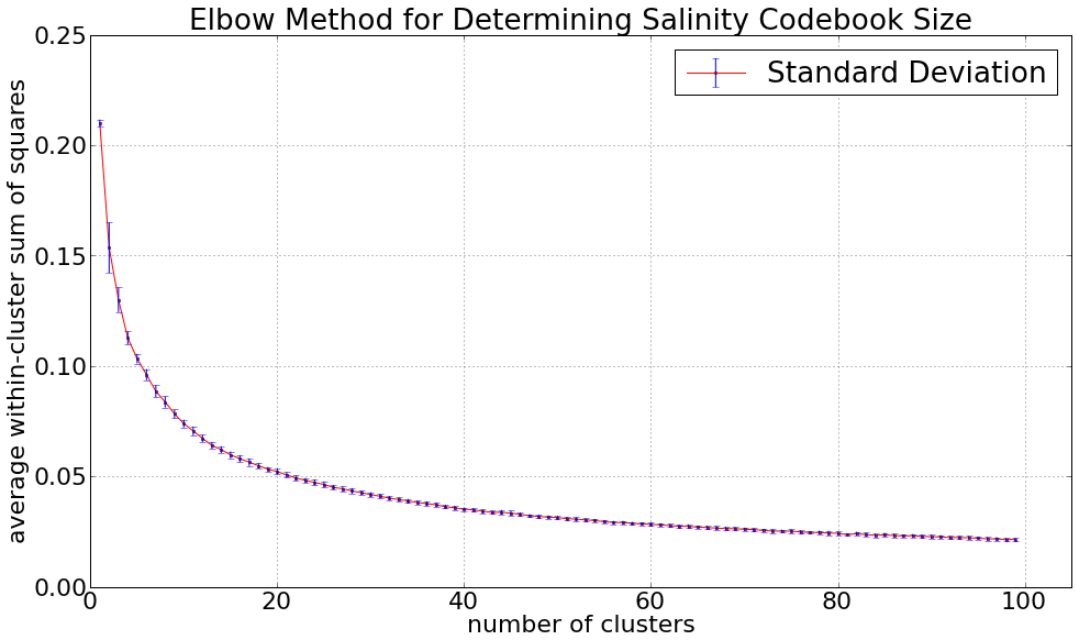

Figure 5.10: Determining the optimal size of salinity codebook using the Elbow method

5.9 and 5.10. The graphs show that both the salinity and turbidity ASSE errors drop dramatically when the codebook size is smaller than 20 and decrease gradually when K is greater than 20. Also, the standard deviation values become small and stable when the codebook consists of more than 20 words. These suggest that a codebook with more than 20 words is a good representation of the anomalous sensor reading detected by MoPBAS. However, adding more words to the codebook will still increase the accuracy. As discussed previously, a smaller codebook may result in an over-clustering model with higher intra-class distortion. This means that the anomalies within the same cluster may have bigger distances between each other. In other words, two anomalies may be assigned to the same word in contrast to different words when using a larger size codebook. Thus, smaller codebook will result of less unique events constructed. Unique events mean that the event has a different feature than all other events in the dataset in contrast to equal events, which have the same feature values extracted. However, the raw sensor readings of equal events may be still different. Figure 5.11 and 5.12 show the number of unique turbidity and salinity abnormal events generated using codebook size from 5 to 80 with step of 5. The results show that increasing the number of words does produce more unique events. For turbidity measurements, approximate 100 unique events are generated when

using the codebook with 5 words and over 350 unique events are constructed when codebooks consisting of more than 75 words are applied. Similar to turbidity, the number of unique salinity abnormal events constructed is 48, when the codebook has only 5 words, and over 90, when the codebooks with more than 65 words are applied. In addition, both of the plots show that when codebooks with 5 to 25 words are used, the number of dissimilar events increases rapidly. In contrast, the increasing ratio becomes small and stable when the number of words is over 25. This suggests that in order to differentiate events constructed, the codebook should consist of at lease 25 words. However, choosing an optimised codebook size for abnormal event detection is still a challenge. Thus, we use a sequence of codebook models from size 5 to 80 with step of 5 and explore how they affect the abnormal events detection results. Once a codebook is created, it can be reused without the need of rebuilding again.

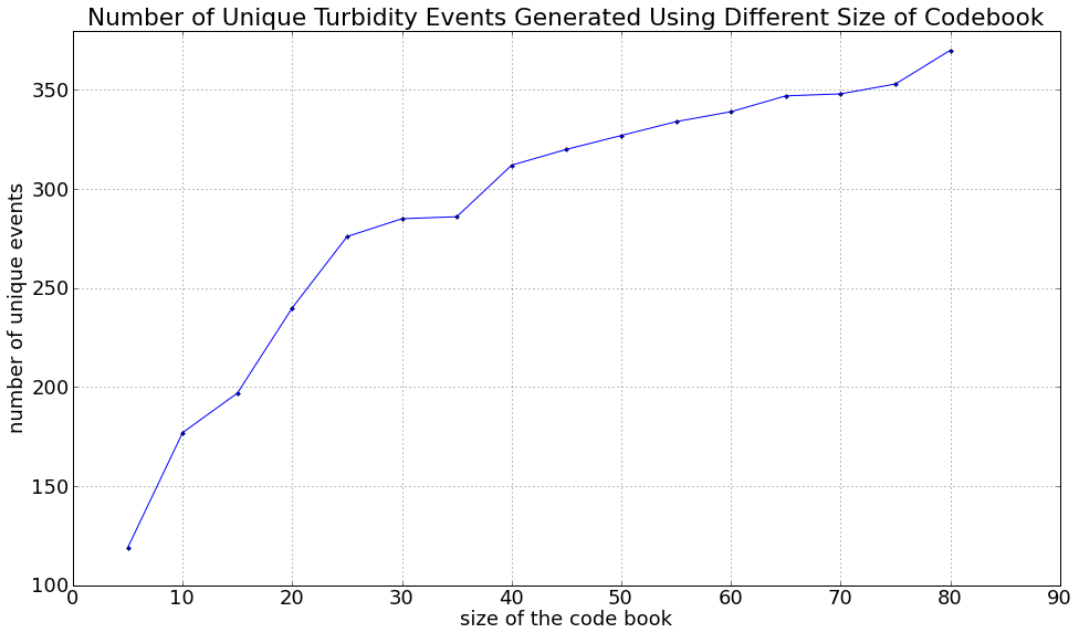

Figure 5.11: Number of unique turbidity events generated using different size of codebook

When constructing an event, T_{gap} is set to 1 to avoid sensor noise and sensor reliability issues. This means that two anomalies are merged into the same event if the gap between them is smaller than 2 samples. This value generally depends on the sampling rate, reliability of the *in-situ* sensor and the complexity of the monitoring site. T_{gap} should be increased if the sampling rate is high, the reliability of the sensor is low or the monitoring site has high variance.

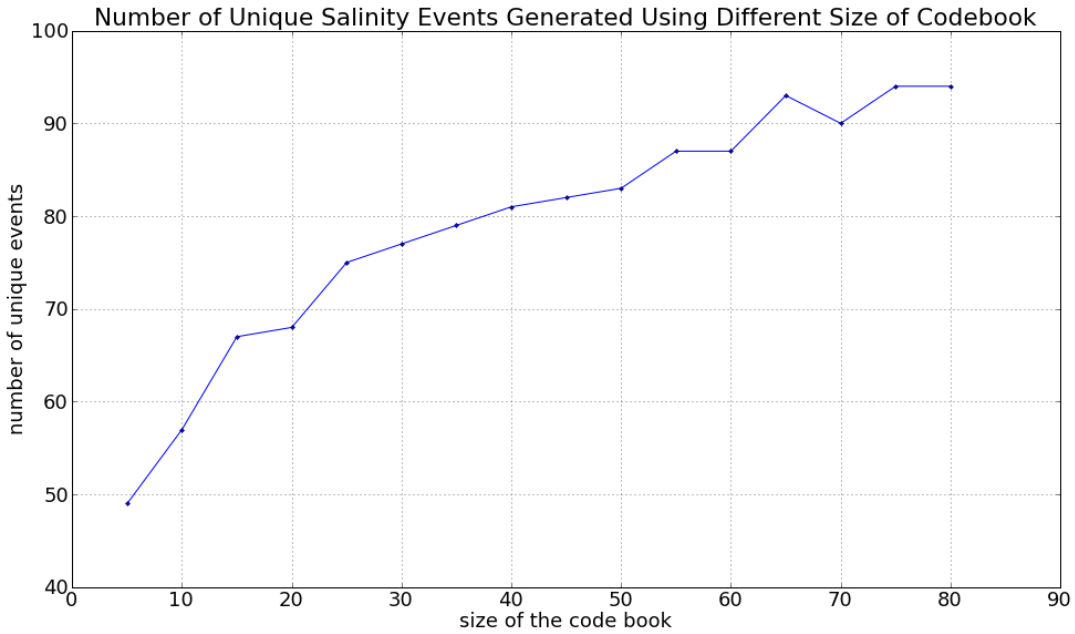

Figure 5.12: Number of unique salinity events generated using different size of codebook

The robust on-line clustering method requires a specified number of clusters. Ideally, this value should be the same or slightly larger than the number of factors that may cause an event at the observation site. However, there are many reasons why this may cause rapid changes in sensor readings, some are known, for example, rainfall events, flood events or shipping events, some are unknown. Thus, choosing a suitable number of abnormal event clusters is complex. Similar to evaluating the size of a codebook, the average within cluster error is calculated to illustrate how the number of the clusters affects the model.

Figure 5.13 and 5.14 illustrate the ASSE value using different codebook sizes and numbers of clusters. The two results show that the ASSE values decrease when the number of cluster centres grow. This suggests that increasing the number of the cluster centres will reduce the within cluster error. Both turbidity and salinity ASSE values drop dramatically when the cluster centres increase from 10 to 20 and decline uniformly when the number of cluster centres is more than 20. This indicates that less than 20 clusters may cause an over-fitted model. The differences among events in a cluster may be much bigger. Although both of the turbidity and salinity within cluster errors show that codebooks with less than 25 words achieved better results, however, the error is much bigger when the number of the cluster centres is small and varies significantly when increasing the number of clus-

ters. This is due to the fact that a smaller codebook will produce an over-clustered model with higher intra-cluster distortion, which results in less unique events to be generated as previously discussed. Events cannot be differentiated when smaller codebooks are used. This also can be seen from Figure 5.13 and 5.14, with the same number of cluster centres, where the distribution of the ASSE values are much larger when the codebook size is smaller than 25 which also suggests that codebooks with less than 25 words may not separate abnormal events accurately and will lead to an over-fitted model. Moreover, Figure 5.13 and 5.14 show that a codebook with more than 25 words achieved comparable but much more stable results for both salinity and turbidity events clustering, which again indicates that less than 25 codewords may cause over-clustering when building a codebook and consequently, can not be used represent the abnormal event precisely. Therefore, the results suggest that a codebook with 50 codewords is a better selection which keeps high accuracy of event representation while keeping computation costs low. Further increasing this number does not reduce ASSE values much. In addition, 50 cluster centres for turbidity event clustering, and 30 cluster centres for salinity event clustering, achieved relatively low within cluster errors and produced stable clustering models. Thus, these two values will be used for the subsequent turbidity and salinity events clustering experiments.

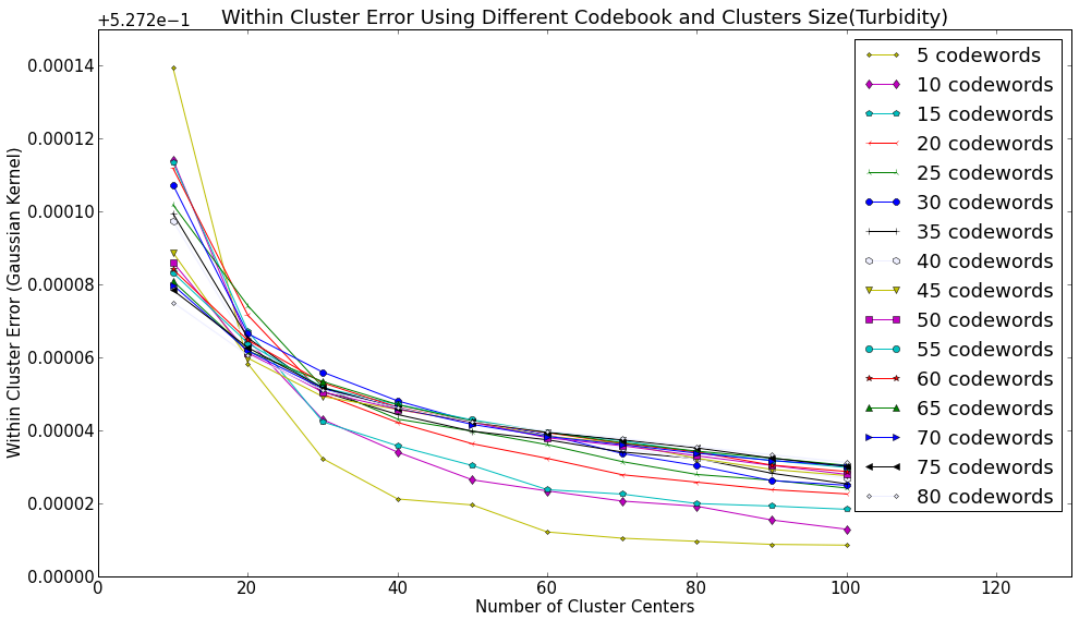

Figure 5.13: Average within cluster error using different codebook size and number of clusters (turbidity)

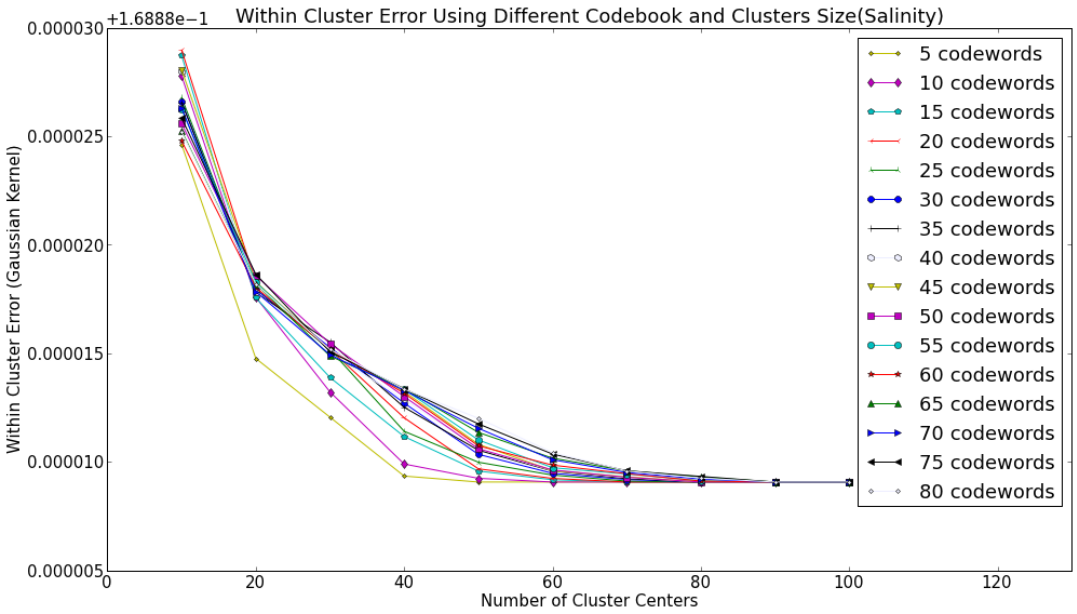

Figure 5.14: Average within cluster error using different codebook size and number of clusters (salinity)

5.7 Salinity Experiment Results

Applying the described MoPBAS anomaly detection, using the optimised set of parameters obtained from Section 5.6, to the entire test dataset results in 861 out of $20,544$ salinity measurements being classified as anomalies. Figure 5.15 shows a 10-day window of the anomaly detection results. The red dots indicate salinity anomalies detected, while the blue line is the sensor measurements and the green solid line is the closest matching entry in the background trend model. As illustrated in Figure 5.15, most of the abnormal salinity readings are detected accurately. Figure 5.16 demonstrates adaptation of the detection threshold and background learning rate based on variation in the mean minimum distance ($\overline{d}_{min}$) between sensor measurements and background trend model. The red line at the bottom represents the background learning ratio. The decision threshold is shown in blue and the minimum distance between sensor readings and the best match entry in the model is shown in green. However, as can be seen from Figure 5.15, the spike occurs (vertical magenta dash line after Oct 10 2010) after the last event is ignored by the anomaly detection system. This is due to the fact that after an event happened, the water body is typically very turbid before it settles down. This can be seen from Figure 5.15,

the raw salinity measurements after Oct 10 2010 are much noisier than sensor readings prior to Oct 07 2010. However, the overall trend of the sensor readings falls back to a similar range as before. During this settle down period, the sensor readings are normally very noisy which may not reflect the true property of the water body. Thus, the increase of the threshold will ignore small spikes during this stabilizing period, especially after a significant event occurs. An example of this is shown in Figure 5.15 (vertical red dash line); even though the absolute value of the salinity reading is lower than the majority of the anomalous detected, the system still classifies it as a normal reading. The threshold decreases towards the lowest value (T_{lower}) after the event terminates. The duration of this decreasing interval approximately equals to the settle down period, thus the system will start capturing small events again after the water body calms. But if the operators need to capture these spikes, higher $T_{inc/dec}$ and lower T_{lower} values are required to shorten the threshold dropping period and increase the anomaly detection sensitivity. However, in the current implementation with static $T_{inc/dec}$ and T_{lower} values, this will also increase the overall sensitivity of the system.

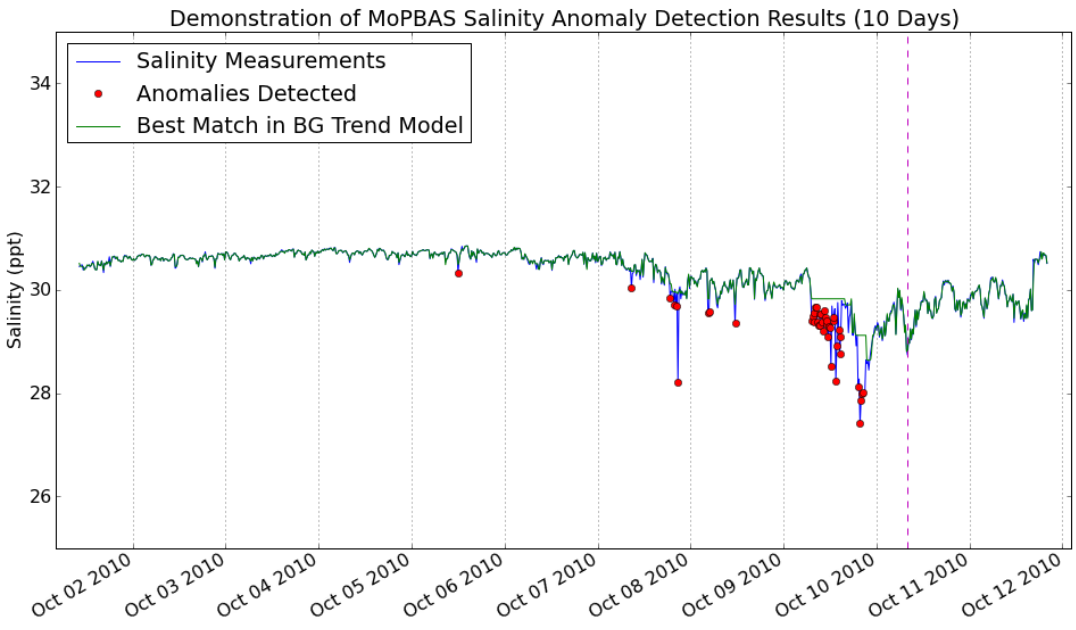

Figure 5.15: A 10-day window of the MoPBAS salinity anomaly detection results. Vertical dash line indicates the settling down period (a short time window after a significant event) where relatively large variation will be ignored.

In order to cluster events into groups based on their similarity, detected anomalies are

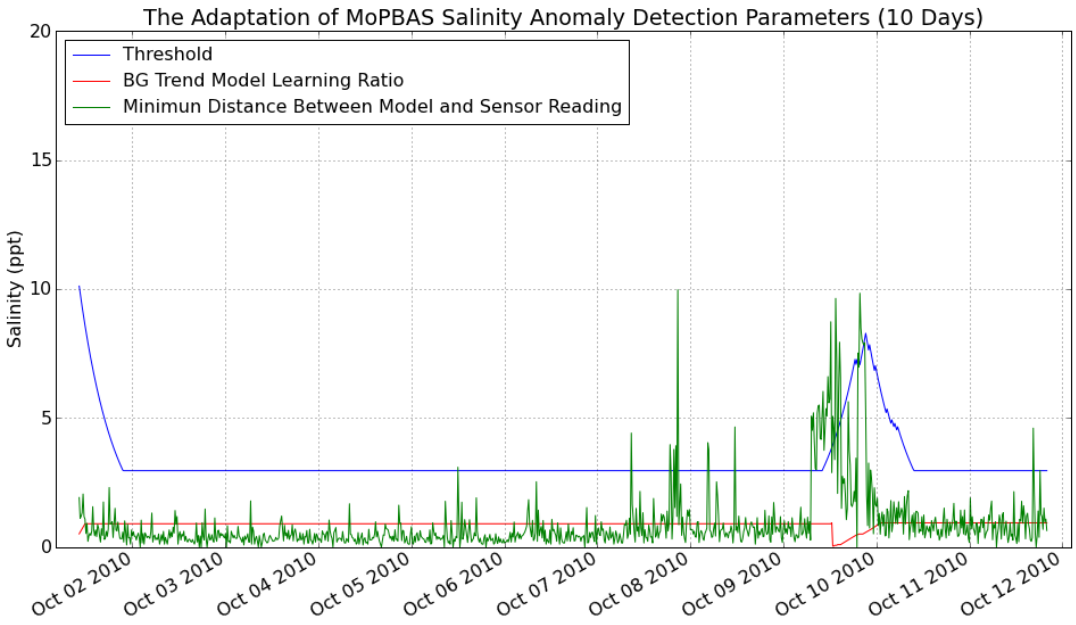

Figure 5.16: Detection threshold, background trend model learning rate and minimum distance between input value and best match element in model.

merged into events based on their timestamps. From the 861 outliers detected, 222 salinity events are constructed using the agglomerative hierarchical clustering method with T_{Gap} equal to 1. For each salinity anomaly detected, a set of features is extracted as the feature vector of the sample. Each feature set of the anomalous value is normalised as a "word" using the codebook that previously built. The histogram of the occurrence of each word for each event constructed is used as the feature set of the event.

Table 5.4: Clustering results, showing the number of similar events within each cluster group.

Clusters	Number of events	Events
Clusters 0	179	Event 0, 2, 5, 25, 107, 109, etc.
Clusters 1	3	Event 205, 206, 213
Clusters 2	3	Event 35, 220, 221
Clusters 3-39	1 (in each)	Event 6, 7, 22,23,30,31, 40 Event 44, 45, 47, 53, 61, 63 Event 65, 70, 71, 72, 73, 74 Event 82, 111, 121, 126, 129 Event 139, 149, 151, 152, 157 Event 158, 159, 160, 168, 173 Event 174, 209, 218

After applying the described clustering methods to the whole dataset, a total of 40 ($N =$

40) clusters are created. The number of events in each cluster is shown in Table 5.4. ROC is a tree-like clustering method; under any cluster center, there is still a sub binary tree structure that consists of nodes and elements. A node could contain sub-level nodes or elements or their combinations.

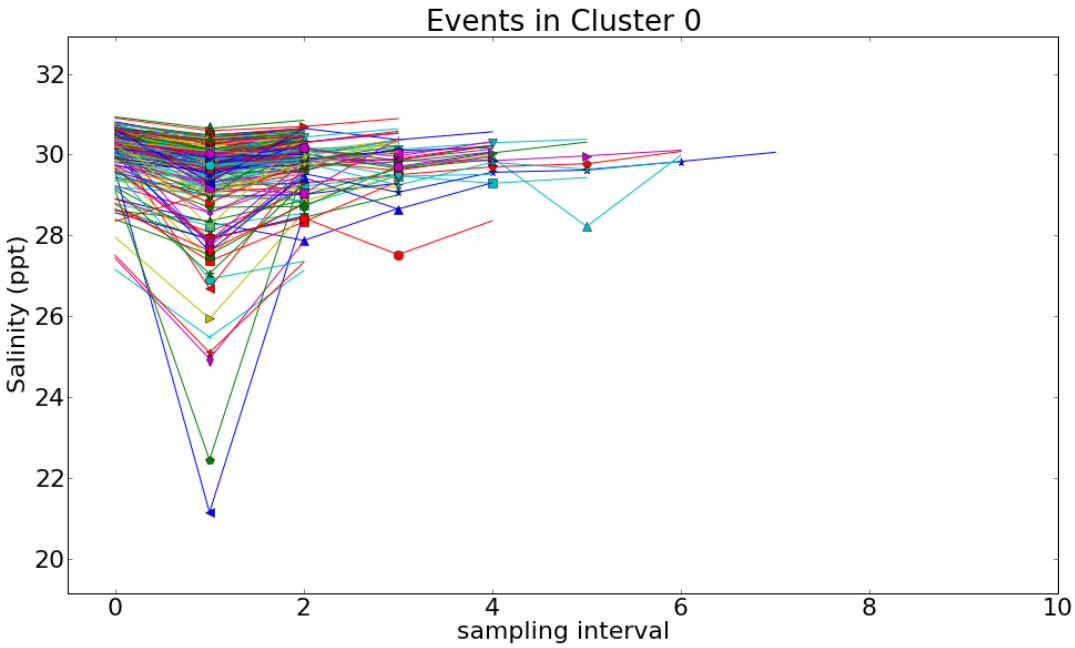

Figure 5.17: Plot of the salinity measurements of all events in cluster 0.

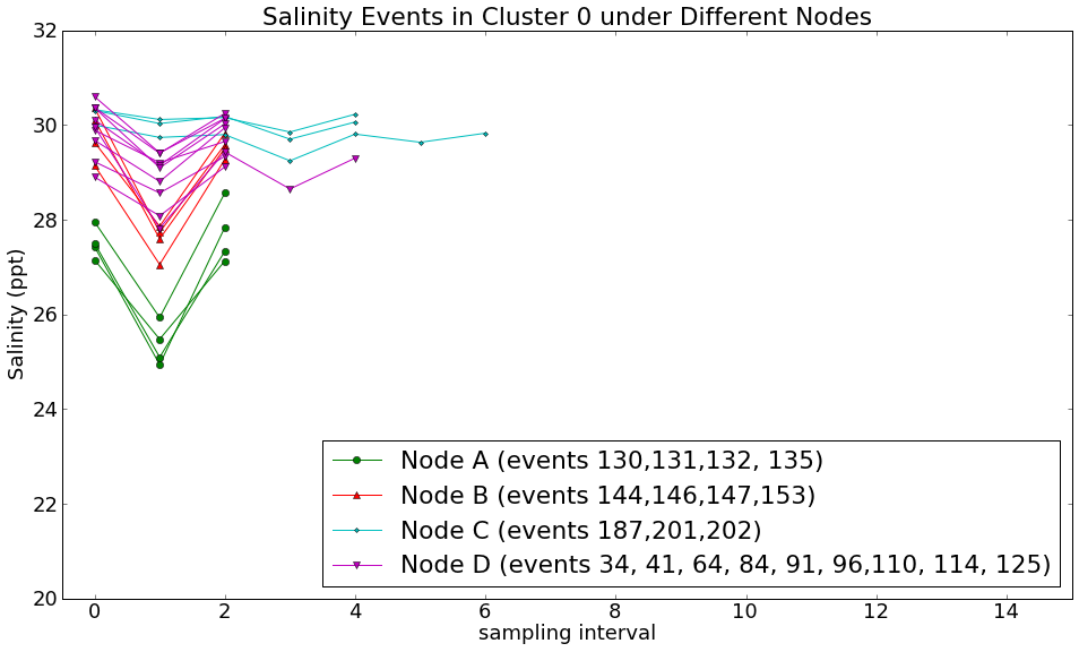

Figure 5.18: An example of the salinity measurements of some events that under the same node and different nodes in cluster 0.

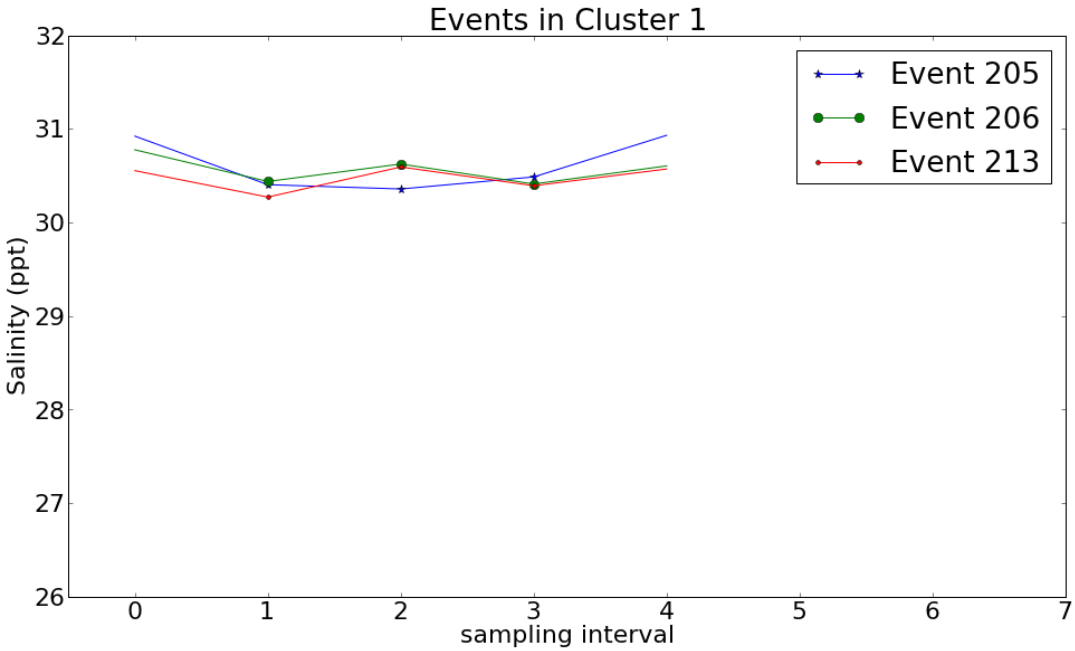

Figure 5.19: Plot of the salinity measurements of the three events in cluster 1.

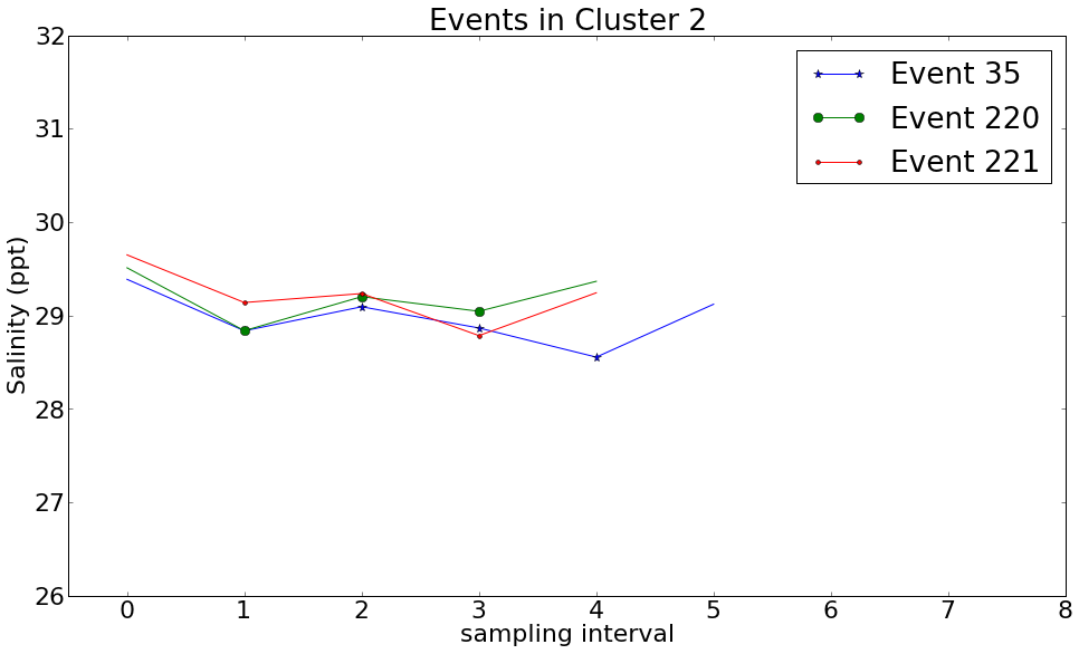

Figure 5.20: Cluster 2 consists of three salinity events.

Figure 5.17 plots the salinity sensor measurements of all events in cluster 0. As can be seen from the figure, cluster 0 contains the highest number of events. Figure 5.18 shows events within cluster 0 under different nodes. As shown, the events under the same node are very similar and there are some connections between different nodes, such as, all events under node A and B have downwards 'V' shape but are offset vertically. Cluster

1 consists of 3 similar events and there are also 3 events in cluster 2. Cluster 3 to cluster 39 only contain 1 event in each. Figure 5.19 demonstrates the three events in cluster 1, the results show that events are similar to each other within the cluster. All of the three events have a 'W' like shape, which have a decreasing reading at the beginning and increasing measurements at the end. Event 206 and 213 have a peak in the middle but event 205 has not, however, the gap is relatively small. Figure 5.20 shows all the events in cluster 2 where it can be seen that tree events do have similar variations (a rotated 'W' shape). Although event 35 contains more samples (longer duration) than the other two events in the cluster, it still has a similar 'W' shape to the others. Figure 5.21 illustrates the difference between events in different clusters. As can be seen from the graph, events within the same cluster have similar trends but events in different clusters have very different profiles. For visualisation purposes, every 5th cluster, from cluster 3 to the others, are plotted

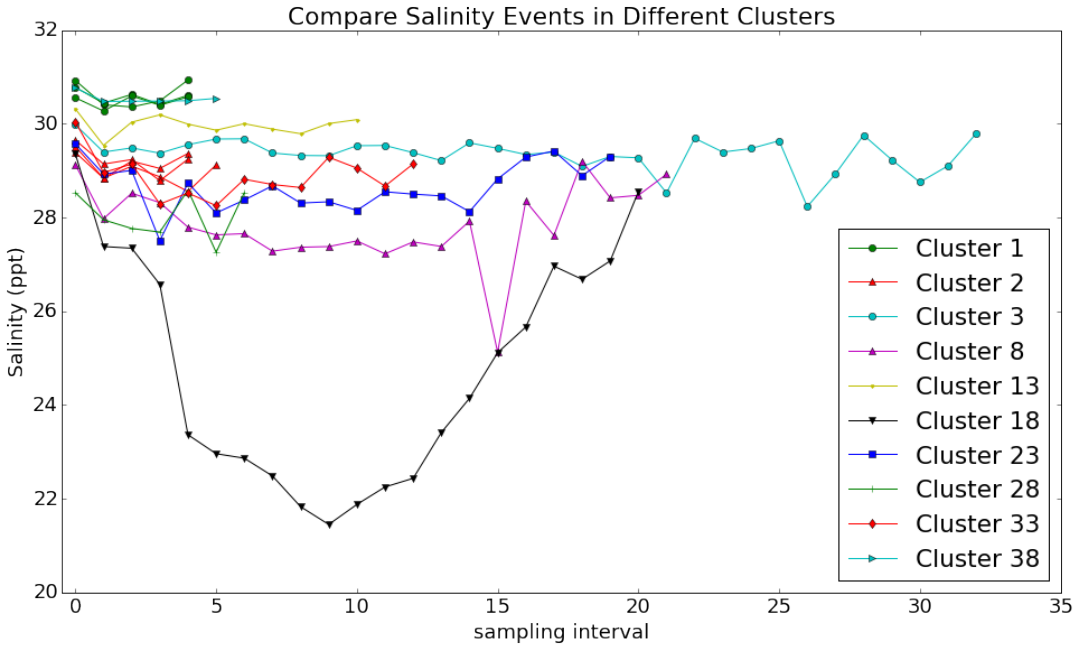

Figure 5.21: Comparison of salinity events in different clusters.

5.8 Turbidity Experiment Results

Applying the same procedures to turbidity data, $2,706$ sensor measurements are classified as anomalies. Figure 5.22 demonstrates a 10-day subset of turbidity anomaly detection results. The red dots are the turbidity anomalies detected, the blue line is the sensor measurements and the green solid line is the closest matching entry in the background trend model. Figure 5.23 demonstrates adaptation of the detection threshold and background learning rate based on variation in the mean minimum distance ($\overline{d}_{min}$) between sensor measurements and background trend model. As with detection of anomalies in the salinity dataset, the classification threshold increases when readings become highly variable and decreases when measurements do not change rapidly. In contrast, the model learning rate decreases sharply when events are happening and increases slowly when sensor readings are stabilising.

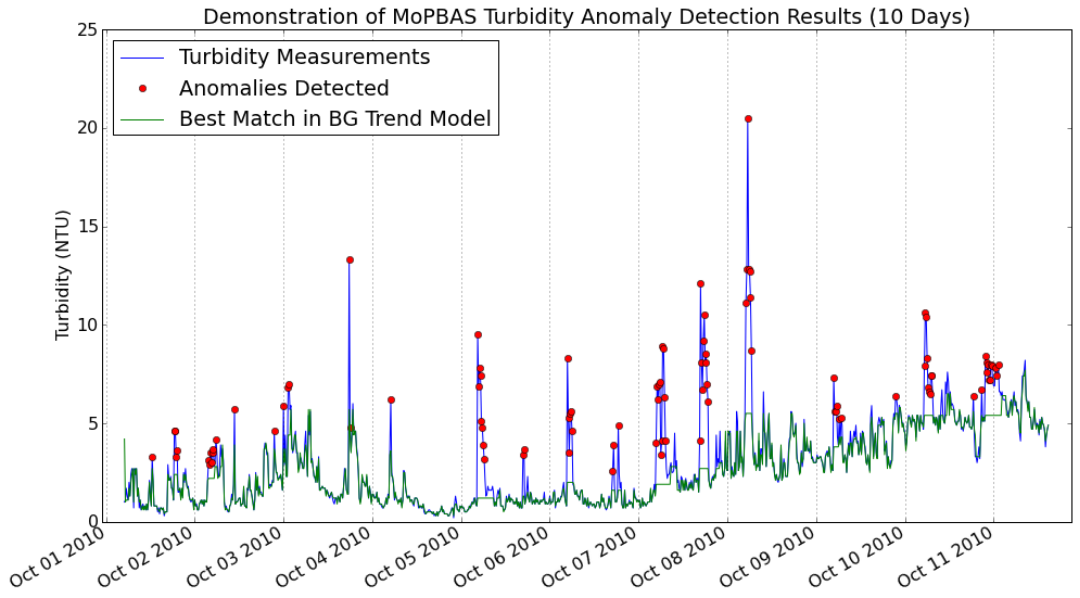

Figure 5.22: A 10-day window of the MoPBAS turbidity anomaly Detection Results.

Turbidity anomalies are grouped into events according to their timestamps. For the whole dataset, 693 events are constructed from the classified anomalies. Table 5.5 lists the clustering results and the turbidity events in each cluster.

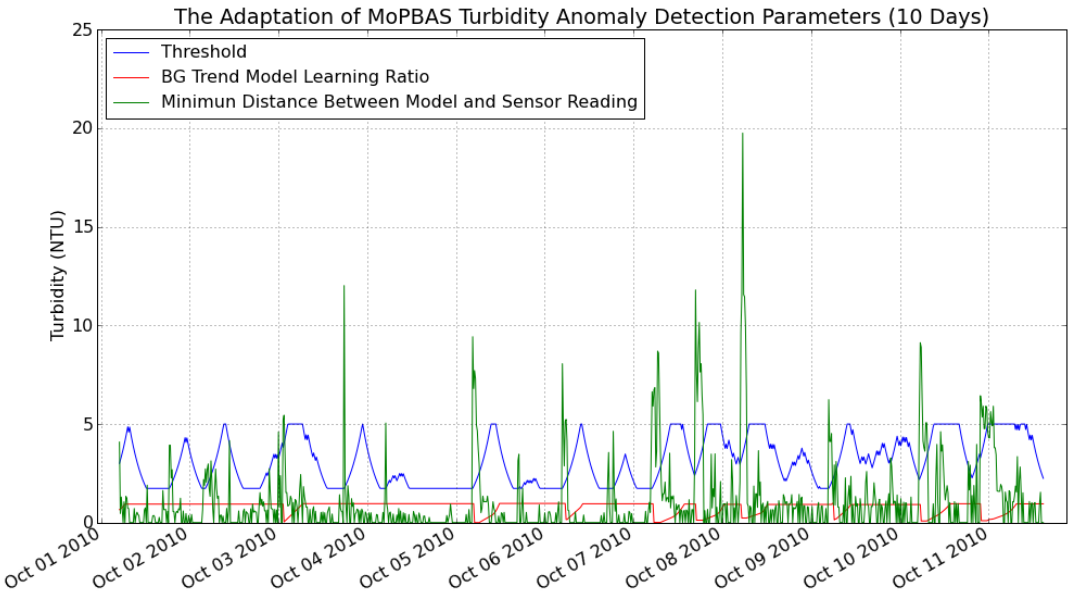

Figure 5.23: Detection threshold, background trend model learning rate and minimum distance between input value and best matching element in the background model.

Table 5.5: Results of turbidity event clustering, showing the number of similar events in each cluster group.

Clusters	Number of Turbidity Events	Events
Clusters 0	628	Event 0, 1, 10, 21, 152, 577, etc.
Clusters 1	4	Event 150, 175, 289, 349
Clusters 2	2	Event 649, 683
Clusters 3	2	Event 133, 288
Clusters 4	2	Event 64, 252
Clusters 5-59	1(in each)	Event 15, 16, 35, 53, 57, 84, 87 Event 92, 94, 119, 123, 126, 129, 141 Event 174, 177, 179, 180, 226, 230 Event 233, 235, 239, 273, 300, 301 Event 316, 326, 328, 347, 366, 368 Event 372, 381, 388, 392, 421, 496 Event 505, 522, 552, 555, 570, 607 Event 608, 615, 620, 641, 642, 674 Event 681, 687, 690, 691, 692

Figures 5.24 and 5.25 show all events in the corresponding cluster where it can be seen that the events within the same cluster have similar variations. Three out of four events in cluster 1 have a rapid increase at the beginning followed by a small rise and then settle down. Although, event 150 does not have a rapid change at the start, its overall trend is very similar to the other three events in the cluster. It has a very similar variation but offset

to the right by a few samples. As can be seen in Figure 5.25, the two events in cluster 2 are different in length. However, both of them show an 'M' like pattern. This shows the advantage of bag-of-words approach, which encode anomaly features as constant length descriptors. Events in cluster 3 are shown in Figure 5.26. It can be easily seen that both of the two turbidity events have comparable appearance. Events shown in Figure 5.27 once again demonstrates the advantage of the bag-of-words approach. Although, the two events do not have an exact pattern, the variations are very similar. Both of the two turbidity events have an increased reading at the beginning followed by a concave shape then rise quickly again before settling down.

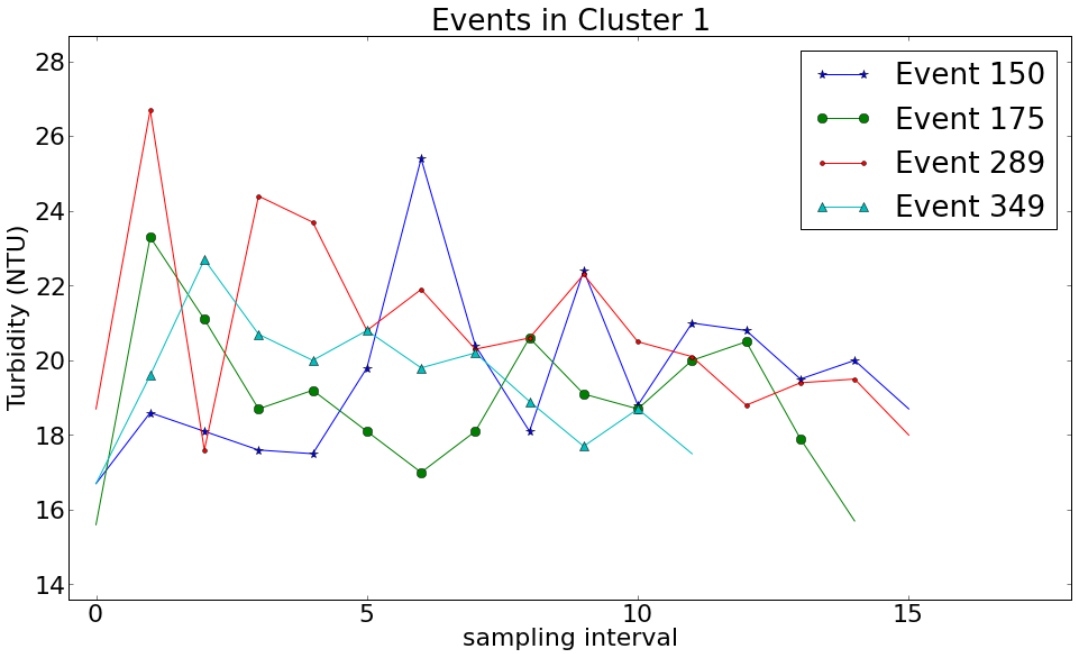

Figure 5.24: Plot of the turbidity measurements arising from events classified as being in cluster 1.

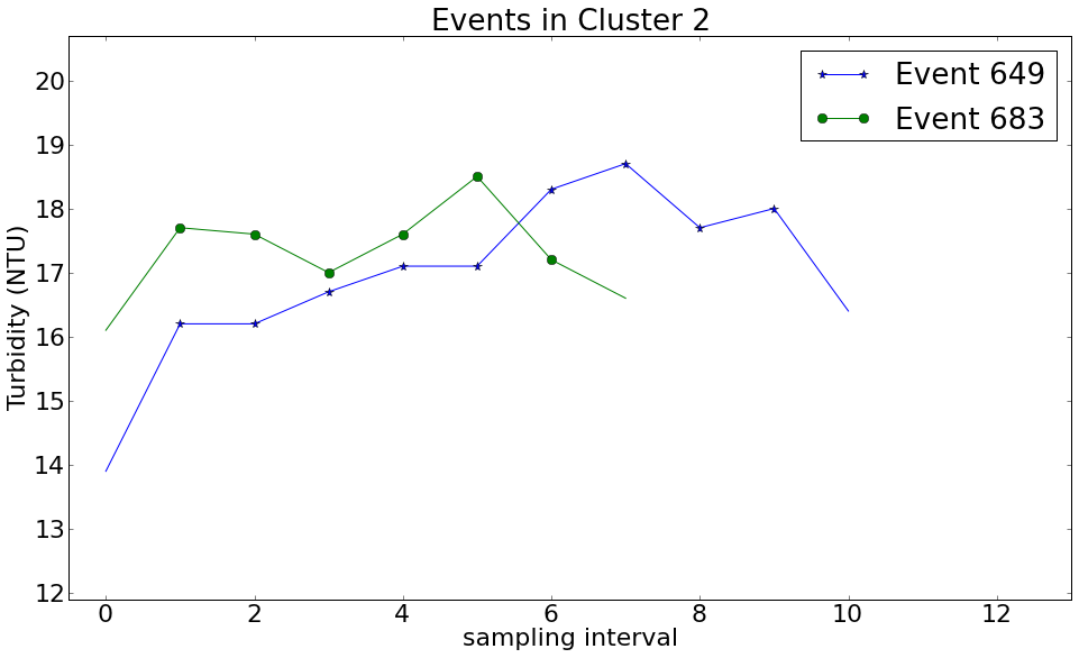

Figure 5.25: Plot of the turbidity measurements from events in cluster 2.

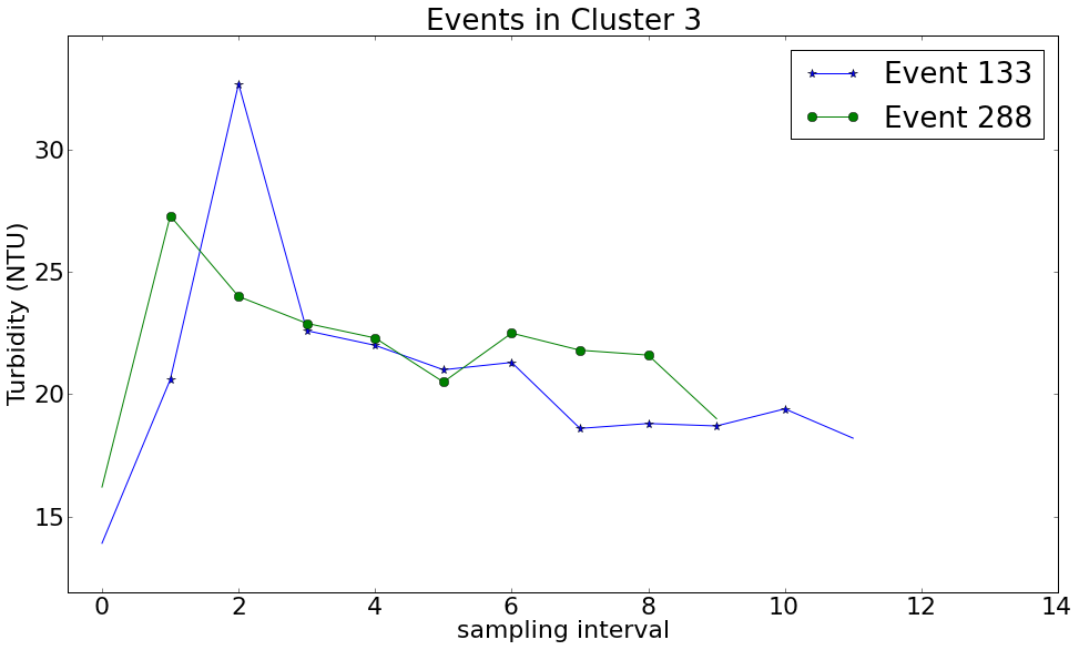

Figure 5.26: Plot of the turbidity measurements from events in cluster 3.

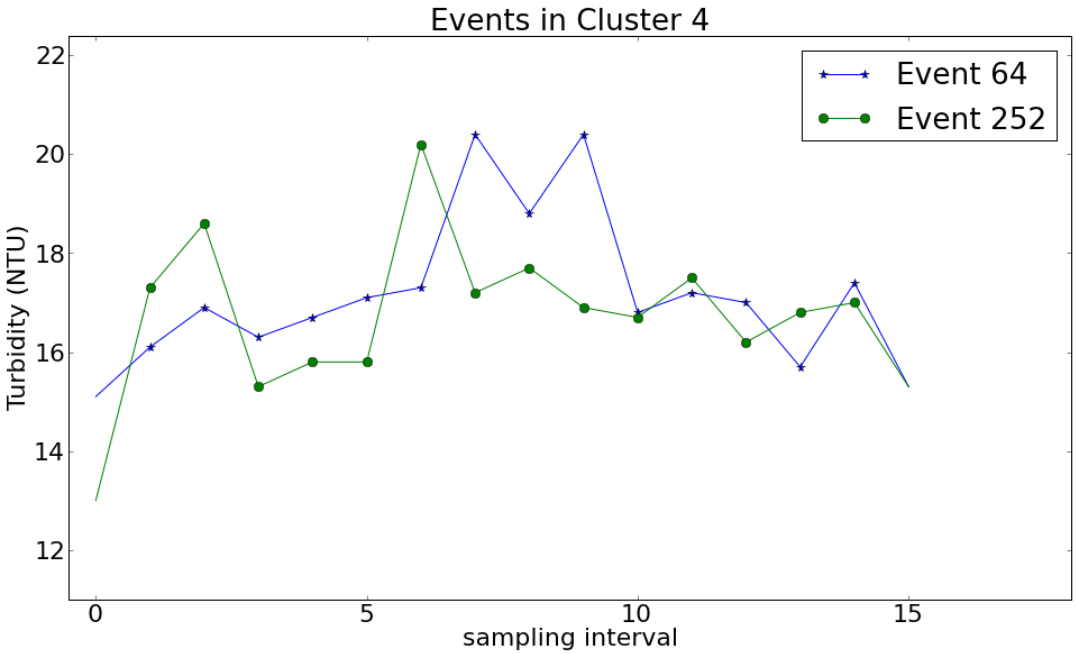

Figure 5.27: Plot of the turbidity measurements from events in cluster 4.

Figure 5.28 shows a comparison of events in different clusters. The plot illustrates that events within different clusters do have disparate trends. A sample of unique turbidity events (event in every 10th cluster from cluster 5 to 55) is shown in Figure 5.29.

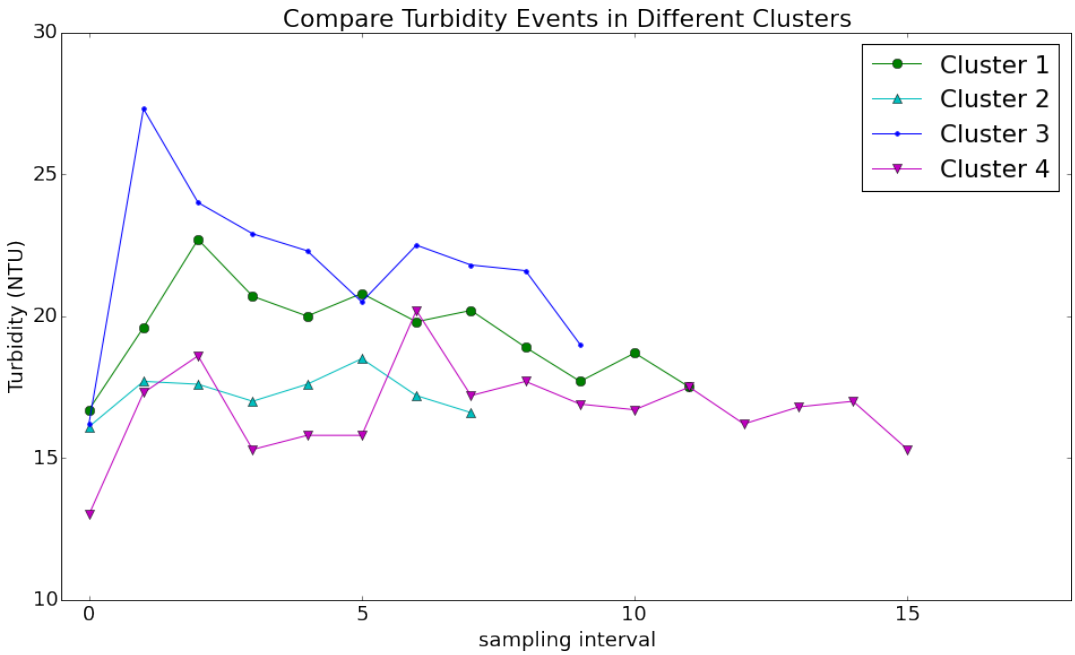

Figure 5.28: Comparison of events in different clusters (Cluster 1,2,3,4). For illustration purposes, only one event in each cluster is shown.

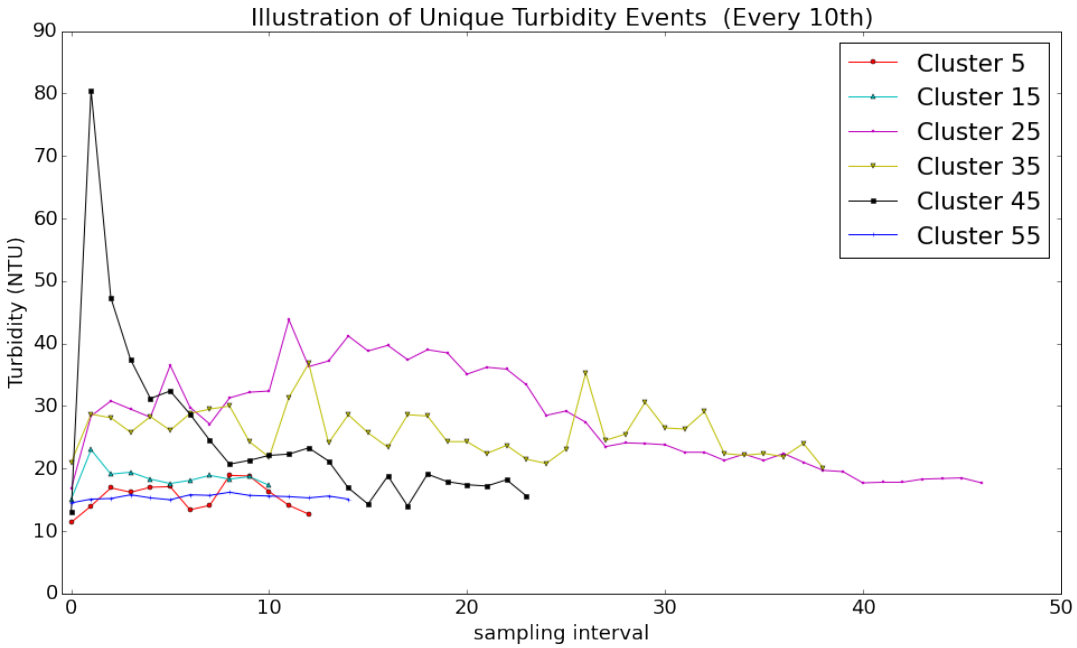

Figure 5.29: Illustration of the differences in turbidity readings between assigned clusters.

5.9 Discussion

Both salinity and turbidity anomaly detection results show that the MoPBAS method is suitable for detection of anomalous sensor readings. The MoPBAS method not only detects upward turbidity unusual sensor readings but downward abnormal salinity measurements. Real-time updating of the background trend model provides the capacity to model the trend of both a highly variable data stream and gradual changes such as tide or seasonal effects. The dynamic threshold and model updating rate are appropriate for detection of environmental events in estuaries. As can be seen from Figures 5.16 and 5.23, the classification threshold is increased when an anomaly is detected. This is due to the fact that after an event happens, there is usually a period of time where the sensor measurements return to a baseline (i.e. these readings usually alter in step changes rather than monotonic increases). During this settling down period, the water body is turbid, which results in a much noisier sensor reading. The raising of the threshold can handle this effect and reduce false positives. The threshold falls back slowly when the water body starts settling down. Another advantage of this adapted threshold is that the system only detects large

variations during periods of high fluctuation while small changes will be captured during periods of relative stability. In contrast, the background learning rate remains high during stable periods and decreases rapidly when an anomaly is detected. This is because the background model should simulate the trend of the water quality parameters but ignore sudden variations. However, as the threshold is raised, the input is likely to be classified as normal even though it is relatively different to the average trend. So the model learning rate is increased and the trend model will be updated as soon as the sensor readings are returning to normal.

Figures 5.21 and 5.29 show that the ROC clustering method successfully discriminates between events, assigning them to clusters where events within the same cluster are relativity similar to each other. Unique events are treated as new cluster centres (such as clusters 5, 15 and 25 in the turbidity clustering example). This feature is very important from a water quality event detection perspective as these events have no analogous events in the past, and thus are potentially of greater importance to operators. These are the significant events, which would trigger an alert when being detected, thus allowing operators to react accordingly.

5.10 Summary

In this chapter, a case study is carried out to illustrate how abnormal events can be detected and further catalogued into groups from *in-situ* salinity and turbidity measurements. By applying state-of-the-art machine learning techniques, such processes can be fully automated. The system provides an opportunity to convert raw sensor readings into a more human understanding and accessible format, which is more suitable for management. This also introduces intelligence into the *in-situ* sensor network, for example, alerting operators when an abnormal event is being detected. In addition, the system can potentially process *in-situ* data at a greater scale, which enables the monitoring of marine environment over a much larger region. Ultimately, such information can potentially provide an improved operator view of the functioning of environments such as estuaries, and

hence improve decision making capability. The system can support decision makers in constructing new policies to better protect environmental and coastal resources.

CHAPTER 6

VISUAL DATA PROCESSING

6.1 Introduction

Visual systems have been identified as effective tools for aquatic environment monitoring. Automated analysis of image data for detecting environmental processes has been studied in a wide variety of contexts.

Davidson et al. [139] described the CoastView project, which focuses on the development of a video-derived coastal state indicating system in support of coastal zone management. The CoastView project illustrated how the use of fixed remote video sensing system can potentially ameliorate issues associated with *in-situ* sensing. Goddijn-Murphy et al. [38] used an off-the-shelf digital camera to estimate near shore water color by calculating yellow substance and chlorophyll concentrations from the image data stream. In [39], Wang et al. built a Short-Term Rainfall Nowcasting system using rainfall radar images. By using image processing and morphology analysis techniques, they achieved a high accuracy in predicting short-term rainfall over a large area. Research in the Fish4Knowledge project [40] demonstrated the use of under water cameras for fish detection, species identification and behaviour recognition. Over $3,000$ different species of fish were observed during the three years deployment period.

Other studies have investigated the use of cameras and analysis of the resulting image data for other forms of environmental monitoring applications. Graham et al., in [140], investigated the use of cameras in determining the dynamics of expanding leaf area for Rhododendron Occidental. In [141], Richardson et al. explored whether digital images could be used to monitor spring green-up in a deciduous northern hardwood forest. They all concluded that cameras offer an inexpensive means by which environmental changes can be quantified.

Analysis of the *in-situ* sensor data obtained from our pilot system along with on-site observations and discrete grab sampling demonstrates that when shipping traffic occurred at the port it often coincided with rapid changes in data from the turbidity sensor. The same effects are not seen with the activity of small boats in the area. Isolating such events that are caused by known factors from the sensor measurements stream automatically is greatly desired from an environmental monitoring perspective. It can significantly reduce the amount of data that needs to be further analysed since the causes of these events are identified. Moreover, when analysing and modelling long term environmental variations, such as climate changes, these data points need to be removed as they are caused by local activities and do not reflect the global characteristics of the water body. However, there were turbidity events without associated shipping events. These turbidity variations are highly interesting to marine scientists as their causes are unknown and require further investigation. In addition, successfully identifying such events can be used to indicate when a grab sampling should be carried out to increase the efficiency and effectiveness of these manual processes.

The benefits of using visual sensing for environmental monitoring can be summarized as follows:

- Cameras provide visual evidence that can be used to verify *in-situ* sensor variations.
- By combining outcomes from visual sensors and *in-situ* sensor modalities, the amount of data that requires further analysis can be reduced.
- Visual analysis in multi modality sensor networks increases the accuracy of long

term environmental modelling by removing variations caused by local factors.

- Multi-modal smart sensing system can be used as an indicator of when a sophisticated grab sampling should be performed to increase the efficiency and effectiveness of the manual processes.

In this chapter, a case study of how shipping events can be detected using image data captured by a visual sensor and how this information can be used to complement *in-situ* sensor abnormal event detection from *in-situ* data process stream is presented. A series of experiments were carried out to evaluate the performance of the proposed system.

This chapter is organized as follows. Section 6.2 explains how motion of large size ships affects water quality such as turbidity levels, at coastal areas, both from the results reported in the literature and on-site discrete sampling analysis outcomes. The proposed detection framework is introduced in Section 6.3 and the methodology is described in detail in Section 6.4. The dataset used for evaluating the performance of the proposed system is described in Section 6.5. Parameter selection for low level feature extraction, high level descriptor construction and event classification is carried out in Section 6.6. The performance of the proposed system is evaluated and the results are discussed in Section 6.7. The combination of turbidity event detection results from *in-situ* data processing stream and the shipping event detection from visual data processing stream is illustrated in Section 6.8. Based on the results obtained, further experiments were carried out in Section 6.9 to detect a more specific shipping event (P&O arrival) at the scene by altering the settings of the proposed system. A summary of the visual data processing stream is drawn in Section 6.10.

6.2 Shipping Traffic and Turbidity at Estuaries

Turbidity events are largely related to vessel activity at Dublin Port, caused by re-suspension of sediments by vessel propulsion systems [106]. The effect of shipping traffic to the local marine ecosystem has previously been discussed in Section 5.2.2. At the test site,

on-site discrete sampling was carried out by colleagues on 15th Aug and 7th Sep 2012 to investigate how shipping events can affect turbidity levels and other water quality parameters.[106]. Figures 6.1 and 6.2 (Source: [106]) show the analyses of water samples collected at different depths (0.5, 2.5 and 4.5 m) before (approx. 15 mins), shortly after (approx. 10 mins) and after (approx. 45 mins) a P&O ferry arrival event along with the turbidity levels measured from *in-situ* sensor.

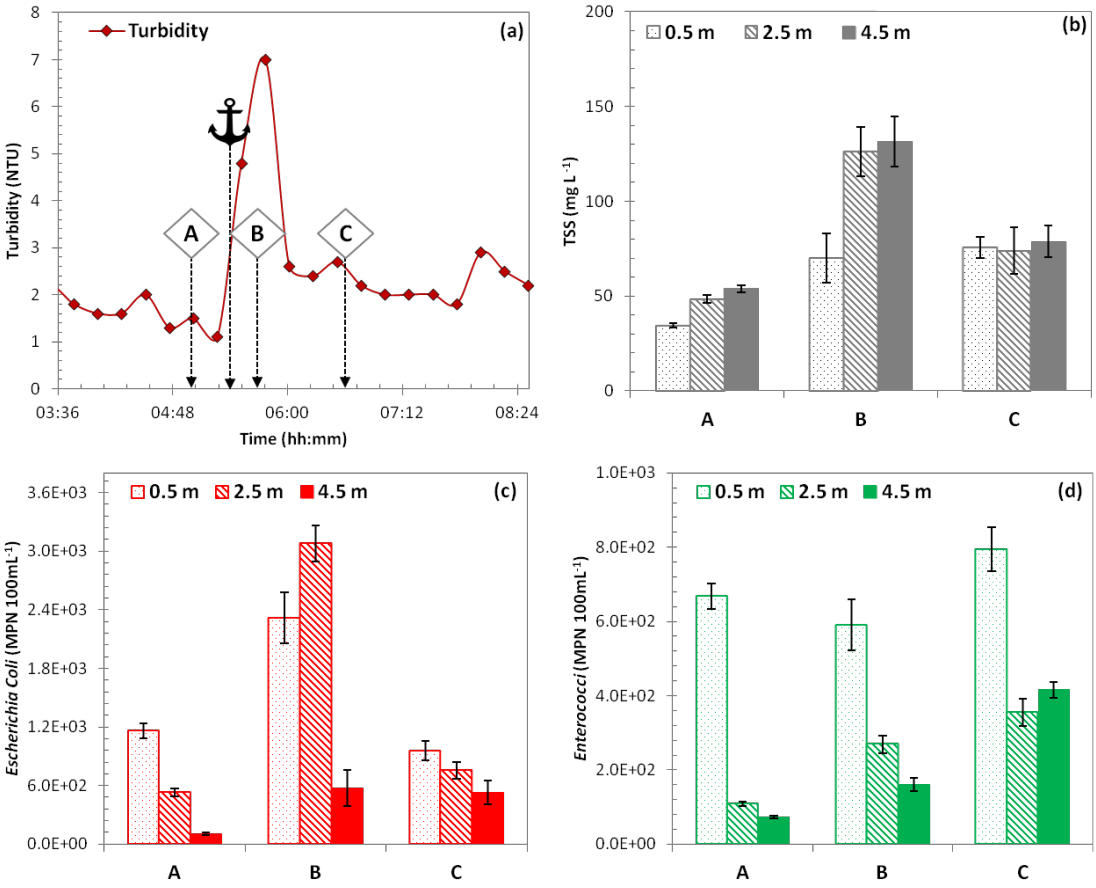

Figure 6.1: Analysis of discrete water samples collected on 15th August 2012. (a) Turbidity measurements from *in-situ* sensor; A, B and C represent the sampling times and the anchor represents the P&O ferry docking time. (b) Total Suspended Solids, (c) E. coli and (d) Enterococci levels from grab sample. Source: Environ Monit Assess (2014) 186:5561-5580.

Total Suspended Solids (TSS) is a water quality measurement listed as a conventional pollutant in the U.S. Clean Water Act. It is the dry-weight of particles trapped by a filter, typically of a specified pore size. Although TSS is not exactly the same as turbidity, they both refer to particles present in the water column, directly or indirectly. Both E. coli and enterococci are used as microbial indicators of water quality. E. coli is an indicator for

freshwater faecal pollution while enterococcus is used for seawater water or seawater. It can be seen from the results that all the turbidity, TSS, E. coli and enterococci levels increased rapidly when a shipping event occurred at the site. Apart from enterococci, which remained constantly high, turbidity, TSS and E. coli settled down after approximately two hours. This indicates that a shipping event does contribute to turbidity, TSS and E. coli variations at the site. In addition, there are strong monotonic relationship among turbidity, TSS and E. coli levels when a shipping event occurs at the test site.

P&O ferry arrival events are selected for the grab sampling due to the fact that it is the closest shipping event to the bank wall that can be accessed.

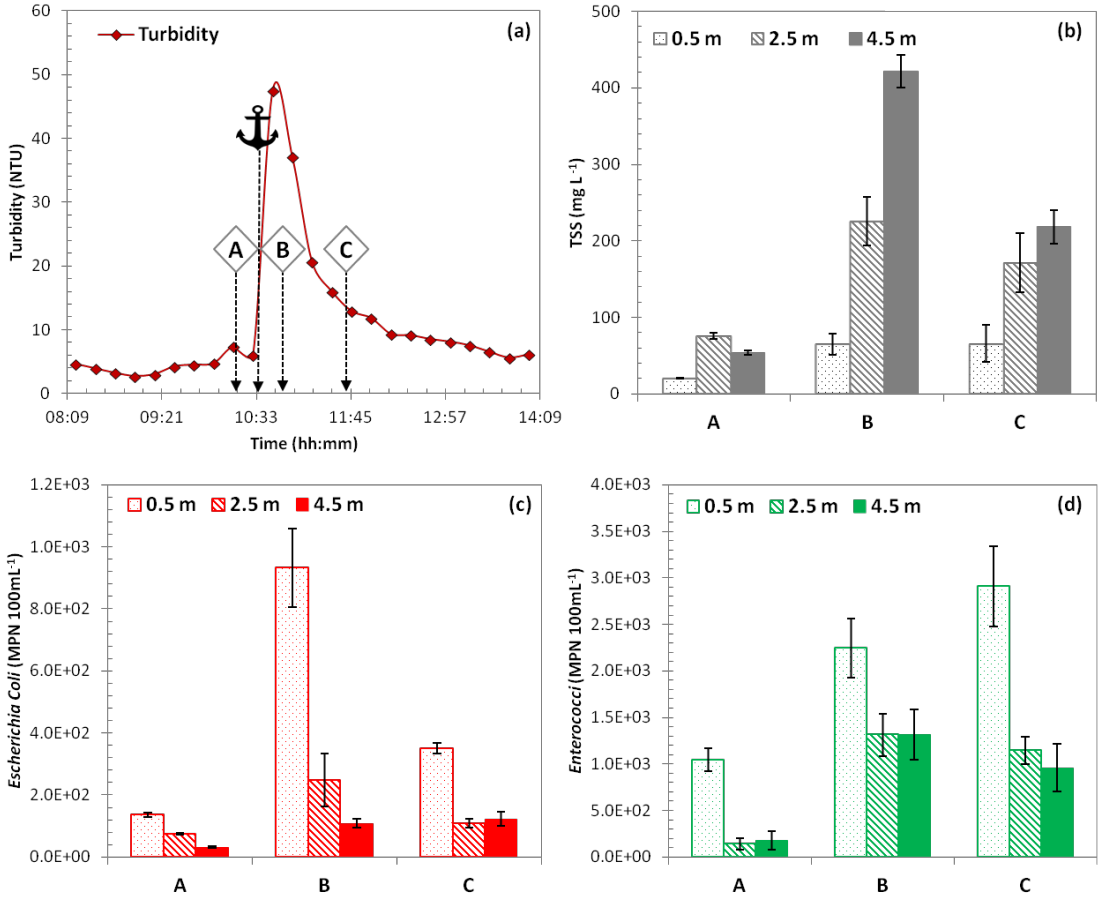

Figure 6.2: Analysis of discrete water samples collected on 9th September 2012. (a) Turbidity measurements from *in-situ* sensor; A, B and C represent the sampling times and the anchor represents the P&O ferry docking time. (b) Total Suspended Solids, (c) E. coli and (d) Enterococci levels from grab sample. Source: Environ Monit Assess (2014) 186:5561-5580

6.3 Proposed Solution

Using a camera to automatically monitor shipping traffic through a port has obvious benefits in terms of security and logistical monitoring. However, with the simultaneous deployment of a turbidity sensor, it can also provide an indication of the effect of the traffic on turbidity levels at the site. Initial analyses of *in-situ* and camera data demonstrated that at times the shipping traffic seemed to contribute to large variations in turbidity measurements. However, this relationship appeared to depend on a number of factors such as water level, type of vessel etc. Therefore, without further analysis, it is unclear that these rapid increases in turbidity measurements are directly attributable to shipping traffic. Automated detection of ships in the images would greatly accelerate and improve such analysis. This would lead to a better understanding of how commercial activities are influencing the local environment and be relevant in subsequent decision making tools for port management. Although some agencies supply shipping schedule information, such data may not always be publicly available or may not provide sufficient meta-data on vessel type and trajectory into the port which can create significant variation in relation to turbidity readings.

Thus, in the following we present a novel approach for automatically detecting shipping events in data collected from the camera deployed at our test site. This is a challenging image dataset, but despite this, a very high accuracy rate for shipping event detection is demonstrated.

Figure 6.3 illustrates an overview structure of the proposed shipping events detection system. The framework consists of three layers, corresponding to raw feature extraction, high level feature construction and classification. This follows the same high-level structure for event detection in *in-situ* data which is introduced in Chapter 5.

- In the image raw feature extraction layer, low level image features from each individual frame in an image sequence or a video segmentation are extracted. Although temporal features require information from preceding frames, a feature set is still assigned to a single frame.

- In the high level feature construction layer, low level features are grouped into high level descriptors. Common techniques include fixed length sliding window and activity triggered dynamic windowing.

- In the classification layer, high level descriptors are catalogued into different classes based on some kind of similarity measurement method.

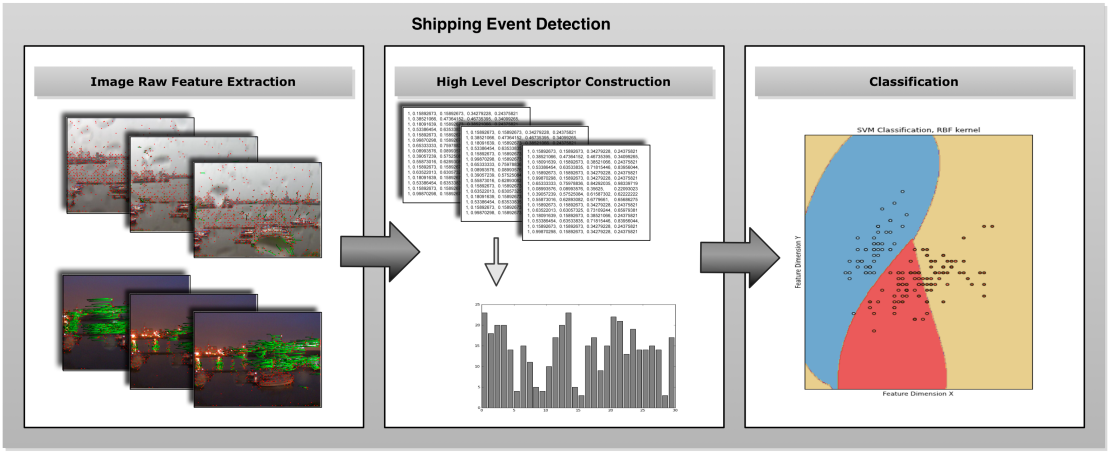

Figure 6.3: Block diagram of shipping event detection framework.

6.4 Methodology

Since our objective is to be able to detect when large ships (150-200 m long) enter or leave the harbour that may cause a rapid change in turbidity measurements, we need to extract a set of features that are sufficiently discriminative to allow us to classify such events. Traditional image processing research work focuses on spatial information only [142, 143, 144], which may not be sufficient to represent events that occupy a duration of time. Recently in the image processing domain, the focus has been shifted to extract temporal information from video segments or a sequence of images. Interesting points are first extracted from a single frame, then tracked over a short of period (few consecutive frames). In [145], Laptev and Lindeberg introduced a method called Harris3D for detection of space-time local regions by extending the Harris corner detector [146] and this has been successfully used for human action recognition [147, 148]. The Gabor3D

interest point detection method, introduced by Dollar et al. [149], is based on two 1D Gabor filters. It has been used in many event detection tasks including facial expression detection, mouse behaviour analysis [149] and human activity identification [150]. Work in [150] shows that Gabor3D method achieved over 90 % accuracy when detecting single person action. However, both Gabor3D and Harris3D are not scale-invariant, which means they can not detect similar objects or actions if they are captured at different scales, e.g. one is closer to the camera than the other. Hessian3D, proposed by Willems et al. [95], is another interest point detector, which is a spatio-temporal extension of the Hessian blob detector [151]. Experiments in [152] compared Harris3D, Gabor3D with Hessian3D. The author concluded that Hessian3D outperformed the other two interest point detection methods. Wang et al. [153] proposed a densely sampled interest point detector named Dense. The Dense detector samples interest points in spatial and temporal coordinates at multiple overlapping scales. Compared with other detectors, Dense provides a richer amount of points to be tracked. The overlapped scaling mechanism is able to deal with actions at different scale. A series of experiments was carried out by the author and the results showed that the Dense detector outperforms Harris3D, Gabor3D and Hessian3D, especially when the dataset represents a more real word environment.

Inspired by the success of Dense detector, Wang and Klaser further introduced the dense trajectory descriptor [154] that captures the shape of motion of the dense interest points, named Trajectory, and combining with Histogram of Oriented Gradients (HOG) [155], Histogram of Optical Flow (HOF) [156] and Motion Boundary Histogram (MOH) [157]. A sequence of experiments was carried out in [154] using various standard benchmarking datasets include KTH, YouTube, Hollywood2, Olympic Sports etc. Results on all datasets showed that the dense Trajectory approach outperformed current state-of-the-art methods. The dense Trajectory feature is selected for this work. To extract dense trajectory features, interesting points $P_t = (x_t, y_t)$ are sampled on a grid space by W pixels at frame t and tracked to the next frame $t+1$ by median filtering in a dense optical flow field $\omega = (u_t, v_t)$. W is the width of the grids, which is pre-defined. M is the median filtering kernel and $(\bar{x}_t, \bar{y}_t)$ is the rounded position of (x_t, y_t). The median filter is a non-linear transformation

that replaces the value at a point by the median value of a small region around the point.

$$P_{t+1} = (x_{t+1}, y_{t+1}) = (x_t, y_t) + (M * \omega)|_{(\bar{x}_t, \bar{y}_t)} \tag{6.1}$$

Interesting points tend to drift from their initial location during tracking due to image noise. To avoid this, the points are tracked within L frames. As soon as a trajectory exceeds length L, it is removed from the tracking process. Trajectory-aligned descriptors are also extracted in a 3D volume along trajectories. HOG, HOF and MBH are calculated within a local neighbourhood of $N*N$ pixels over M consecutive frames (a fraction of L). The use of full dense trajectory feature describes each scene with finer details. However, due to the limitation of the annotated dataset available and to reduce the complexity, only the Trajectory feature is used in this work. Using full dense trajectory feature results in a dispersive feature space (426 dimensions) which very likely leads to an over-fitted model on a small dataset. Figure 6.4 and 6.5 demonstrate the Trajectory feature points extracted from an image of a static scene and an image of a shipping event occurring.

A key factor in continuous real-time event detection is how to select the set of raw features extracted from each frame to be aggregated for event classification. These low level features need to be added up into fragments that can be mapped to specific events. In this work, features extracted from each individual frame are grouped into temporal overlapping windows as shown in Figure 6.6. Each image may produce varying numbers of raw features. In order to compare these features and further classify shipping events, a vector quantization method known as "bag-of-visual-words" is adopted. With this method, each trajectory feature is passed to a pre-built codebook using K-means clustering method and represented by the clustering centre ("a visual word") to which it belongs. The histogram of all visual words within a time window is calculated as the descriptor of the window.

Fixed-length sliding window is a common grouping technique and has been widely used in the literature [158, 159, 160]. In contrast to fixed-length sliding window, activity triggered dynamic grouping is another common solution. The system monitors the overall activity level at the scene or within a pre-defined triggering region; it starts grouping fea-

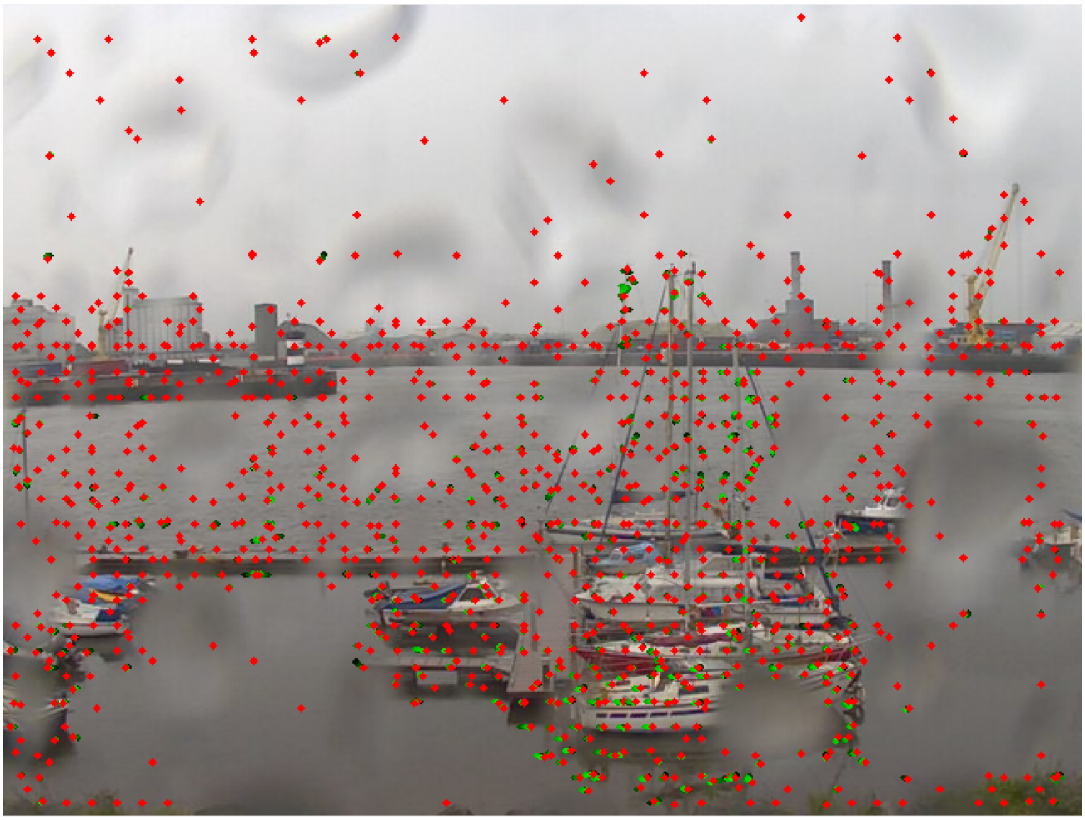

Figure 6.4: A sample image demonstrates Trajectory feature points that are extracted from an image of a static scene at the observation site.

tures if the activity level is over a certain threshold and stops when the activity level drops below the terminating threshold. The window length as well as both thresholds are normally dynamically derived at run-time. The main advantage of activity trigger grouping is that the window always starts when an event occurs and stops when the event terminates. However, for this work, due to the low frame rate of the visual sensing system as previously discussed and the nature of marine environment, determining suitable thresholds is difficult. The low frame rate results in large gradual changes, which may be caused by the change of lighting condition, moving cloud, waves and water surface reflection, between successive frames. To differentiate such gradual changes from the true unusual activity, which is required to define the triggering and terminating thresholds, is challenging. In addition, activity triggering requires a large amount of training data to model events compared to the sliding window method. Modelling these events is much more complicated in contrast to fixed-length time window, especially when multiple events occur simultaneously. Thus, this method often applies when large scale benchmarking data is available.

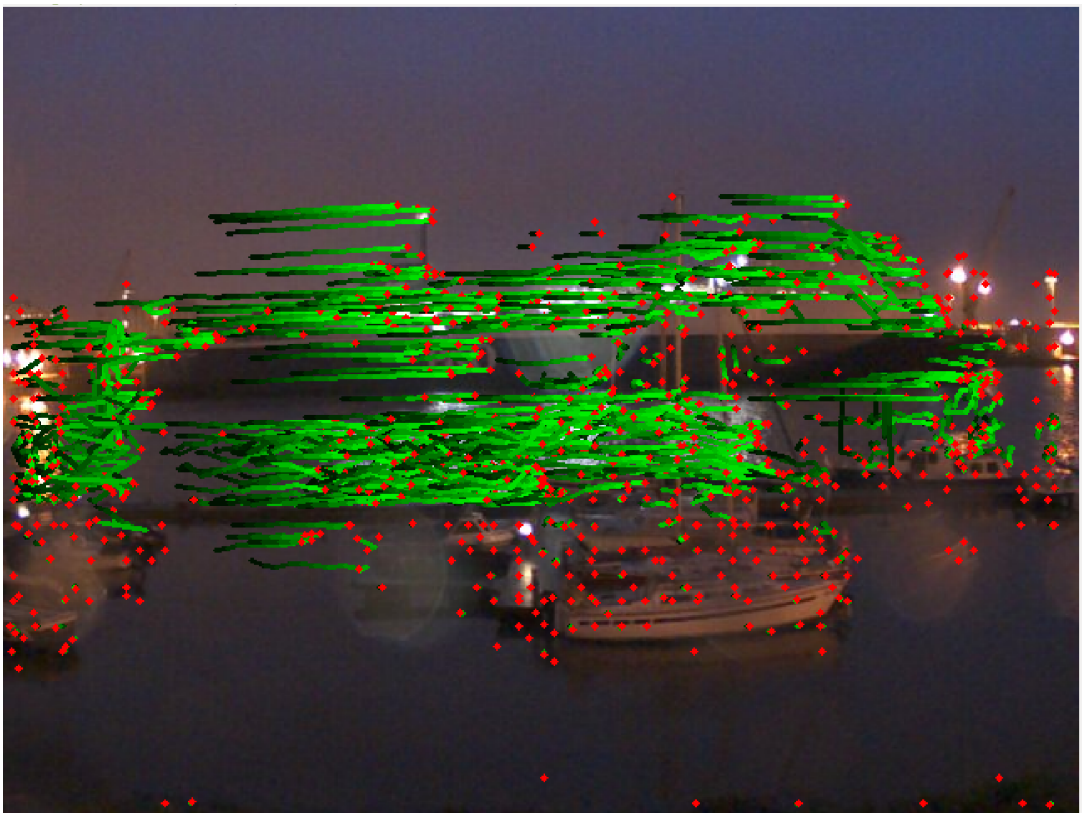

Figure 6.5: A sample image demonstrates Trajectory feature points that are extracted from an image with a shipping event occurring at the observation site.

In this work, we only focus on the detection of shipping events and do not differentiate event type in this case and thus overlapped fixed-length time window is sufficient enough to perform this operation. The major limitation of this method is that a single event may lead to multiple true samples, especially when the event does not start at the beginning of a time window, which produces nosier classification results. However, the majority of these noisy outputs do not affect the final event detection results and can be ignored. This is further discussed in the result and discussion section.

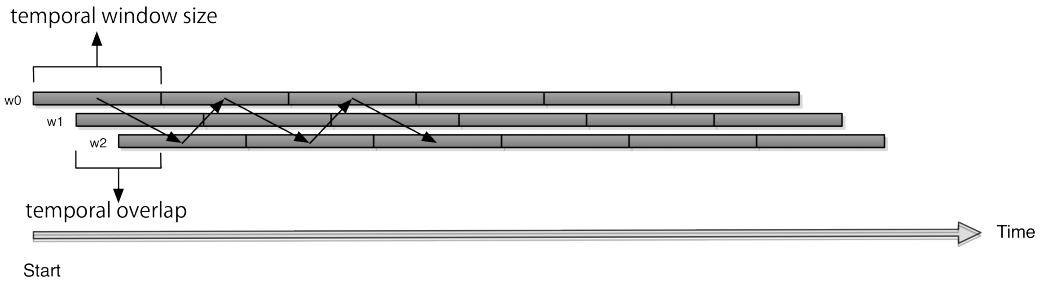

Figure 6.6: Temporal windowing, overlapping windows are distributed equidistantly over a sequence of frames.

Once the time window based descriptors are constructed, they are passed to a classifier. There are a variety of classification methods in the literature, all have their advantages and disadvantages. Some commonly used classifiers are Bayesian [161], Decision Tree [162], Neural Network [163], k-Nearest Neighbours [164] and Support Vector Machines(SVM) [165]. The strength and weakness of each classification method are well defined in the literature. A fundamental discussion can be found in Toby Segaran's *Collective Intelligence* [166] and a more detailed introduction is provided by Ian H. Witten's *Data Mining* book [167]. Selecting the best classifier is always task dependent. The objective of this work is to illustrate how a visual sensor can provide additional information to enhance *in-situ* sensing and to further assist environmental scientists to better understand marine ecosystems. Comparing and contrasting the optimized classifier for the shipping event detection system is beyond the scope of the current work. In this work, classification is performed using the Support Vector Machines (SVM) classification method. SVM is a state-of-art classifier which was introduced in 1992 by Boser, Guyon and Vapnik [168]. In its simplest form, an SVM finds a linear separating hyperplane with the best possible separation between two classes. SVM is widely used in many research areas such as machine vision [169, 170, 171], audio processing [172, 173], and text categorisation [128, 174]. Previous results show that SVM is a very powerful classifier and is likely to work as well as or better than other classification methods [166]. One of the strengths of a SVM is that by using kernel functions, feature vectors can be mapped onto a higher dimensional space, where non-linear or very difficult classification problems can be effectively solved. Moreover, after a model is built, it is very fast to classify new inputs, since classification is simply done by determining on which side of the hyperplane an input lies. One disadvantage of SVM is that it may over-fit the training data with a small dataset, especially when a non-linear kernel is applied or when processing imbalanced data. To avoid this, cross-validation is normally performed. Generally, there are two steps to perform SVM classification: determine which kernel to used and select an optimal set of parameters. Some of the most common kernel functions are linear, polynomial, sigmoid and radial basis function (RBF).

- Linear kernel is defined as:

$$k(x, x') = x^T x' + b \tag{6.2}$$

It is the simplest kernel function, x and x' are two samples represented as feature vector in some input space. B is called the bias, where $x^T x' + b = 0$ defines a hyperplane, which is the decision boundary of the classifier. It divides the input data into two categories, positive (e.g. is an unusual event) and negative (e.g. is not an unusual event).

- Polynomial kernel is defined as:

$$k(x, x') = (x^T x' + b)^d \tag{6.3}$$

where d is the polynomial degree. The most common degree is $d = 2$, since larger degrees tend to build an over-fitted model. In general, polynomial kernel performs well on normalized data. Polynomial kernel is very popular in natural language processing.

- Sigmoid kernel is defined as:

$$k(x, x') = tanh(x^T x' + b) \tag{6.4}$$

It is also known as Hyperbolic Tangent kernel. It is commonly used in the neural network field as an activation function for artificial neurons.

- RBF kernel is defined as:

$$k(x, x') = exp(-\gamma \left\| x - x' \right\|^2), where - \gamma > 0 \tag{6.5}$$

where $\|x - x'\|^2$ is the squared distance between two vectors, γ is a free parameter that defines how far the influence of a single training example reaches, where low values means 'far' (the influence of a single training entry is significant to the

decision boundary) and high values means 'close'.

An SVM also consists of a soft margin parameter C for all kernels, which trades off misclassification of training examples against simplicity of the decision surface. A low value of C makes the decision surface smooth, while a high value of C aims at classifying all training examples correctly. An RBF kernel is chosen as the kernel function for the following event classification process due to its ability to generalize data well and it can also handle a non-linear decision boundary.

6.5 Visual Test Data: Dublin Bay

A month of image data from the 1st May 2012 to 31st May 2012 (total of 255,956 images captured at 1 frame every 10 seconds) was used to evaluate the proposed shipping traffic detection method. The first 50 % of continuous data was used to train a model and the following 25 % of sequential data was used for classification parameter optimization. The remaining 25 % of data was used for testing. The data exhibits a wide variety of lighting and weather conditions, as well as many different types of ships and trajectories. Figure 6.7 demonstrates the complexity of the dataset. The dataset contains daytime images as well as nighttime images with reflections of lighting on water surface. A variety of weather conditions, such as sunny, cloudy, light shower, heavy rainfall and storm, are also present in the dataset. Human activities, such as a yacht race, also occurred during the data capture period. Technical issues, such as the failure of the control board, which extracts image data from the camera and uploads to a cloud data centre, loss of mobile network connection, which results in a short period of missing image data, are also present in the dataset. Therefore, the image dataset used for the following experiments truly reflects the nature of a practical deployment.

A total of $255,956$ color images of 640×480 pixels were annotated as the ground truth of the dataset. To reduce the amount of data that needs to be processed, a region of interest (x : 0, y : 100, $width$: 640, $height$: 200) is drawn on the original image before ex-

Figure 6.7: Samples of the image data, which exhibit a wide variety of lighting and weather condition, demonstrate the complexity of the dataset.

tracting features. This is due to two reasons. Firstly, image processing is computationally expensive; processing data within the region of interest significantly reduces processing time. Secondly, shipping events only occur in certain areas within the image, e.g. within the channel, and so unrelated information extracted from outside the region of interest provides no useful information to the classifier and may interfere with the results. Initial analysis on the dataset shows that the duration of the majority of shipping events is between 3 to 7 mins. Thus, raw image features were grouped into 15 mins time intervals, which is approximately twice as large as a long shipping event, with 10 mins (2/3) overlapping (e.g 15:00 to 15:15 and 15:05 to 15:20). If a large part of the event (90 %) falls into a time interval, it is annotated as true. Because of the overlapping mechanism, a shipping event may lead to multiple positive entries in the dataset. However, these entries are temporally close to each other (successive samples). Feature sets were categorised into two classes: no shipping events and shipping events. The total amount of shipping events in the training, evaluation and testing set are 176, 51 and 54 respectively; the total amount of positive samples are 387, 100 and 117.

6.6 Parameter Settings

The Elbow method, discussed in Chapter 5, was applied to determine an optimized codebook. The plot of the average within cluster sum of squared error (ASSE) against a series of sequential cluster levels is shown in Figure 6.8 and the explained variance ratio is illustrated in Figure 6.9. Due to the limitation of hardware resources, every 10th sample in the training data is used for the evaluation process and the range of cluster center is set from 1 to 50 with a step of 5 (e.g 1, 5, 10, 15) and 50 to 3000 with a step of 50 (e.g. 50, 100, 150). However, building a codebook does not require the calculation of ASSE, thus, the full training dataset was used to build the final codebook.

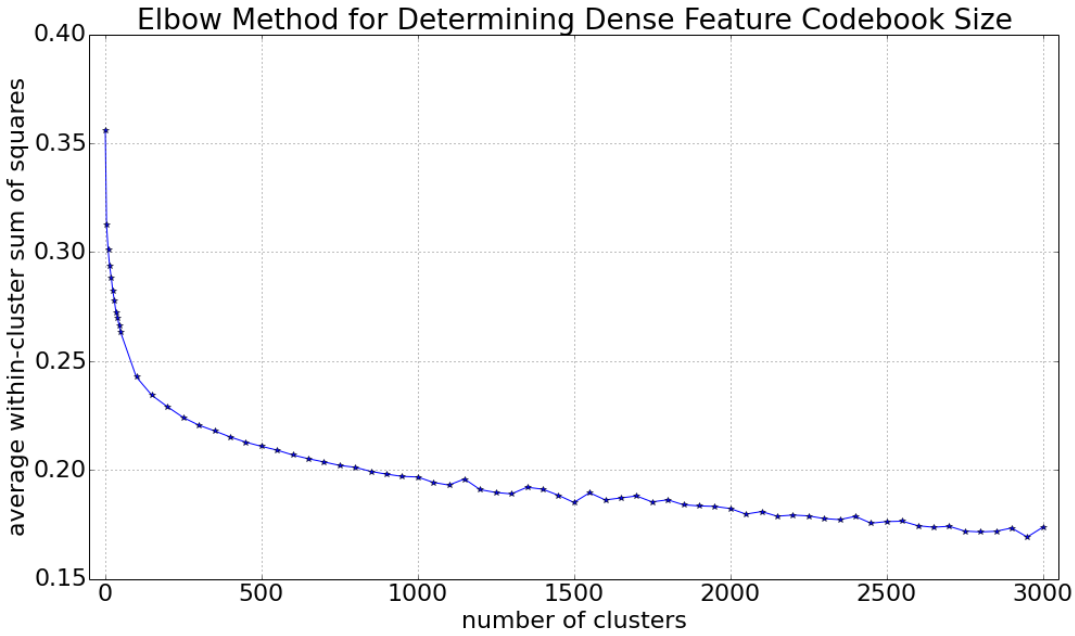

Figure 6.8: Average within-cluster sum of squared error vs. the number of clusters in the codebook. A lower error value means that the codebook model is a closer representation of the whole dataset.

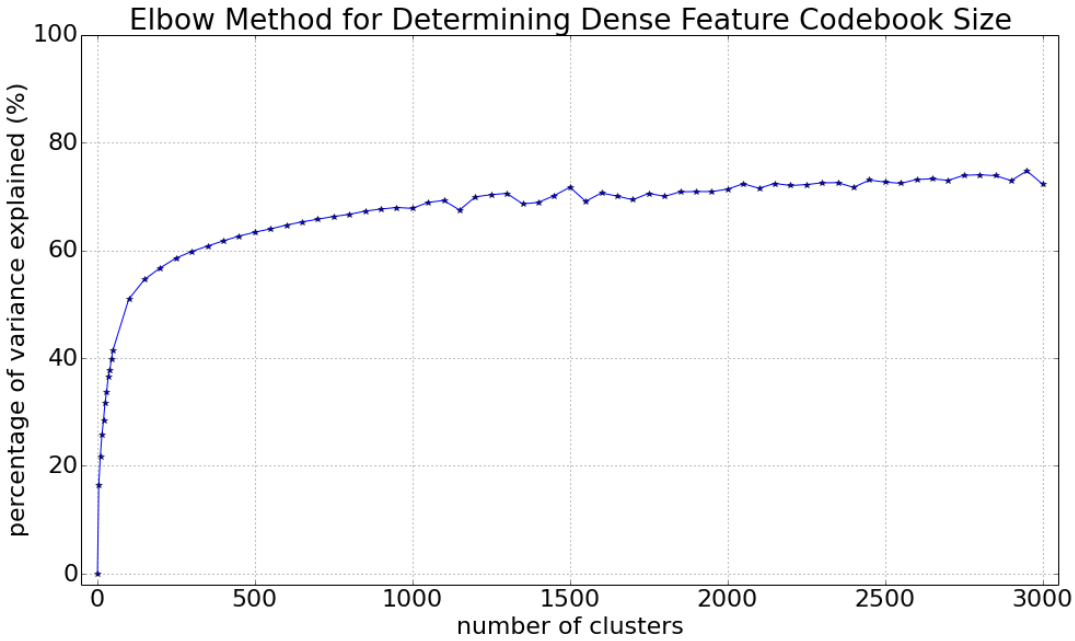

Figure 6.9: Percentage of variance explained vs. the number of clusters in the codebook. The higher percentage means the better that the codebook represents the original data.

As shown in Figure 6.8, the ASSE decreases rapidly when the number of clusters is small. When the number of clusters is greater than 100 the decrease becomes smaller. After 500 clusters, the changes of ASSE are very small and the decreasing rate becomes steady. These suggest that a codebook with at least 100 words is a good representation of the raw feature data. In addition, using more than 500 words does not increase the accuracy by much. Further increasing the number of words still improves performance but it also increases the computational complexity and may lead to a dispersive descriptor, which increases the possibility of producing an over-fitted classification model. The same conclusion can be drawn from Figure 6.9; the increase of explained variance ratio becomes small when the number of clusters exceeds 100 and steady when the codebook contains more than 500 words. This suggests that a codebook with the number of words between 100 (less accurate but computationally inexpensive) and 500 (more accurate but computationally expensive) is a good representation of the Dense feature. To keep the balance between accuracy and computation requirement, a codebook with 200 words is chosen as the model for the feature representation process.

When training a SVM with the RBF kernel, two parameters must be considered: C and

γ. To obtain an optimised set of parameters, grid search [175] was applied. Grid search is one of the standard methods of performing hyperparameter optimization. Various pairs of (C, γ) values are tried and the one with the highest evaluation accuracy is picked. In [175], the author suggests that trying exponentially growing sequences of C and γ is a practical method to identify good parameters. Thus, we set the range of C from $1e^{-2}$ to $1e^{9}$ and the range of γ from $1e^{-7}$ to $1e^{3}$. The classification F1 scores on the training and evaluation dataset are shown in Figure 6.10 and 6.11. Evaluation results suggest that $C = 100$ and $\gamma = 1e^{-5}$ are the optimal parameter values for the SVM classifier on the dataset.

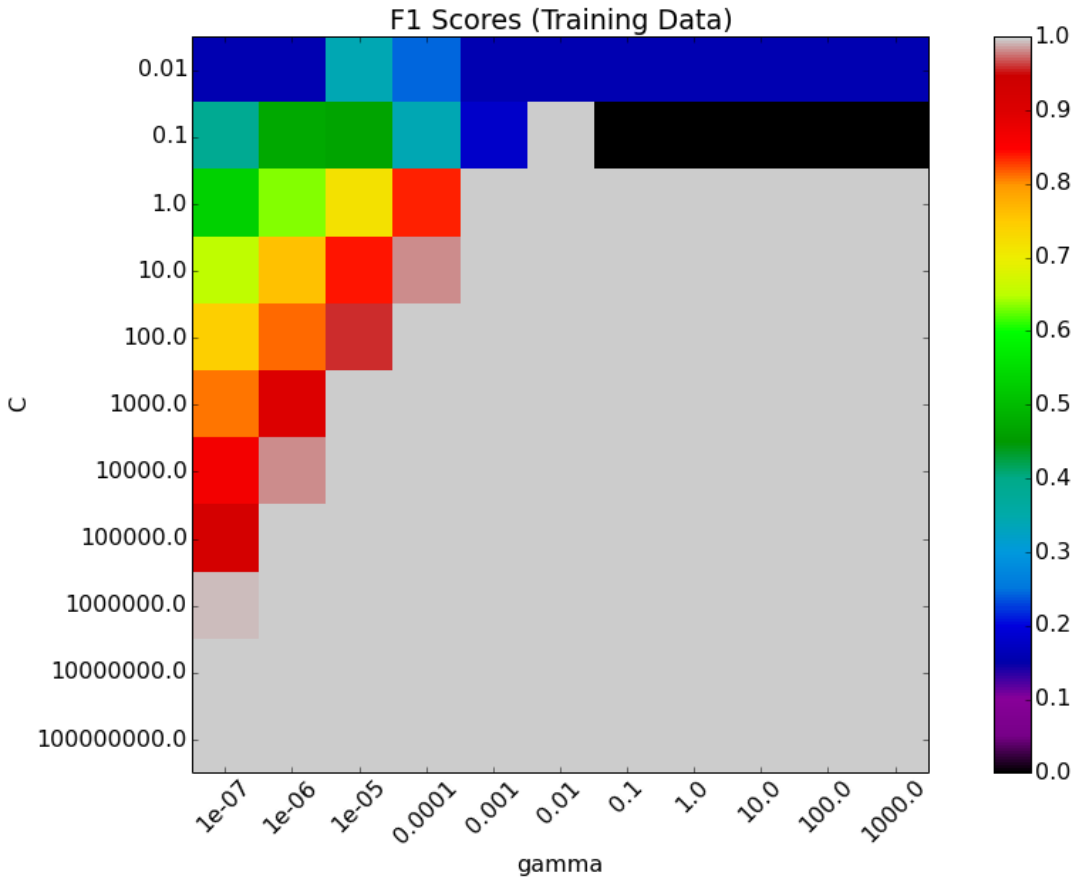

Figure 6.10: Grid search results for RBF kernel parameters C and γ on training data. The result shows that the classifier achieved good results when the C and γ values are in the grey region.

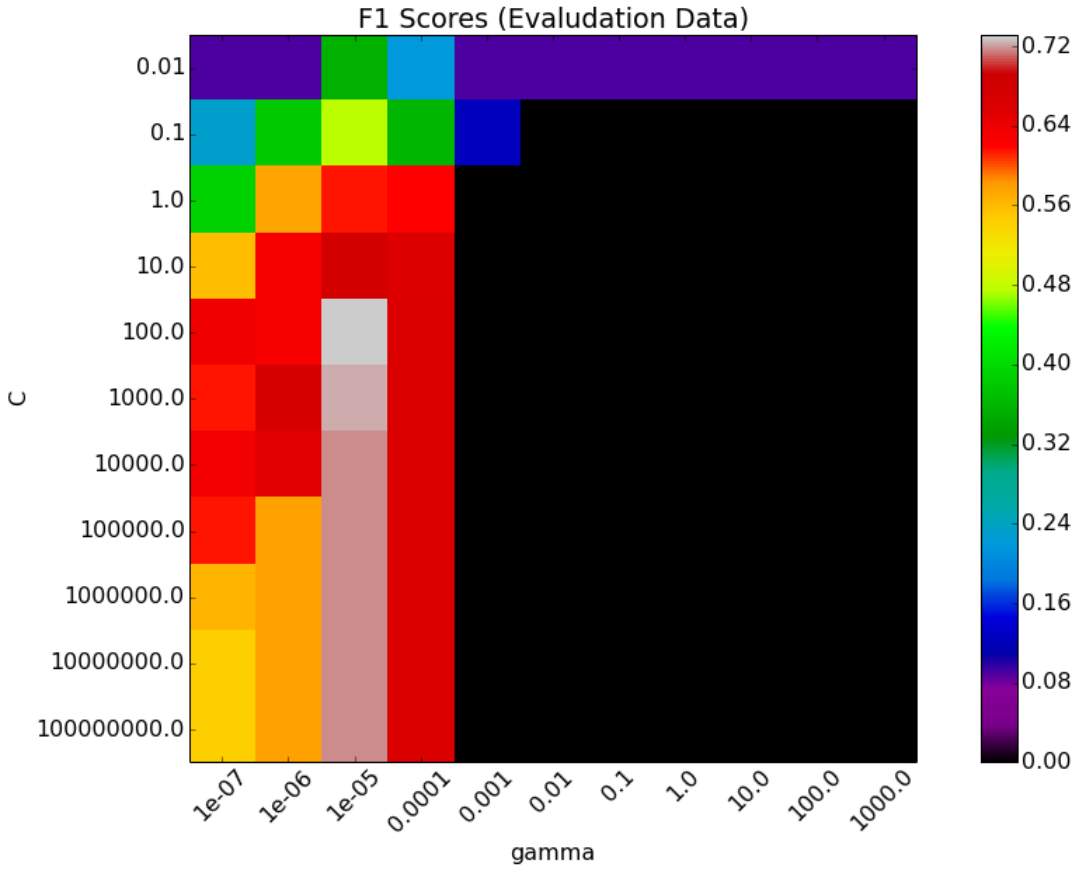

Figure 6.11: Grid search results for RBF kernel parameters C and γ on evaluation data. The highest classification accuracy is obtained with parameter values $C = 100$ and $\gamma = 1e^{-5}$, which suggests this value pair is the optimal parameter set for classification of shipping events.

6.7 Results and Discussion

Applying the described shipping event detection method, using the optimized set of parameters obtained from Section 6.6, to the test data results in 143 (FP+TP) out of 2232 (TN+FN+FP+TP) descriptor sets being classified as positive samples. The classification confusion matrix and the F1 scores are shown in Table 6.1 and the Receiver Operating Characteristic (ROC) curve is shown in Figure 6.12.

Table 6.1: Training, evaluation and testing confusion matrix of shipping detection using SVM classifier with RBF kernel and the optimized parameter values.

			Training		Evaluation		Testing	
No Shipping Events	TN	FP	4041	34	2079	46	2064	37
Shipping Events	FN	TP	0	385	18	87	23	106
F1 Score					0.73		0.78	

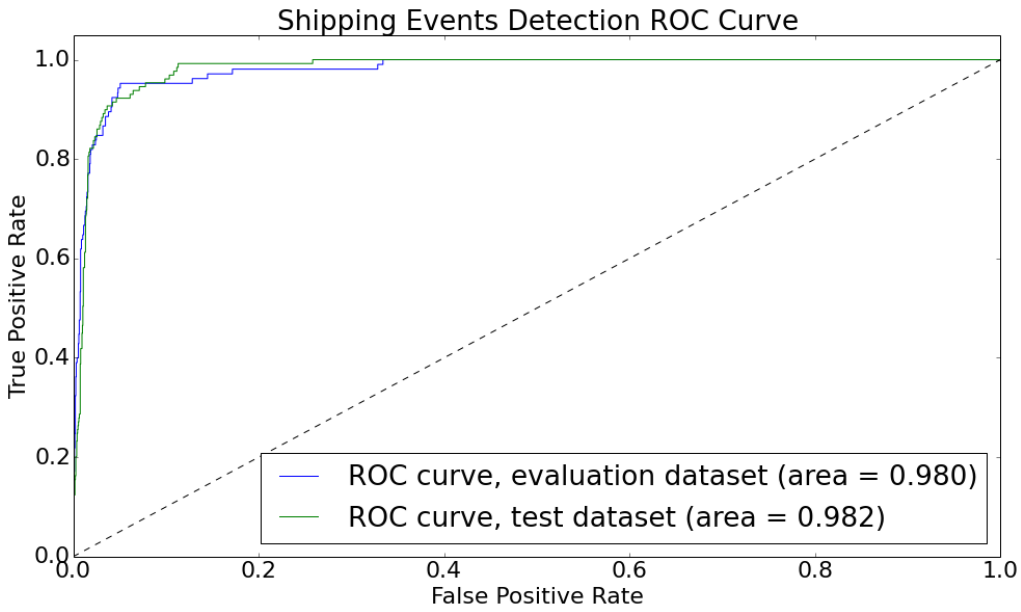

Figure 6.12: Shipping events classification evaluation and test dataset ROC curves.

As can be seen from the confusion matrix, 46 out of $2,125$ negative samples (TN+FP) and 18 out of 105 positive samples (FN+TP) are misclassified in the evaluation dataset and 37 out of $2,102$ negative samples (TN+FP) and 23 out of 129 (FN+TP) positive samples are misclassified in the test data. The evaluation and testing F1 scores are 0.73 and 0.78 respectively. As previously discussed, a ship entering event may result in multiple true samples in the data set due to the overlapping fixed-length window based grouping mechanism applied. Depending on preceding and succeeding outputs, the classification error can be further grouped in three categories:

- Type I - Event Missed: No descriptor is classified as True, a shipping event is completely missed by the detection system.
- Type II - Event Incorrectly Detected: System returns positive, but no event occurred at the site.
- Type III - Don't Care Error: Descriptor is wrongly classified, but shipping event is still detected.

To illustrate this, a sample shipping event and the descriptors constructed during the period of this event are shown in Figure 6.13. For convenience purposes, they are named

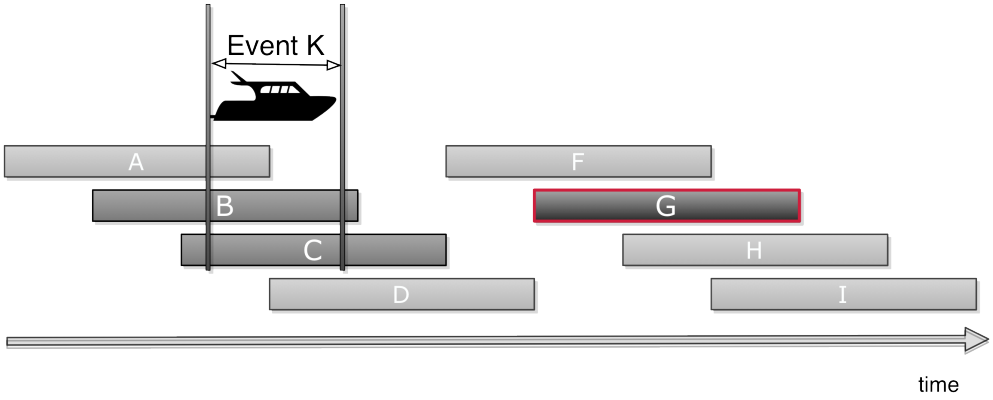

Figure 6.13: This example shows three types of classification errors that may occur. Both descriptor B and C are labelled as true since both of them cover shipping event K. Descriptor G is labelled as false since there is no shipping event but it is classified as true by the system.

as A to I, which represent successive descriptors constructed from the low level features that are extracted from images. Descriptor A and D are negative samples since they only cover small portion of the shipping event. B and C are annotated as true samples since both of them cover a shipping event. If either of these two descriptors is incorrectly classified while the other one is correctly detected (assume descriptor A and D are correctly identified), a shipping event is still detected by the system. Thus, this classification error is a type III error, which does not affect the shipping event detection result since the event is still captured by the system. However, if both descriptor set B and C are wrongly classified, event K will be missed by the detection system, which results a type I error. As illustrated in Figure 6.13, descriptor set G is classified as true by the detector, however, there is no shipping event at the time, which results a type II error (false detected).

Since only type I and type II errors affect shipping detection accuracy, type III errors can be ignored. This results in 4 out of 54 shipping events missed and 2 events wrongly classified in the test dataset, which results in an overall shipping events detection rate of 93.2% (48 out of 54). A more visualised classification result is shown in Figure 6.14. The red bars are the outputs from the classifier and the blue bars are the ground truth. The variant width of the bar indicates that there are multiple successive descriptors that are labelled or detected as positive sample. A sample of type I and type II error are also illustrated in the graph. Some aligned red and blue bars have different width which are

caused by type III errors, however, it does not affect the overall system accuracy as events are still detected. As can be seen from Figure 6.14, the proposed system achieved a very high shipping event detection accuracy.

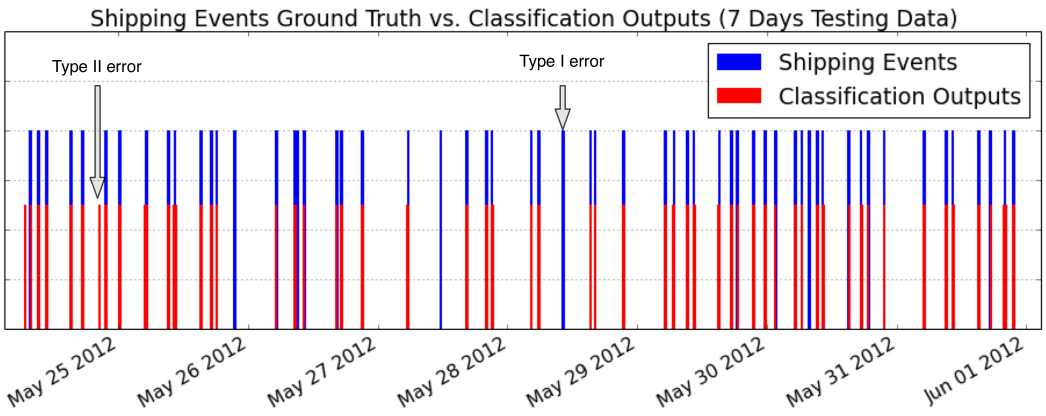

Figure 6.14: Classification outputs vs. ground truth indicates that the system achieved very high shipping events detection accuracy. A sample of type I and II error are illustrated.

Figure 6.15 and 6.16 show some example images of the two incorrectly detected events (Type II error). As can be been from the sample frames, the first wrongly detected event is caused by one speed boat and one fishing boat crossing the channel. The velocity of the speed boat is very high, which generates strong waves over a short period of time. The wake generates a lot of motion features, which affect the classification results. In addition, the impact of wake caused vibration of the pontoon and docked boats, which generate motion features that also affects the classifier. The second wrongly detected event is caused by a large size sailing boat and a tug boat crossing the channel, which generates a lot of motion within the image. These classification errors are mainly cased by the limitation of bag-of-words representation and the sliding window mechanism. Bag-of-words along with the sliding window approach discards local temporal information to reduce descriptor complexity. For example, raw features extracted from two individual medium size boat events are simply accumulated, which may appear as a similar to features extracted from a large size vessel. One potential solution to solve this issue is to extract spatial information, such as activity regions. Multiple medium or small size boat events generate multiple small, high density activity regions and large vessels generate single large

activity regions, which can be used to discriminate above events. A more sophisticated solution could be to combine Dense feature with other local shape features, such as HOG, which may discriminate above events. However, to evaluate these solutions requires a much larger labelled dataset, which is currently not available.

Figure 6.15: Sample images of the first wrongly classified shipping event. Speed boat, fish boat and the impact of wake creates large amount of motion, which affects classification results.

Figure 6.16: Sample images of the second wrongly classified shipping event. Tug boat and sail boat appeared at the scene, which leads to incorrect classification.

Figure 6.18 to 6.20 show example images of the four missed events (type I error). The first two missed events are a P&O ferry departure from the left of the channel to the right. The reason why these two events are missed by the classifier needs to be further studied.

There are 18 similar P&O departure events in the test data set, 16 were correctly detected by the system. The third missed event is the Shoalway trailing suction hopper dredging ship turning at the right edge of the image region. Although this event is annotated as true, the ship only appears partially at the scene which may not provide enough information for the classifier. The final undetected event is a medium sized passenger ship coming into the harbour, turning anti-clockwise and docking against the wall at the far side. The key reason for this error is that this event only occurred once in the whole dataset. No similar events are available for training the classification model. A supervised classification method tends to perform well if sufficient training data is provided. Here, only binary classification is performed, thus, if an event is not 'similar' to a positive sample in the training set or has not been observed before, it is likely to be catalogued as false.

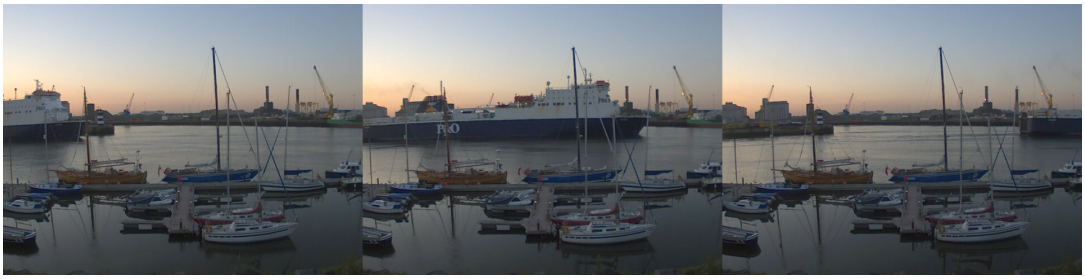

Figure 6.17: Sample images of the first missed shipping event.

Figure 6.18: Sample images of the second missed shipping event.

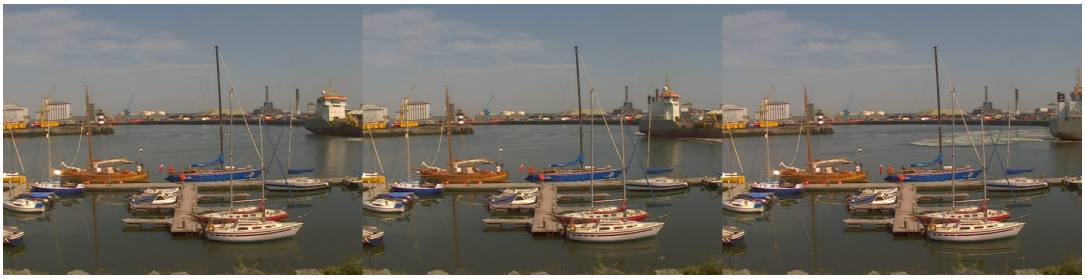

Figure 6.19: Sample images of the third missed shipping event.

Figure 6.20: Sample images of the fourth missed shipping event.

6.8 Combination of Visual and In-Situ Data Processing Results

In order to better understand and subsequently model the environmental dynamics at the observation site, the output of visual sensor modality is combined with the turbidity events detected to further distinguish whether a turbidity event is caused by shipping traffic. This provides an opportunity of filtering out turbidity variations that are caused by local activities and to determine the abnormal events that need to be further analysed. The turbidity anomalies detected, as shown in Figure 6.21, are grouped into events by applying the event construction method introduced in Chapter 5. Figure 6.21 also shows a combination of turbidity occurrences and shipping events.

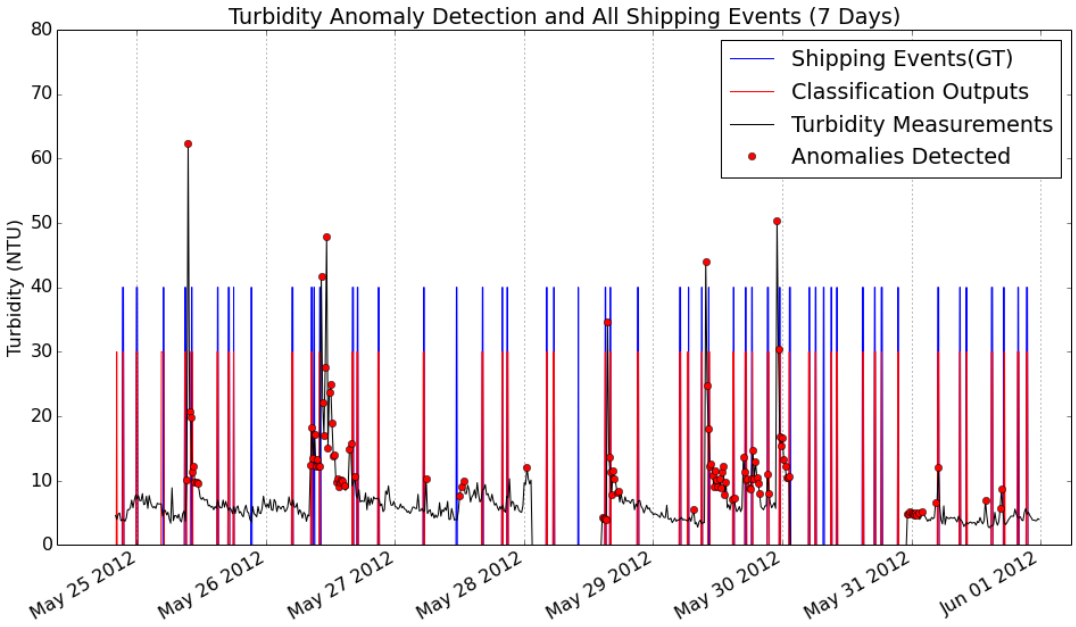

Figure 6.21: Matching of shipping and turbidity events by their timestamps. The graph shows that not all shipping events lead to a rapid change in turbidity sensor data stream.

From Figure 6.21, it can be seen that the majority of shipping events do not affect turbidity measurements collected by the *in-situ* sensor at the site. Further analysis of the images and *in-situ* data shows that P&O ferries are more likely to cause a rapid change in turbidity reading than other shipping events. This is mainly due to the following facts:

- Single Point Sensor: As discussed in the previous section, purchase, deployment and maintenance of an *in-situ* sensor system is costly and is a subject to restrictions in hosting permission. Thus, to prove the concept, only one multi-parameter sonde is deployed at Dublin bay. The drawback of the current system is that it is a single point system, which may not capture the overall water quality dynamics of the entire site. As shown in Figure 6.22, the YSI sonde is deployed opposite of Terminal 3 (anchor point), the shipping events that occur at the far side of the channel may not be reflected in the sensor reading. Events such as these may cause a rapid change in turbidity values but it may not be captured by the deployed sensor.

- Manoeuvring: When a P&O ferry is entering the terminal, it manoeuvres first then reverses to the dock. During this process, the vessel has to use its bow thrusters to change the direction, which cause turbulence. Also, the stern main engine is also at its high load, which disturbs the water body as well. The impact of this intensive mixing and stirring has been observed visually on-site and is shown in Figure 6.22. Moreover, as these events often occur in the middle of the channel, there is a high chance for the *in-situ* sensor to capture these effects compared to other large scale vessel events, which appear at the far end of the channel. In contrast, when a P&O ferry departures from the terminal, the bow thrusters are not applied and the speed of the ferry is relatively low. As a consequence, P&O departure events do not lead to a rapid change in turbidity measurements.

Thus, in the following section, we altered the setting of the proposed system to detect only P&O arriving events.

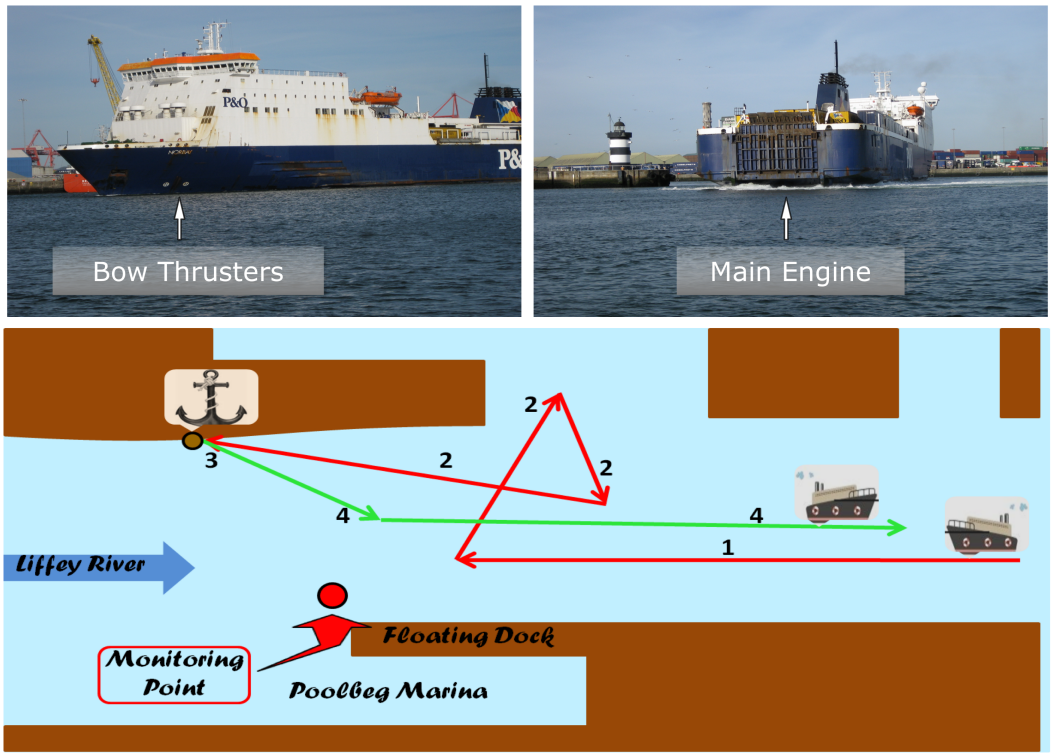

Figure 6.22: Demostration of a P&O ferry entering port terminal.

6.9 P&O Ferry Arrival Event Detection

To further evaluate how shipping events affect the *in-situ* sensor measurements, we altered the settings of the previous experiments to detect P&O ferry arrival events. In order to estimate the generalization of the proposed detection framework, a different set of test data is used for evaluation.

Two weeks of image data from the 8th Nov 2012 to 21st Nov 2012 (109, 143 images) was annotated and used for the subsequent experiments. Following the same procedure of the previous test, dense feature within the region of interest is first extracted from each individual frame and passed to the codebook previously built. The 'words', output from the codebook model, are used as the representation of low level raw features (the Trajectory feature). Since the low level dense feature describes the motion characteristic of an interesting point, this does not require to rebuilding the codebook. These words are further grouped together using fixed-length overlapping sliding window mechanism and the frequency of their occurrence is used as the high level descriptors. Descriptors

are catalogued into two groups corresponding to P&O arrival events, which were labelled as positive samples and all others, such as no shipping or other shipping events, were labelled as negatives entries. The data shows a very different characteristic than previous test dataset due to seasonal effects. For example, the sunshine hours during this period is much shorter than the former dataset, which results in the majority of P&O ferries arriving in the dark mornings or evenings in contrast to bright daylight time, even though these events may occur approximately at the same time of the day as before. In addition, other activities, such as yacht races, dredging, the traffic of cargo freighters, are less intensive than in the summer time. Thus, a different classifier needs to be built for this period of time. The first week (50% continuous) data is used to train a model and the remaining week data is used for testing. All the parameters are set to the optimized values that are obtained from Section 6.6 ($C = 100 and \gamma = 1e^{-5}$). The test data classification confusion matrix is shown in Table 6.2

Table 6.2: Testing confusion matrix of P&O arrival shipping detection using SVM classifier with RBF kernel and the optimized parameter values that were obtained from the previous experiment.

P&O Entering Events	TN	FP	1967	17
All Ohters	FN	TP	3	27
F1 Score			0.73	

Further analysis of the classification output indicates that there is 1 event missed due to the type I error and 1 event is incorrectly detected by the classifier (type II error) out of 17 events in total. The system achieved 88.25% (15 out of 17) overall event detection accuracy. A more visualised classification result is shown in Figure 6.23. The red bars are the outputs from the classifier and the blue bars are the ground truth. Sample images of missed and incorrectly classified events are shown in Figure 6.24. The top row shows three sample frames of the missed P&O arrival event and the bottom row presents three sample frames of incorrectly classified event. As can be seen from the graph, the type II error is caused by a giant Sea Star cargo ship. By further examining the image data, we found that the vessel first left the dock at the far side and then entered the channel. Dragged by the pilot boats, the vessel manoeuvred clockwise and accelerated to the right.

The trajectory of this event is very similar to a P&O arrival event apart from the reverse order of the action. This illustrates a limitation of the descriptor used, it can not differentiate actions with inverse patterns. The descriptor counts the frequency of the occurrence of each visual word within a sliding window but does not take into account when it happens within the time period. The same solutions, as discussed in previous section (Section 6.7), can be applied to avoid this limitation. However, the causes of the type I error need to be further investigated.

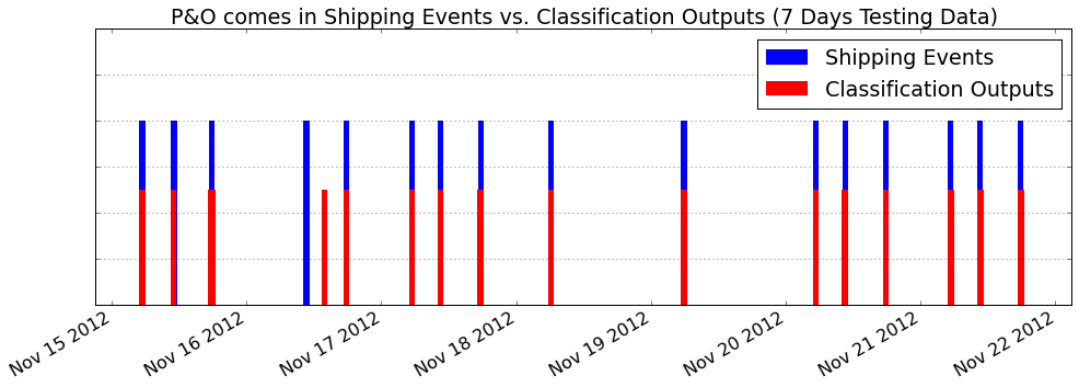

Figure 6.23: P&O entering events classification output vs. ground truth.

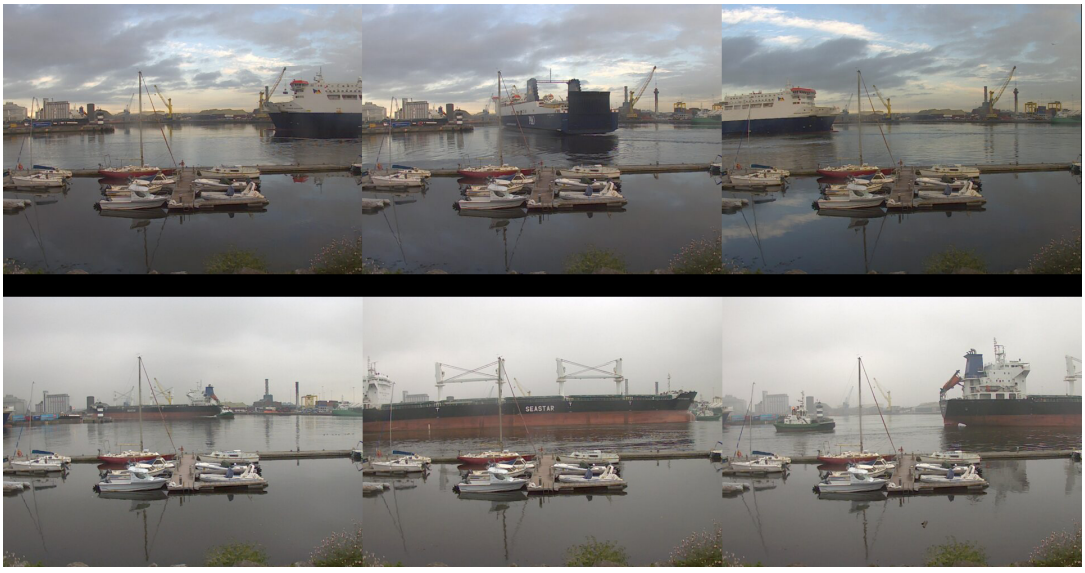

Figure 6.24: Samples image of missed and incorrectly classified events. Top row: missed P&O arrival event, bottom row: incorrectly classified event.

A combination of turbidity event detection results and P&O ferry arrival event classification results over the same period of time are shown in Figure 6.25. The graph shows that large amounts of turbidity variations are likely caused by the arrival of P&O ferries.

However, it also indicates that there are turbidity events that do not have shipping activities associated with them, such as the event that occurred at around mid-night of Nov 19th and two events which happened at mid-day on Nov 20th. Interestingly, not all shipping activities lead to a rapid change in turbidity sensor measurements. Four shipping events within the testing time period, three on Nov 18th and one on Nov 19th, do not affect turbidity readings at all. Moreover, although P&O ferries follow a similar trajectory when they come into the port and berth at the dock, the turbidity signatures do not always show a similar pattern. This can be seen from the graph where the turbidity trends associated with the first two shipping events have similar shapes; the turbidity data captured after shipping event 4 and 13 have similar variations, however, the majority of the turbidity events associated with these shipping events have diverse patterns.

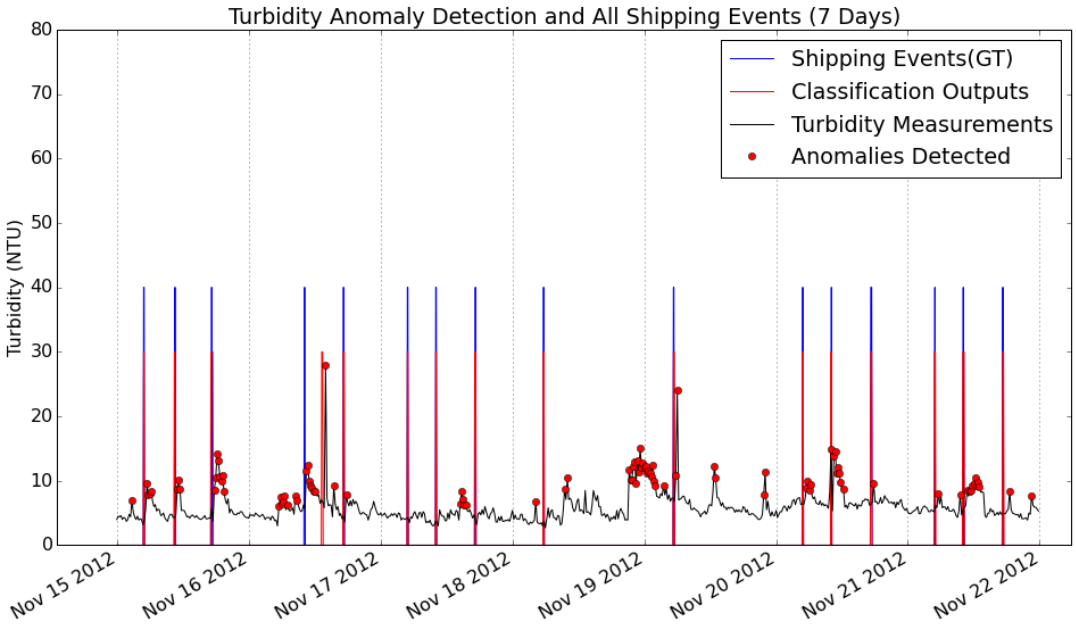

Figure 6.25: Combination of turbidity event detection and P&O arrival events classification output.

6.10 Summary

In this chapter, we firstly introduced how visual sensing can be used as an alternative sensing modality for many forms of environmental monitoring. Many other works in the literature demonstrated that a low cost off-the-shelf camera can provide much richer

content based information that can be used to enhance *in-situ* sensors. Inspired by these research works, a visual sensing modality was installed at our pilot site to complement the *in-situ* sensor deployed. Due to the unique characteristics of our test site, we firstly focused on the detection of large scale vessels present at the site since these type of ships potentially affect turbidity levels at estuaries. The contribution of shipping events to local turbidity variation has been studied in the past, however, only from a manual perspective and verified by discrete sampling, which cannot be quantified for long term water quality monitoring and subsequent modelling. We proposed an automated shipping event detection system that determines when a large scale ship is appearing at the scene. A series of experiments were carried out to evaluate the proposed method and results show that shipping events can be identified accurately. However, mapping all occurrences of shipping transits with abnormal event detection results obtained from *in-situ* sensor measurements using the method described from Chapter 5, we found that most of the occurrences do not lead to a rapid change in turbidity readings. As discussed, the potential causes of these phenomena are the location of where the *in-situ* sensors are deployed and the trajectories of the shipping events. Further analysis on the data suggested that, at the test site, the arrival of a P&O ferry often leads to rapid changes in the sensor readings while other shipping events do not have such an effect. Thus, we altered the settings of our proposed framework and adapted the system to detect P&O arrival events only. Results show that significant amount of turbidity events are caused by the arrival of P&O ferries. However, the results also demonstrated that the same shipping events may not necessarily generate a turbidity variation, due to the complexity of the environment. Turbidity is affected by many factors. Although shipping events do have a significant contribution, but it also relies on other constraints. For example, speed and direction of water flow, sediments at the channel, water depth at the time of shipping transit occurs, wind etc. all provide different outcomes of turbidity patterns. It can also be seen from the results that the turbidity variations associated with the same shipping events certainly do not show similar trends. However, the results suggest that *in-situ* sensor variations can be verified by visual sensors. The output of visual sensors can be used to enhance the event detection results

from *in-situ* sensor data. Events from *in-situ* sensor can be further classified as being caused by a local activity, which can then be filtered out, or classified as unknown. The environmental scientists can then focus on the remaining events only.

The case study carried out in this chapter demonstrates the advantage of coupling a visual sensor with an *in-situ* sensing unit, which addresses research questions 3 and 4 and further validates our hypothesis 1, in Chapter 1. By applying state-of-the-art machine learning methods, *in-situ* and visual data streams can be processed automatically. Unusual events can be isolated from data streams and catalogued into sub-groups. This also enables the opportunity of monitoring the marine environment on a much greater scale. Visual sensing provides context information that can be used to verify events detected from *in-situ* sensor measurements. The system provides context based information rather than raw sensor reading based information to assist scientists in better understanding the marine ecosystem. New policies can then be developed to further protect these environments. Feedback can be applied to hardware infrastructure, e.g. change location, angle or altering sampling rate, to make the deployed system more effective.

CHAPTER 7

CONCLUSION

7.1 Thesis Overview

In this thesis, the requirements for a multi-modality smart marine monitoring system are identified. Results obtained from the case studies show that marine environmental monitoring applications will strongly benefit from the integration of multiple sensing modalities. Different sensing modalities can complement each other to provide more robust and comprehensive information that is more suitable for decision making, especially in a large scale setting. Such information can potentially provide an improved operator view of the functioning of environments and hence improve decision making capability. A summary of the findings in each chapter is provided and the research hypotheses are revisited. The research contribution and limitations of this study are also discussed followed by suggestions for future research.

In the introductory chapter, the need for high spatial and temporal monitoring of marine environment is identified from both economical and ecosystem well-being perspectives. Current state-of-the-art research works carried out in other research domains which motivate this work are discussed. The aims and objectives of this research work are outlined. The research hypotheses and the expanded research questions that are investigated

throughout the thesis are listed followed by the outline of this thesis.

An overview of some key concepts from the literature in relation to marine environmental monitoring is provided in Chapter 2. This chapter starts with an introduction of the concept of WSNs, which provides the fundamental physical infrastructure for environmental monitoring systems, followed by the discussion of current progress together with the issues that WSNs are facing. Visual sensing as an alternative sensing modality for marine environmental monitoring is introduced. Current existing marine monitoring systems are introduced and the main focus of these systems is outlined. Anomaly detection, the first step of introducing intelligence to WSNs, is highlighted in this chapter followed by the discussion of unusual event detection and clustering in WSNs. Standard classification performance evaluation methods, which are used to evaluate the experimental results in this work, are also introduced.

In Chapter 3, a multi-modal smart sensing system framework has been designed and the structure of the system is discussed. The framework is architected in a flexible manner that can be deployed on a computing cloud, which meets the requirement of futuristic large scale multi-modality smart sensor networks. High level content-based knowledge (the output from the back end smart system using machine learning techniques) is provided, which can be more easily understood and accessed by end users. The system also provides a user interface that allows a rich set of queries from end users.

Dublin Bay, Ireland, is the site used as the location for practical deployment of the proposed system and is described in Chapter 4. This test site presents a real challenge in environmental monitoring due to the complex interactions of parameters such as tide, stratification and human activities. Both of the *in-situ* and visual sensing modalities, which are deployed at the site, are described in detail in this chapter along with issues concerning deployment in the real environment.

The first case study is carried out in Chapter 5, which illustrated how raw *in-situ* sensor data can be converted into organized content based information. This chapter begins with the introduction of the importance of salinity and turbidity at estuaries followed by

abnormal event detection from these two sensor parameters. The experiments carried out in this section address the first two research questions, which validates our first hypothesis.

The second case study is carried out in Chapter 6, which illustrated event detection from visual sensing and the combination of event detection results from both visual and *in-situ* sensing modalities. A shipping traffic event detection system has been proposed and evaluated. The results show that the appearance of a large vessel at the scene can be identified accurately. However, it has been found that most of the occurrences do not lead to a rapid change in turbidity readings. Further analysis on the data suggested that, at the test site, the arrival of a P&O ferry often leads to rapid changes in the sensor readings while other shipping events do not have such affect. This is mainly due to the location where the *in-situ* sensor is deployed. Thus, we alter the settings of the shipping event detection system and adapt the system to detect P&O arrival events only. Results shown that a significant amount of turbidity events were caused by the arrival of P&O ferries. The results found in this case study demonstrate the advantage of coupling multiple sensing modalities, where visual sensor provides context information that can be used to verify events detected from *in-situ* sensor measurements. The case study carried out in this chapter demonstrates the advantage of multi-modality sensing system, which addresses research questions 3 and 4 and validates our second hypothesis.

7.2 Analysis and Discussion of Hypotheses

In this thesis, a number of research questions in conjunction with research hypotheses are explored to investigate how computer science techniques can improve the efficiency and effectiveness of current marine monitoring systems. In the following, the research questions are examined with respect to the experimental results obtained.

1. ***Can machine learning methods be used to automate the detection of abnormal events in the marine environment from in-situ sensing modalities?***

   This research question is explored in Chapter 5. Anomaly detection, as the first step

of abnormal event detection, is carried out using a modified background modelling technique (MoPBAS) originally from the image processing domain. The system achieved very high F1 scores on both salinity and turbidity test data. Abnormal events are then created using agglomerative hierarchical clustering based on the temporal information of the anomalies detected. From 861 salinity anomalies detected, 222 salinity events are constructed. In contrast, 693 turbidity events are constructed from the classified turbidity anomalies. The experiments carried out illustrated that it is possible to identify unusual water quality parameter variations from continuous sensor data stream.

2. ***Can machine learning techniques further group automatically detected abnormal events into catalogues based on their similarities to assist marine scientists in finding their causes?***

   This research question is also investigated in Chapter 5. ROC clustering method was employed to catalogue the detected abnormal events into sub-classes. Results show that detected abnormal events can be assigned into groups based on their similarity measurements. Events in the same group have similar variations but have very different trends compared with events in other groups. Significant events, which are potentially of greater importance to marine scientists, are assigned to new categories since there are no analogous events in the past.

3. ***What information can be extracted from a visual sensor to enhance the deployed wireless sensor network? Can this information be used to classify the abnormal events detected by in-situ sensors to assist the marine scientists in better understanding and modelling the ecosystem?***

   In Chapter 6, the second case study shows that shipping traffic at the test site can be accurately identified from a visual sensor. This content based information provided by the visual sensing modality can be used to validate the abnormal events detected from *in-situ* water quality sensors. The abnormal events, associated with the shipping traffic, can then be further classified as caused by local activity, which

can be ignored. Marine scientists only need to focus on investigating the causes of the remaining detected events.

4. ***Can a multi-modal smart sensor framework combine various data sources to provide a broader picture of monitoring sites and to assist the operators in monitoring large scale marine environments more efficiently and effectively?***

   In Chapter 3, a multi-modal smart sensing system is designed. The two case studies carried out in Chapter 5 and Chapter 6 illustrated the data processing from various sensing modalities. Although the designed system is not fully implemented, the case studies carried out in this research work demonstrated an example of how each building block of the designed system performs. Significant events that are detected by the system are also isolated (catalogued in new clusters). The system also aligns the events detected from all sensing modalities, thus providing richer information to marine scientists. The output of the studies shows that raw data can be converted to structured high level information that can potentially assist operators in monitoring large scale marine environments more efficiently and effectively.

7.3 Research Contributions

The contributions of this research consist of the following:

- An investigation into the need for multi-modal smart sensing network for marine environmental monitoring and the design of such a smart sensing system.
- The adaptation of a foreground extraction technique from image processing domain to anomaly detection from *in-situ* water quality sensor measurements.
- An evaluation of abnormal event detection and clustering from *in-situ* sensor data.
- An evaluation of shipping traffic event detection from visual sensor data.
- An investigation of the combination of event detection results from multi sensor modalities in a particular marine monitoring application scenario.

7.4 Future Work

During this research work, only one test site is deployed and maintained due to very practical concern such as the necessity for a hosting permission agreement, labour intensive maintenance requirements and high cost. This may limit the generalization of the outcomes from this research work. However, following the success of this work, we are now deploying sensors at two more test sites along the River Liffey in collaboration with Intel Labs Europe, Dublin City Council (DCC) and The Commissioners of Irish Lights (CIL). The architecture for these deployments follow the same framework as the designed site. New datasets will be collected in the near future, which can be used to further improve the proposed system. The location of the new sites, Dublin Bay Buoy and Strawberry Beds are shown in Figure 7.1. Strawberry Beds is located at the upper stream of the Liffy River, which is a fresh water environment. In contrast, the other new test site is located at Dublin Bay, where is the location that the Liffy River reaches the Irish Sea.

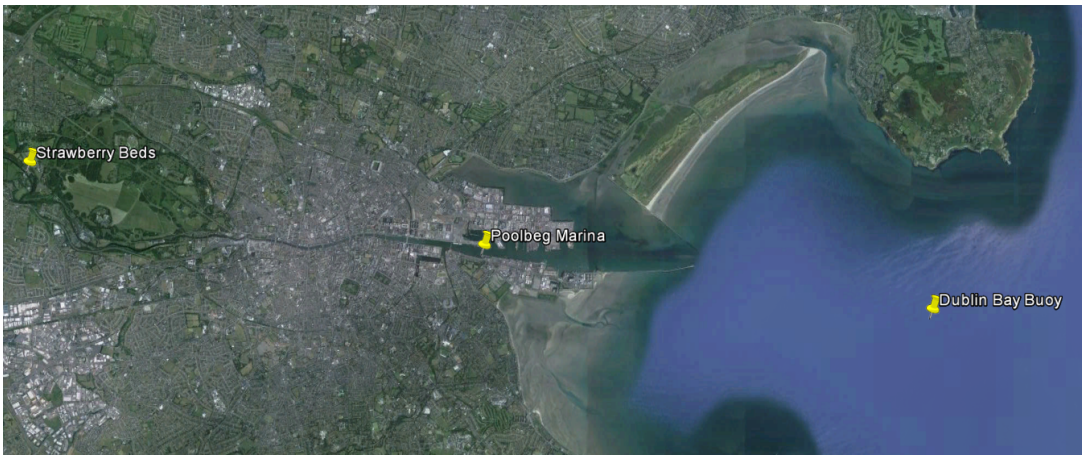

Figure 7.1: A map shows the location of the two new test sites, Dublin Bay Buoy and Strawberry Beds, which are currently under construction (source: http://maps.google.ie).

There are a wide range of novel opportunities for marine environment monitoring with the help of new developed hardware and software platforms. Marine well-being is also a key research area under the EU research and innovation program Horizon 2020. The findings of this research poses many new research possibilities:

Visual Sensing Recent released embedded systems, such as Raspberry Pi, Banana Pi, BeagleBoard etc. enables the development of a low cost self-powered mobile visual

sensing system that could be deployed at any marine site. Projects developed based on the used of these embedded systems, such as Feeder Tweeter [1] have shown the potential of such system that can be used for long-term environmental monitoring.

In terms of image analysis, future work involves extraction of additional information from image data. An example of this is estimating water levels from the relative position of a reference object or objects in the image. Such systems can provide validation information to water level sensors or a replacement if visual sensor can achieve a relative high accuracy. Water level sensors then can be removed to reduce cost and maintenance.

External Data Sources Integration of other data sources, such as weather forecasts, can provide additional information that can potentially assist the marine scientists in better understanding the nature process. For example, a heavy rainfall will result in a large volume of fresh water into the test site, which may have significant effect on *in-situ* sensor readings. Although, in this research work, only two sensing modalities were investigated, the designed multi-modality smart sensing framework has the capability of integrating external sources into the smart system.

System Implementation In this work, a multi-modality smart sensing system framework for environmental monitoring has been proposed. Two case studies have been carried out and evaluated to illustrate how the proposed system performs. However, in order to benefit the marine scientists, a fully functional system is required. Various components of the system have been developed during this work, the next step would be to integrate these components into a complete system and also to create a Graphical User Interface (GUI) that allows user to interact with the smart sensing system.

[1] Feeder Tweeter: http://www.feedertweeter.net/

BIBLIOGRAPHY

[1] "Harnessing our ocean wealth: An integrated marine plan for ireland," July 2012. Accessed on Dec 2014. 1

[2] D. P. Company, "Facts and figures," 2014. Accessed on 15th Dec 2014. 1

[3] E. M. Board, "Integrating marine science in europe," *European Science Foundation Marine Board Position Paper*, vol. 5, p. 148, 2002. 1

[4] A. Prüss-Üstün, R. Bos, F. Gore, J. Bartram, *et al.*, *Safer water, better health: costs, benefits and sustainability of interventions to protect and promote health.* World Health Organization, 2008. 1

[5] A. Prüss-Ustün, J. Bartram, T. Clasen, J. M. Colford, O. Cumming, V. Curtis, S. Bonjour, A. D. Dangour, J. De France, L. Fewtrell, *et al.*, "Burden of disease from inadequate water, sanitation and hygiene in low-and middle-income settings: a retrospective analysis of data from 145 countries," *Tropical Medicine & International Health*, vol. 19, no. 8, pp. 894–905, 2014. 2

[6] F. Collins, D. Orpen, D. Maher, J. Cleary, C. Fay, and D. Diamond, "Distributed chemical sensor networks for environmental sensing," 2011. 2

[7] J. H. Porter, E. Nagy, T. K. Kratz, P. Hanson, S. L. Collins, and P. Arzberger, "New eyes on the world: advanced sensors for ecology," *BioScience*, vol. 59, no. 5, pp. 385–397, 2009. 2

[8] L. Delauney, C. Compere, and M. Lehaitre, "Biofouling protection for marine environmental sensors," *Ocean Science*, vol. 6, no. 2, pp. 503–511, 2010. 3

[9] D. V. Manov, G. C. Chang, and T. D. Dickey, "Methods for reducing biofouling of moored optical sensors," *Journal of Atmospheric and Oceanic Technology*, vol. 21, no. 6, pp. 958–968, 2004. 3, 18

[10] P. Teillet, R. Gauthier, A. Chichagov, and G. Fedosejevs, "Towards integrated earth sensing: The role of in situ sensing," *International Archives of Photogrammetry Remote Sensing and Spatial Information Sciences*, vol. 34, no. 1, pp. 249–254, 2002. 3

[11] P. Chave, "The eu water framework directive," 2001. 5

[12] E. Directive, "60/ec of the european parliament and of the council of 23 october 2007 on the assessment and management of flood risks," *Official Journal of the European Union L*, vol. 288, no. 27, p. 2007, 2007. 5

[13] S. M. Glenn, T. D. Dickey, B. Parker, and W. Boicourt, "Long-term real-time coastal ocean observation networks," *OCEANOGRAPHY-WASHINGTON DC-OCEANOGRAPHY SOCIETY-*, vol. 13, no. 1, pp. 24–34, 2000. 5

[14] T. S. Moore, K. M. Mullaugh, R. R. Holyoke, A. S. Madison, M. Yücel, and G. W. Luther III, "Marine chemical technology and sensors for marine waters: potentials and limits," *Annual review of marine science*, vol. 1, pp. 91–115, 2009. 5

[15] T. Voigt, F. Osterlind, N. Finne, N. Tsiftes, Z. He, J. Eriksson, A. Dunkels, U. Bamstedt, J. Schiller, and K. Hjort, "Sensor networking in aquatic environments-experiences and new challenges," in *Local Computer Networks, 2007. LCN 2007. 32nd IEEE Conference on*, pp. 793–798, IEEE, 2007. 5

[16] B. O'Flynn, F. Regan, A. Lawlor, J. Wallace, J. Torres, and C. O'Mathuna, "Experiences and recommendations in deploying a real-time, water quality monitoring system," *Measurement Science and Technology*, vol. 21, no. 12, p. 124004, 2010. 6, 29

[17] C. Albaladejo, P. Sánchez, A. Iborra, F. Soto, J. A. López, and R. Torres, "Wireless sensor networks for oceanographic monitoring: A systematic review," *Sensors*, vol. 10, no. 7, pp. 6948–6968, 2010. 6, 13, 18

[18] P. W. Rundel, E. A. Graham, M. F. Allen, J. C. Fisher, and T. C. Harmon, "Environmental sensor networks in ecological research," *New Phytologist*, vol. 182, no. 3, pp. 589–607, 2009. 6

[19] T. Erickson, M. Podlaseck, S. Sahu, J. D. Dai, T. Chao, and M. Naphade, "The dubuque water portal: evaluation of the uptake, use and impact of residential water consumption feedback," in *Proceedings of the SIGCHI Conference on Human Factors in Computing Systems*, pp. 675–684, ACM, 2012. 6

[20] T. Erickson, M. Li, Y. Kim, A. Deshpande, S. Sahu, T. Chao, P. Sukaviriya, and M. Naphade, "The dubuque electricity portal: evaluation of a city-scale residential electricity consumption feedback system," in *Proceedings of the SIGCHI Conference on Human Factors in Computing Systems*, pp. 1203–1212, ACM, 2013. 6

[21] C. Fay, A. R. Doherty, S. Beirne, F. Collins, C. Foley, J. Healy, B. M. Kiernan, H. Lee, D. Maher, D. Orpen, *et al.*, "Remote real-time monitoring of subsurface landfill gas migration," *Sensors*, vol. 11, no. 7, pp. 6603–6628, 2011. 7

[22] H. Kopetz, "Internet of things," in *Real-time systems*, pp. 307–323, Springer, 2011. 12

[23] R. H. Weber and R. Weber, *Internet of Things*. Springer, 2010. 12

[24] J. Spohrer and P. Maglio, "Working together to build a smart planet," *ICSOC, Service-Oriented Computing*, 2010. 12

[25] K. Su, J. Li, and H. Fu, "Smart city and the applications," in *Electronics, Communications and Control (ICECC), 2011 International Conference on*, pp. 1028–1031, IEEE, 2011. 12

[26] J. Yick, B. Mukherjee, and D. Ghosal, "Wireless sensor network survey," *Computer networks*, vol. 52, no. 12, pp. 2292–2330, 2008. 12

[27] E. OConnor, *Trust and reputation in multi-modal sensor networks for marine environmental monitoring*. PhD thesis, Dublin City University, 2012. 12, 18, 19, 20

[28] M. Li and B. Yang, "A survey on topology issues in wireless sensor network.," in *ICWN*, p. 503, 2006. 14

[29] A. Flammini, P. Ferrari, D. Marioli, E. Sisinni, and A. Taroni, "Wired and wireless sensor networks for industrial applications," *Microelectronics Journal*, vol. 40, no. 9, pp. 1322–1336, 2009. 14

[30] G. Xu, W. Shen, and X. Wang, "Applications of wireless sensor networks in marine environment monitoring: A survey," *Sensors*, vol. 14, no. 9, pp. 16932–16954, 2014. 14

[31] C. Eklund, R. B. Marks, K. L. Stanwood, S. Wang, *et al.*, "Ieee standard 802.16: a technical overview of the wirelessman air interface for broadband wireless access," *IEEE communications magazine*, vol. 40, no. 6, pp. 98–107, 2002. 15

[32] I. C. S. L. M. S. Committee *et al.*, "Wireless lan medium access control (mac) and physical layer (phy) specifications," 1997. 15

[33] A. Ericsson, "Ericsson mobility report, on the pulse of the networked society," 2012. 16

[34] J. Decuir, "Bluetooth 4.0: Low energy," *Cambridge, UK: Cambridge Silicon Radio SR plc*, 2010. 16

[35] D. Diamond, K. T. Lau, S. Brady, and J. Cleary, "Integration of analytical measurements and wireless communicationscurrent issues and future strategies," *Talanta*, vol. 75, no. 3, pp. 606–612, 2008. 18, 20

[36] X. Xu, X. Gao, J. Wan, and N. Xiong, "Trust index based fault tolerant multiple event localization algorithm for wsns," *Sensors*, vol. 11, no. 7, pp. 6555–6574, 2011. 18

[37] K. Ni, N. Ramanathan, M. N. H. Chehade, L. Balzano, S. Nair, S. Zahedi, E. Kohler, G. Pottie, M. Hansen, and M. Srivastava, "Sensor network data fault types," *ACM Transactions on Sensor Networks (TOSN)*, vol. 5, no. 3, p. 25, 2009. 18

[38] L. Goddijn-Murphy, D. Dailloux, M. White, and D. Bowers, "Fundamentals of in situ digital camera methodology for water quality monitoring of coast and ocean," *Sensors*, vol. 9, no. 7, pp. 5825–5843, 2009. 19, 88

[39] P. Wang, A. F. Smeaton, L. Songyang, E. O'Connor, Y. Ling, and N. E. O'Connor, "Short-term rainfall nowcasting: Using rainfall radar imaging," *Eurographics Ireland 2009: The 9th Irish Workshop on Computer Graphics*, 2009. 19, 88

[40] B. J. Boom, J. He, S. Palazzo, P. X. Huang, C. Beyan, H.-M. Chou, F.-P. Lin, C. Spampinato, and R. B. Fisher, "A research tool for long-term and continuous analysis of fish assemblage in coral-reefs using underwater camera footage," *Ecological Informatics*, 2013. 19, 88

[41] Y. Li, *What makes the city pulse*. PhD thesis, Dublin City University, 2014. 19

[42] T. Sakaki, M. Okazaki, and Y. Matsuo, "Earthquake shakes twitter users: real-time event detection by social sensors," in *Proceedings of the 19th international conference on World wide web*, pp. 851–860, ACM, 2010. 19

[43] "Trends in social media: Use in natural disasters." http://www.mysecurecyberspace.com/articles/classroom/

trends-in-social-media-use-in-natural-disasters.html. Accessed: 2015-02-23. 20

[44] K. Starbird, L. Palen, A. L. Hughes, and S. Vieweg, "Chatter on the red: what hazards threat reveals about the social life of microblogged information," in *Proceedings of the 2010 ACM conference on Computer supported cooperative work*, pp. 241–250, ACM, 2010. 20

[45] M. G. C. Torres, *Energy consumption in wireless sensor networks using gsp*. PhD thesis, University of Pittsburgh, 2006. 20

[46] N. Giannadakis, A. Rowe, M. Ghanem, and Y.-k. Guo, "Infogrid: providing information integration for knowledge discovery," *Information Sciences*, vol. 155, no. 3, pp. 199–226, 2003. 20

[47] L. Xiao, S. Boyd, and S. Lall, "A scheme for robust distributed sensor fusion based on average consensus," in *Information Processing in Sensor Networks, 2005. IPSN 2005. Fourth International Symposium on*, pp. 63–70, IEEE, 2005. 20

[48] K. Sambhoos, R. Nagi, M. Sudit, and J. T. Rickard, "Hierarchical higher level data fusion using fuzzy hamming and hypercube clustering.," *J. Adv. Inf. Fusion*, vol. 3, no. 2, pp. 90–106, 2008. 20

[49] A. F. Smeaton, E. O'Connor, and F. Regan, "Multimedia information retrieval and environmental monitoring: Shared perspectives on data fusion," *Ecological Informatics*, vol. 23, pp. 118–125, 2014. 20

[50] T. D. Little, J. Konrad, and P. Ishwar, "A wireless video sensor network for autonomous coastal sensing," in *Proceedings of the conference on coastal environmental sensing networks (CESN 2007), Boston, MA, USA*, Citeseer, 2007. 20

[51] E. O'Connor, A. F. Smeaton, N. E. O'Connor, and D. Diamond, "Integrating multiple sensor modalities for environmental monitoring of marine locations," in *Proceedings of the 6th ACM conference on Embedded network sensor systems*, pp. 405–406, ACM, 2008. 20, 34

[52] E. O'Connor, A. F. Smeaton, and N. E. O'Connor, "A multi-modal event detection system for river and coastal marine monitoring applications," in *OCEANS, 2011 IEEE-Spain*, pp. 1–10, IEEE, 2011. 21, 34

[53] A. Khan and L. Jenkins, "Undersea wireless sensor network for ocean pollution prevention," in *Communication Systems Software and Middleware and Workshops, 2008. COMSWARE 2008. 3rd International Conference on*, pp. 2–8, IEEE, 2008. 21

[54] C. A. Pérez, M. Jiménez, F. Soto, R. Torres, J. López, and A. Iborra, "A system for monitoring marine environments based on wireless sensor networks," in *OCEANS, 2011 IEEE-Spain*, pp. 1–6, IEEE, 2011. 21

[55] A. Alkandari *et al.*, "Wireless sensor network (wsn) for water monitoring system: Case study of kuwait beaches," *International Journal of Digital Information and Wireless Communications (IJDIWC)*, vol. 1, no. 4, pp. 709–717, 2011. 22

[56] F. Regan, A. Lawlor, B. O'Flynn, J. Torres, R. Martinez-Catala, C. O'Mathuna, and J. Wallace, "A demonstration of wireless sensing for long term monitoring of water quality," in *Local Computer Networks, 2009. LCN 2009. IEEE 34th Conference on*, pp. 819–825, IEEE, 2009. 22

[57] C. Alippi, R. Camplani, C. Galperti, and M. Roveri, "A robust, adaptive, solar-powered wsn framework for aquatic environmental monitoring," *Sensors Journal, IEEE*, vol. 11, no. 1, pp. 45–55, 2011. 22

[58] H. Yang, H. Wu, and Y. He, "Architecture of wireless sensor network for monitoring aquatic environment of marine shellfish," in *Asian Control Conference, 2009. ASCC 2009. 7th*, pp. 1147–1151, IEEE, 2009. 22

[59] J. Tateson, C. Roadknight, A. Gonzalez, T. Khan, S. Fitz, I. Henning, N. Boyd, C. Vincent, and I. Marshall, "Real world issues in deploying a wireless sensor network for oceanography," in *Workshop on Real-World Wireless Sensor Networks REALWSN05*, 2005. 22

[60] M. Iacono, E. Romano, and S. Marrone, "Adaptive monitoring of marine disasters with intelligent mobile sensor networks," in *Environmental Energy and Structural Monitoring Systems (EESMS), 2010 IEEE Workshop on*, pp. 38–45, IEEE, 2010. 22

[61] P. Jiang, H. Xia, Z. He, and Z. Wang, "Design of a water environment monitoring system based on wireless sensor networks," *Sensors*, vol. 9, no. 8, pp. 6411–6434, 2009. 22

[62] R. V. Kulkarni, A. Forster, and G. K. Venayagamoorthy, "Computational intelligence in wireless sensor networks: A survey," *Communications Surveys & Tutorials, IEEE*, vol. 13, no. 1, pp. 68–96, 2011. 23

[63] V. Chandola, A. Banerjee, and V. Kumar, "Anomaly detection: A survey," *ACM Comput. Surv.*, vol. 41, pp. 15:1–15:58, July 2009. 23

[64] A. Patcha and J.-M. Park, "An overview of anomaly detection techniques: Existing solutions and latest technological trends," *Computer Networks*, vol. 51, no. 12, pp. 3448–3470, 2007. 23

[65] V. J. Hodge and J. Austin, "A survey of outlier detection methodologies," *Artificial Intelligence Review*, vol. 22, no. 2, pp. 85–126, 2004. 23

[66] S. Ramaswamy, R. Rastogi, and K. Shim, "Efficient algorithms for mining outliers from large data sets," in *Proceedings of the 2000 ACM SIGMOD International Conference on Management Data*, SIGMOD '00, (New York, NY, USA), pp. 427–438, ACM, 2000. 24

[67] F. Angiulli and C. Pizzuti, "Fast outlier detection in high dimensional spaces," in *Principles of data mining and knowledge discovery*, pp. 15–27, Springer, 2002. 24

[68] S. Staniford, J. A. Hoagland, and J. M. McAlerney, "Practical automated detection of stealthy portscans," *Journal of Computer Security*, vol. 10, no. 1, pp. 105–136, 2002. 24

[69] B. Schölkopf, J. C. Platt, J. Shawe-Taylor, A. J. Smola, and R. C. Williamson, "Estimating the support of a high-dimensional distribution," *Neural computation*, vol. 13, no. 7, pp. 1443–1471, 2001. 24

[70] J. Ma and S. Perkins, "Time-series novelty detection using one-class support vector machines," in *Neural Networks, 2003. Proceedings of the International Joint Conference on*, vol. 3, pp. 1741–1745, IEEE, 2003. 24

[71] A. Valdes and K. Skinner, "Adaptive, model-based monitoring for cyber attack detection," in *Recent Advances in Intrusion Detection*, pp. 80–93, Springer, 2000. 24

[72] W. Lee and S. J. Stolfo, "Data mining approaches for intrusion detection," in *Usenix Security*, 1998. 24

[73] J. E. Dickerson and J. A. Dickerson, "Fuzzy network profiling for intrusion detection," in *Fuzzy Information Processing Society, 2000. NAFIPS. 19th International Conference of the North American*, pp. 301–306, IEEE, 2000. 24

[74] Z. He, X. Xu, and S. Deng, "Discovering cluster-based local outliers," *Pattern Recognition Letters*, vol. 24, no. 9, pp. 1641–1650, 2003. 24

[75] X. Song, M. Wu, C. Jermaine, and S. Ranka, "Conditional anomaly detection," *Knowledge and Data Engineering, IEEE Transactions on*, vol. 19, no. 5, pp. 631–645, 2007. 24

[76] H. He and E. A. Garcia, "Learning from imbalanced data," *Knowledge and Data Engineering, IEEE Transactions on*, vol. 21, no. 9, pp. 1263–1284, 2009. 24

[77] N. V. Chawla, N. Japkowicz, and A. Kotcz, "Editorial: special issue on learning from imbalanced data sets," *ACM Sigkdd Explorations Newsletter*, vol. 6, no. 1, pp. 1–6, 2004. 24

[78] G. H. Nguyen, A. Bouzerdoum, and S. L. Phung, "A supervised learning approach for imbalanced data sets," in *Pattern Recognition, 2008. ICPR 2008. 19th International Conference on*, pp. 1–4, IEEE, 2008. 24

[79] M. Galar, A. Fernandez, E. Barrenechea, H. Bustince, and F. Herrera, "A review on ensembles for the class imbalance problem: bagging-, boosting-, and hybrid-based approaches," *Systems, Man, and Cybernetics, Part C: Applications and Reviews, IEEE Transactions on*, vol. 42, no. 4, pp. 463–484, 2012. 24

[80] R. Batuwita and V. Palade, "Fsvm-cil: fuzzy support vector machines for class imbalance learning," *Fuzzy Systems, IEEE Transactions on*, vol. 18, no. 3, pp. 558–571, 2010. 24

[81] R. R. Sillito and R. B. Fisher, "Semi-supervised learning for anomalous trajectory detection.," in *BMVC*, pp. 1–10, 2008. 25

[82] K. Wang, J. J. Parekh, and S. J. Stolfo, "Anagram: A content anomaly detector resistant to mimicry attack," in *Recent Advances in Intrusion Detection*, pp. 226–248, Springer, 2006. 25

[83] G. Blanchard, G. Lee, and C. Scott, "Semi-supervised novelty detection," *The Journal of Machine Learning Research*, vol. 11, pp. 2973–3009, 2010. 25

[84] V. Chandola, A. Banerjee, and V. Kumar, "Anomaly detection: A survey," *ACM Computing Surveys (CSUR)*, vol. 41, no. 3, p. 15, 2009. 25

[85] K. Kapitanova, S. H. Son, and K. Kang, "Event detection in wireless sensor networks," in *Second International Conference, ADHOCNETS*, pp. 18–20, 2010. 25

[86] S. Anwar and C. Zhang, "Event detection in wireless sensor networks," *Handbook of Research on Mobility and Computing: Evolving Technologies and Ubiquitous Impacts: Evolving Technologies and Ubiquitous Impacts*, vol. 1, p. 237, 2011. 25, 26

[87] R. Govindan, J. Hellerstein, W. Hong, S. Madden, M. Franklin, and S. Shenker, "The sensor network as a database," tech. rep., Citeseer, 2002. 25

[88] S. Li, S. H. Son, and J. A. Stankovic, "Event detection services using data service middleware in distributed sensor networks," in *Information Processing in Sensor Networks*, pp. 502–517, Springer, 2003. 25

[89] J. M. Hellerstein, W. Hong, S. Madden, and K. Stanek, "Beyond average: Toward sophisticated sensing with queries," in *Information Processing in Sensor Networks*, pp. 63–79, Springer, 2003. 25

[90] M. Li, Y. Liu, and L. Chen, "Nonthreshold-based event detection for 3d environment monitoring in sensor networks," *Knowledge and Data Engineering, IEEE Transactions on*, vol. 20, pp. 1699–1711, Dec 2008. 26

[91] P. Simon, *Too Big to Ignore: The Business Case for Big Data*. John Wiley & Sons, 2013. 26

[92] J. R. Anderson, R. S. Michalski, J. G. Carbonell, and T. M. Mitchell, *Machine learning: An artificial intelligence approach*, vol. 2. Morgan Kaufmann, 1986. 26

[93] A. G. Barto, *Reinforcement learning: An introduction*. MIT press, 1998. 27

[94] J. Davis and M. Goadrich, "The relationship between precision-recall and roc curves," in *Proceedings of the 23rd international conference on Machine learning*, pp. 233–240, ACM, 2006. 28

[95] G. Willems, T. Tuytelaars, and L. Van Gool, "An efficient dense and scale-invariant spatio-temporal interest point detector," in *Computer Vision–ECCV 2008*, pp. 650–663, Springer, 2008. 28, 95

[96] S. Umakanthan, S. Denman, S. Sridharan, C. Fookes, and T. Wark, "Spatio temporal feature evaluation for action recognition," in *Digital Image Computing Techniques and Applications (DICTA), 2012 International Conference on*, pp. 1–8, IEEE, 2012. 28

[97] J. R. Parker, *Algorithms for image processing and computer vision*. John Wiley & Sons, 2010. 29

[98] O. L. Junior, D. Delgado, V. Gonçalves, and U. Nunes, "Trainable classifier-fusion schemes: an application to pedestrian detection," in *Intelligent Transportation Systems*, pp. 1–6, 2009. 29

[99] R. Mehran, A. Oyama, and M. Shah, "Abnormal crowd behavior detection using social force model," in *Computer Vision and Pattern Recognition, 2009. CVPR 2009. IEEE Conference on*, pp. 935–942, IEEE, 2009. 29

[100] V. Mahadevan, W. Li, V. Bhalodia, and N. Vasconcelos, "Anomaly detection in crowded scenes," in *Computer Vision and Pattern Recognition (CVPR), 2010 IEEE Conference on*, pp. 1975–1981, IEEE, 2010. 29

[101] F. Provost and T. Fawcett, "Robust classification for imprecise environments," *Machine learning*, vol. 42, no. 3, pp. 203–231, 2001. 29

[102] P. Mell and T. Grance, "The nist definition of cloud computing," 2011. 31

[103] S. E. R. B. District, "South eastern river basin district management system initial characterisation report @ONLINE." Accessed on 22nd Dec 2014. 37

[104] S. Roth and J. G. Wilson, "Functional analysis by trophic guilds of macrobenthic community structure in dublin bay, ireland," *Journal of Experimental Marine Biology and Ecology*, vol. 222, no. 12, pp. 195 – 217, 1998. 38

[105] J. Wilson, "Productivity, fisheries and aquaculture in temperate estuaries," *Estuarine, Coastal and Shelf Science*, vol. 55, no. 6, pp. 953 – 967, 2002. 38

[106] C. Briciu-Burghina, T. Sullivan, J. Chapman, and F. Regan, "Continuous high-frequency monitoring of estuarine water quality as a decision support tool: a dublin port case study," *Environmental monitoring and assessment*, pp. 1–20, 2014. 38, 39, 50, 90, 91

[107] R. J. Wagner, H. C. Mattraw, G. F. Ritz, and B. A. Smith, *Guidelines and standard procedures for continuous water-quality monitors: Site selection, field operation, calibration, record computation, and reporting*. US Department of the Interior, US Geological Survey, 2000. 41

[108] T. O'Higgins and J. Wilson, "Impact of the river liffey discharge on nutrient and chlorophyll concentrations in the liffey estuary and dublin bay (irish sea)," *Estuarine, Coastal and Shelf Science*, vol. 64, no. 2, pp. 323–334, 2005. 47

[109] C. Raick, K. Soetaert, and M. Grégoire, "Model complexity and performance: How far can we simplify?," *Progress in Oceanography*, vol. 70, pp. 27–57, July 2006. 47

[110] S. B. Lee and G. F. Birch, "Utilising monitoring and modelling of estuarine environments to investigate catchment conditions responsible for stratification events in a typically well-mixed urbanised estuary," *Estuarine, Coastal and Shelf Science*, vol. 111, pp. 1–16, 2012. 48

[111] C. Crain, B. Silliman, Bertness, S.L., and M. Bertness, "Physical and biotic drivers of plant distribution across estuarine salinity gradients," *Ecology*, vol. 85, pp. 2539–2549, 2004. 48

[112] B. Eyre and P. Balls, "A comparative study of nutrient behavior along the salinity gradient of tropical and temperate estuaries," *Estuaries*, vol. 22, no. 2, pp. 313–326, 1999. 48

[113] "Ysi 6-series multiparameter water quality sondes user manual." https://www.ysi.com/File%20Library/Documents/Manuals/069300-YSI-6-Series-Manual-RevJ.pdf, Mar 2012. Accessed: 2015-05-10. 48, 50

[114] S. G. J. Aarninkhof, I. L. Turner, T. D. T. Dronkers, M. Caljouw, and L. Nipius, "Nearshore subtidal bathymetry from time-exposure video images," *Geophysical Research*, vol. 110 (C6), 2005. 49

[115] W. Henley, M. Patterson, R. Neves, and A. D. Lemly, "Effects of sedimentation and turbidity on lotic food webs: a concise review for natural resource managers," *Reviews in Fisheries Science*, vol. 8, no. 2, pp. 125–139, 2000. 49, 50

[116] H. Chanson, M. Takeuchi, and M. Trevethan, "Using turbidity and acoustic backscatter intensity as surrogate measures of suspended sediment concentration in a small subtropical estuary," *Journal of Environmental Management*, vol. 88, no. 4, pp. 1406 – 1416, 2008. 49

[117] J. E. Petersen, L. P. Sanford, and W. M. Kemp, "Coastal plankton responses to turbulent mixing in experimental ecosystems," *Marine Ecology Progress Series*, vol. 171, pp. 23–41, 1998. 49, 50

[118] N. K. Goosen, J. Kromkamp, J. Peene, P. van Rijswijk, and P. van Breugel, "Bacterial and phytoplankton production in the maximum turbidity zone of three european estuaries: the elbe, westerschelde and gironde," *Journal of Marine Systems*, vol. 22, no. 23, pp. 151 – 171, 1999. 49

[119] J. Zhang and C. Liu, "Riverine composition and estuarine geochemistry of particulate metals in chinaweathering features, anthropogenic impact and chemical fluxes," *Estuarine, Coastal and Shelf Science*, vol. 54, no. 6, pp. 1051–1070, 2002. 49

[120] L. Tremblay, S. Kohl, J. Rice, and J. Gagné, "Effects of temperature, salinity, and dissolved humic substances on the sorption of polycyclic aromatic hydrocarbons to estuarine particles," *Marine Chemistry*, vol. 96, no. 1, pp. 21–34, 2005. 49

[121] Y. A. Pachepsky and D. R. Shelton, "Escherichia coli and fecal coliforms in freshwater and estuarine sediments," *Critical Reviews in Environmental Science and Technology*, vol. 41, no. 12, pp. 1067–1110, 2011. 49

[122] D. Lawler, G. Petts, I. Foster, and S. Harper, "Turbidity dynamics during spring storm events in an urban headwater river system: The upper tame, west midlands, uk," *Science of The Total Environment*, vol. 360, no. 13, pp. 109 – 126, 2006.

¡ce:title¿Urban Environmental Research in the UK: The Urban Regeneration and the Environment (NERC URGENT) Programme and associated studies.¡/ce:title¿. 49, 50

[123] R. Uncles, J. Stephens, and R. Smith, "The dependence of estuarine turbidity on tidal intrusion length, tidal range and residence time," *Continental Shelf Research*, vol. 22, no. 11, pp. 1835–1856, 2002. 50

[124] D. H. Wilber and D. G. Clarke, "Biological effects of suspended sediments: A review of suspended sediment impacts on fish and shellfish with relation to dredging activities in estuaries," *North American Journal of Fisheries Management*, vol. 21, no. 4, pp. 855–875, 2001. 50

[125] T. Lindholm, M. Svartstrm, L. Spoof, and J. Meriluoto, "Effects of ship traffic on archipelago waters off the langnas harbour in aland, sw finland," *Hydrobiologia*, vol. 444, pp. 217–225, 2001. 50

[126] Y. A. Yousef, W. M. McLellon, and H. H. Zebuth, "Changes in phosphorus concentrations due to mixing by motorboats in shallow lakes," *Water Research*, vol. 14, no. 7, pp. 841–852, 1980. 50

[127] M. Hofmann, P. Tiefenbacher, and G. Rigoll, "Background segmentation with feedback: The pixel-based adaptive segmenter," in *IEEE Computer Society Conference on Computer Vision and Pattern Recognition Workshops (CVPRW)*, pp. 38–43, 2012. 52, 53

[128] T. Joachims, *Text categorization with support vector machines: Learning with many relevant features*. Springer, 1998. 58, 99

[129] G. Qiu, "Indexing chromatic and achromatic patterns for content-based colour image retrieval," *Pattern Recognition*, vol. 35, no. 8, pp. 1675–1686, 2002. 58

[130] L. Fei-Fei and P. Perona, "A bayesian hierarchical model for learning natural scene categories," in *Computer Vision and Pattern Recognition, 2005. CVPR 2005. IEEE Computer Society Conference on*, vol. 2, pp. 524–531 vol. 2, June 2005. 58

[131] D. Zhang, S. Chen, and K. Tan, "Improving the robustness of online agglomerative clustering methodbased on kernel-induce distance measures," *Neural Processing Letters*, vol. 21, no. 1, pp. 45–51, 2005. 59

[132] E. Jones, T. Oliphant, P. Peterson, *et al.*, "SciPy: Open source scientific tools for Python," 2001–. 61

[133] J. Bergstra, R. Bardenet, Y. Bengio, B. Kégl, *et al.*, "Algorithms for hyper-parameter optimization.," in *NIPS*, vol. 24, pp. 2546–2554, 2011. 65

[134] F. Hutter, "Automated configuration of algorithms for solving hard computational problems," 2009. 65

[135] F. Hutter, H. H. Hoos, and K. Leyton-Brown, "Sequential model-based optimization for general algorithm configuration," in *Learning and Intelligent Optimization*, pp. 507–523, Springer, 2011. 65

[136] C. E. Rasmussen, "Gaussian processes for machine learning," 2006. 65

[137] N. Pinto, D. Doukhan, J. J. DiCarlo, and D. D. Cox, "A high-throughput screening approach to discovering good forms of biologically inspired visual representation," *PLoS computational biology*, vol. 5, no. 11, p. e1000579, 2009. 65

[138] J. Bergstra, D. Yamins, and D. D. Cox, "Hyperopt: A python library for optimizing the hyperparameters of machine learning algorithms," 2013. 65

[139] M. Davidson, M. Van Koningsveld, A. de Kruif, J. Rawson, R. Holman, A. Lamberti, R. Medina, A. Kroon, and S. Aarninkhof, "The coastview project: Developing video-derived coastal state indicators in support of coastal zone management," *Coastal Engineering*, vol. 54, no. 6, pp. 463–475, 2007. 88

[140] E. A. Graham, E. M. Yuen, G. F. Robertson, W. J. Kaiser, M. P. Hamilton, and P. W. Rundel, "Budburst and leaf area expansion measured with a novel mobile camera system and simple color thresholding," *Environmental and Experimental Botany*, vol. 65, no. 2-3, pp. 238 – 244, 2009. 89

[141] A. Richardson, J. Jenkins, B. Braswell, D. Hollinger, S. Ollinger, , and M. Smith, "Use of digital webcam images to track spring green-up in a deciduous broadleaf forest," *Ecosystem Ecology*, vol. 152(2), pp. 323–334, 2007. 89

[142] D. G. Lowe, "Object recognition from local scale-invariant features," in *Computer vision, 1999. The proceedings of the seventh IEEE international conference on*, vol. 2, pp. 1150–1157, Ieee, 1999. 94

[143] K. Sudo, T. Osawa, H. Tanaka, H. Koike, and K. Arakawa, "Online anomal movement detection based on unsupervised incremental learning," in *Pattern Recognition, 2008. ICPR 2008. 19th International Conference on*, pp. 1–4, IEEE, 2008. 94

[144] M. D. Breitenstein, H. Grabner, and L. Van Gool, "Hunting nessie-real-time abnormality detection from webcams," in *Computer Vision Workshops (ICCV Workshops), 2009 IEEE 12th International Conference on*, pp. 1243–1250, IEEE, 2009. 94

[145] I. Laptev, "On space-time interest points," *International Journal of Computer Vision*, vol. 64, no. 2-3, pp. 107–123, 2005. 94

[146] C. Harris and M. Stephens, "A combined corner and edge detector.," in *Alvey vision conference*, vol. 15, p. 50, Manchester, UK, 1988. 94

[147] C. Schuldt, I. Laptev, and B. Caputo, "Recognizing human actions: a local svm approach," in *Pattern Recognition, 2004. ICPR 2004. Proceedings of the 17th International Conference on*, vol. 3, pp. 32–36, IEEE, 2004. 94

[148] A. Kovashka and K. Grauman, "Learning a hierarchy of discriminative space-time neighborhood features for human action recognition," in *Computer Vision and Pattern Recognition (CVPR), 2010 IEEE Conference on*, pp. 2046–2053, IEEE, 2010. 94

[149] P. Dollár, V. Rabaud, G. Cottrell, and S. Belongie, "Behavior recognition via sparse spatio-temporal features," in *Visual Surveillance and Performance Evalu-*

ation of Tracking and Surveillance, 2005. 2nd Joint IEEE International Workshop on, pp. 65–72, IEEE, 2005. 95

[150] M. Bregonzio, S. Gong, and T. Xiang, "Recognising action as clouds of space-time interest points," in *Computer Vision and Pattern Recognition, 2009. CVPR 2009. IEEE Conference on*, pp. 1948–1955, IEEE, 2009. 95

[151] T. Lindeberg, "Feature detection with automatic scale selection," *International journal of computer vision*, vol. 30, no. 2, pp. 79–116, 1998. 95

[152] J. Stöttinger, B. T. Goras, T. Pöntiz, A. Hanbury, N. Sebe, and T. Gevers, "Systematic evaluation of spatio-temporal features on comparative video challenges," in *Computer Vision–ACCV 2010 Workshops*, pp. 349–358, Springer, 2011. 95

[153] H. Wang, M. M. Ullah, A. Klaser, I. Laptev, C. Schmid, *et al.*, "Evaluation of local spatio-temporal features for action recognition," in *BMVC 2009-British Machine Vision Conference*, 2009. 95

[154] H. Wang, A. Klaser, C. Schmid, and C.-L. Liu, "Action recognition by dense trajectories," in *Computer Vision and Pattern Recognition (CVPR), 2011 IEEE Conference on*, pp. 3169–3176, IEEE, 2011. 95

[155] A. Klaser, M. Marszałek, and C. Schmid, "A spatio-temporal descriptor based on 3d-gradients," in *BMVC 2008-19th British Machine Vision Conference*, pp. 275–1, British Machine Vision Association, 2008. 95

[156] I. Laptev and T. Lindeberg, "Local descriptors for spatio-temporal recognition," in *Spatial Coherence for Visual Motion Analysis*, pp. 91–103, Springer, 2006. 95

[157] N. Dalal, B. Triggs, and C. Schmid, "Human detection using oriented histograms of flow and appearance," in *Computer Vision–ECCV 2006*, pp. 428–441, Springer, 2006. 95

[158] M. Stikic, T. Huynh, K. Van Laerhoven, and B. Schiele, "Adl recognition based on the combination of rfid and accelerometer sensing," in *Pervasive Computing*

Technologies for Healthcare, 2008. PervasiveHealth 2008. Second International Conference on, pp. 258–263, IEEE, 2008. 96

[159] S. Nowozin, G. Bakir, and K. Tsuda, "Discriminative subsequence mining for action classification," in *Computer Vision, 2007. ICCV 2007. IEEE 11th International Conference on*, pp. 1–8, IEEE, 2007. 96

[160] J. O. Laguna, A. G. Olaya, and D. Borrajo, "A dynamic sliding window approach for activity recognition," in *User Modeling, Adaption and Personalization*, pp. 219–230, Springer, 2011. 96

[161] P. Domingos and M. Pazzani, "On the optimality of the simple bayesian classifier under zero-one loss," *Machine learning*, vol. 29, no. 2-3, pp. 103–130, 1997. 99

[162] L. Rokach, *Data mining with decision trees: theory and applications*, vol. 69. World scientific, 2008. 99

[163] I. Aleksander and H. Morton, "An introduction to neural computing," 1990. 99

[164] N. S. Altman, "An introduction to kernel and nearest-neighbor nonparametric regression," *The American Statistician*, vol. 46, no. 3, pp. 175–185, 1992. 99

[165] C. Cortes and V. Vapnik, "Support-vector networks," *Machine learning*, vol. 20, no. 3, pp. 273–297, 1995. 99

[166] T. Segaran, *Programming collective intelligence: building smart web 2.0 applications*. " O'Reilly Media, Inc.", 2007. 99

[167] I. H. Witten and E. Frank, *Data Mining: Practical machine learning tools and techniques*. Morgan Kaufmann, 2005. 99

[168] B. E. Boser, I. M. Guyon, and V. N. Vapnik, "A training algorithm for optimal margin classifiers," in *Proceedings of the fifth annual workshop on Computational learning theory*, pp. 144–152, ACM, 1992. 99

[169] H. Jia, Y. L. Murphey, J. Shi, and T.-S. Chang, "An intelligent real-time vision system for surface defect detection," in *Pattern Recognition, 2004. ICPR 2004. Proceedings of the 17th International Conference on*, vol. 3, pp. 239–242, IEEE, 2004. 99

[170] W. E. Snyder and H. Qi, *Machine vision*. Cambridge University Press, 2010. 99

[171] M. Sonka, V. Hlavac, and R. Boyle, *Image processing, analysis, and machine vision*. Cengage Learning, 2014. 99

[172] C.-C. Lin, S.-H. Chen, T.-K. Truong, and Y. Chang, "Audio classification and categorization based on wavelets and support vector machine," *Speech and Audio Processing, IEEE Transactions on*, vol. 13, no. 5, pp. 644–651, 2005. 99

[173] W. M. Campbell, D. E. Sturim, and D. A. Reynolds, "Support vector machines using gmm supervectors for speaker verification," *Signal Processing Letters, IEEE*, vol. 13, no. 5, pp. 308–311, 2006. 99

[174] S. Kiritchenko and S. Matwin, "Email classification with co-training," in *Proceedings of the 2011 Conference of the Center for Advanced Studies on Collaborative Research*, pp. 301–312, IBM Corp., 2011. 99

[175] C.-W. Hsu, C.-C. Chang, C.-J. Lin, *et al.*, "A practical guide to support vector classification," 2003. 105